OSCILLATING FLOW ABOUT TUBE BUNDLES

Mehmet Ali Cinar

NAVAL POSTGRADUATE SCHOOL
Monterey, California

THESIS

OSCILLATING FLOW ABOUT TUBE BUNDLES

by

Mehmet Ali Cinar

September 1979

Thesis Advisor: T. Sarpkaya

UNCLASSIFIED

SECURITY CLASSIFICATION OF THIS PAGE (When Data Entered)

REPORT DOCUMENTATION PAGE		READ INSTRUCTIONS BEFORE COMPLETING FORM
1. REPORT NUMBER	2. GOVT ACCESSION NO.	3. RECIPIENT'S CATALOG NUMBER
4. TITLE (and Subtitle) Oscillating Flow About Tube Bundles		5. TYPE OF REPORT & PERIOD COVERED Master of Science and Mechanical Engineer Degree September 1979 6. PERFORMING ORG. REPORT NUMBER
7. AUTHOR(s) Mehmet Ali Cinar		8. CONTRACT OR GRANT NUMBER(s)
9. PERFORMING ORGANIZATION NAME AND ADDRESS Naval Postgraduate School Monterey, California 93940		10. PROGRAM ELEMENT, PROJECT, TASK AREA & WORK UNIT NUMBERS
11. CONTROLLING OFFICE NAME AND ADDRESS Naval Postgraduate School Monterey, California 93940		12. REPORT DATE September 1979 13. NUMBER OF PAGES 121
14. MONITORING AGENCY NAME & ADDRESS(if different from Controlling Office)		15. SECURITY CLASS. (of this report) Unclassified 15a. DECLASSIFICATION/DOWNGRADING SCHEDULE

16. DISTRIBUTION STATEMENT (of this Report)

Approved for public release; distribution unlimited

17. DISTRIBUTION STATEMENT (of the abstract entered in Block 20, if different from Report)

18. SUPPLEMENTARY NOTES

19. KEY WORDS (Continue on reverse side if necessary and identify by block number)

Harmonic Flow; Tube Bundles; Resistance in Harmonic Flow

20. ABSTRACT (Continue on reverse side if necessary and identify by block number)

The lift, drag, and inertia coefficients have been determined experimentally for various tube bundles and for two cylinders at various relative positions subjected to harmonically oscillating flow. The force coefficients for the inline force have been analyzed through the use of the Morison's equation and the Fourier analysis. The transverse force or the lift force has been expressed in terms of its maximum value.

DD FORM 1 JAN 73 1473 EDITION OF 1 NOV 65 IS OBSOLETE
S/N 0102-014-6601 |
(Page 1)

UNCLASSIFIED
SECURITY CLASSIFICATION OF THIS PAGE (When Data Entered)

The results have shown that the interference between the cylinders can give rise to complex flow patterns and to unexpectedly large force transfer coefficients. The results with two cylinder experiments have shed considerable light on the wake interference in harmonic flows.

Approved for public release; distribution unlimited

Oscillating Flow About Tube Bundles

by

Mehmet Ali Çinar
Lieutenant, Turkish Navy
B.S.M.E., Naval Postgraduate School, 1978

Submitted in partial fulfillment of the
requirements for the degree of

MASTER OF SCIENCE IN MECHANICAL ENGINEERING

and the degree of

MECHANICAL ENGINEER

ABSTRACT

The lift, drag, and inertia coefficients have been determined experimentally for various tube bundles and for two cylinders at various relative positions subjected to harmonically oscillating flow. The force coefficients for the inline force have been analyzed through the use of Morison's Equation and Fourier Analysis. The transverse force or the lift force has been expressed in terms of its maximum value.

The results have shown that the interference between the cylinders can give rise to complex flow patterns and to unexpectedly large force transfer coefficients. The results with two-cylinder experiments have shed considerable light on the wake interference in harmonic flows.

TABLE OF CONTENTS

LIST OF FIGURES

NOMENCLATURE

C_d	Drag coefficient
C_m	Inertia coefficient
D_i	Diameter of individual cylinder comprising riser
D_a	ΣD_i
D_e	$(\Sigma D_i^2)^{\frac{1}{2}}$
L	Length of the cylinder
F	Total force exerted on the cylinder by the fluid
F_m	Measured force
U	Instantaneous velocity, $U=-U_m \cos \omega t$
U_m	Maximum velocity in a cycle
f_v	Frequency of vortex shedding
T	Period of flow oscillation
K	Keulegan-Carpenter Number, $K = \frac{U_m T}{D}$
Re	Reynolds Number, $Re = \frac{U_m D}{\nu}$
St	Strouhal number, $St = \frac{f_v D}{U_m}$
C_L	Lift coefficient
F_L	Lift force
T	Period of flow oscillation
t	Time
ω	Angular frequency $(=\frac{2\pi}{T})$
β	Frequency parameter, $\beta = D^2/\nu T = \frac{Re}{K}$
ν	Kinematic viscosity of fluid
ρ	Fluid density
α	Angle between two cylinder-center line and flow direction

ACKNOWLEDGEMENT

The author would like to express his sincere appreciation to his advisor Professor T. Sarpkaya for his guidance throughout the investigation and for his help with the composition of the thesis.

In addition, the author wishes to acknowledge the help given by the personnel of the machine shop of the Department of Mechanical Engineering in constructing the test apparatus. In particular, I wish to thank Mr. Jack McKay for his superb workmanship.

I. INTRODUCTION

A body's resistance to flow is strongly affected by what surrounds it. When two bodies are in close proximity, not only the flow about the downstream body but also that about the upstream body may be influenced. Examples include condenser tubes in heat transfer; columns in pressure suppression pools of nuclear reactors; risers, piles, and other tubular structures in off-shore engineering; turbine and compressor blades in mechanical or aerospace engineering; and high-rise buildings, cooling towers, and transmission lines in civil engineering. The quantification of the interference effects in terms of the pressure distribution, lift and drag forces on individual members, vortex shedding frequency, and the dynamic response of members of the array in terms of the governing flow and structural parameters constitute the essence of the problem.

There are infinite numbers of possible arrangements of two or more bodies positioned at right or oblique angles to the approaching flow direction. In wavy or time-dependent flows one needs the lift, drag and inertia coefficients for all members of the array. Evidently, the members of the array may not be all parallel and normal to the flow. The quantification of the flow interference on lift, drag and inertia coefficients for cylinders with relative inclinations and spacings in a design-wave environment is an exceedingly

complex problem. In the absence of data on the interaction between drag and inertia coefficients in wavy and harmonic flows for cylinder groups one is tempted to use steady-flow results for the drag coefficient and the unseparated potential flow results for the inertia coefficient. The inertia coefficient for a group of cylinders in inviscid unseparated flow may be obtained through the use of the method of images [1, 2] or through the use of the linear potential theory including wave diffraction [3, 4]. These analyses do not deal with the effects of separation and vortex shedding. Consequently, the results are more appropriate to the determination of earthquake forces and wave forces on large bodies rather than to the evaluation of the inertial components of the force in the drag/inertia dominated regime.

It is evident from the foregoing that experiments must be carried out with carefully selected tube bundles and cylinder combinations in order to develop some understanding of the flow interference and to provide data for body combinations of practical importance.

II. REVIEW OF PREVIOUS INVESTIGATIONS

A careful review of flow interference between two circular cylinders in various arrangements in steady flow has been presented by Zdravkovich [5] where an extensive list of references may be found. Numerous studies have shown that the changes in drag, lift and vortex shedding are not necessarily continuous. In fact, the occurrence of a fairly abrupt change in one or all flow characteristics at a critical spacing is one of the fundamental observations of flow interference in cylinder arrays.

For the tandem arrangement (one cylinder behind the other, see Figure 1), it has been shown that at relative spacings $S/D<3.5$ there is a strong mutual interference between the two cylinders. This critical distance increases with the bluffness of the bodies. For two plates in tandem, the critical spacings is about 10 times the plate width [6]. In general, the tandem arrangement has a strong effect on the drag and is sensitive to spacing. The upstream cylinder takes the brunt of

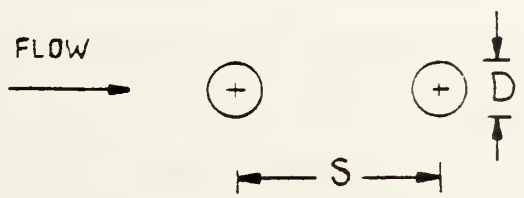

Fig. 1 Tandem arrangement of two cylinders

the burden and the total drag for the group is smaller than the sum of the drag forces acting on each cylinder in isolation in a tunnel with the same blockage. The drag coefficient for the downstream cylinders is reduced partly by shielding and partly by the occurrence of earlier transition in the boundary layers due to the turbulence in the approaching flow.

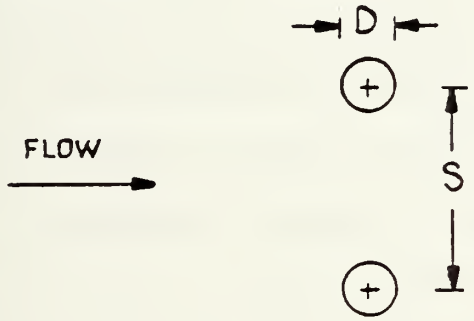

Fig. 2 Side-by-side arrangement of two cylinders

The side-by-side arrangement (see Figure 2) exhibits a discontinuity in the flow and measured forces for spacing ratios smaller than a critical value ($S/D<2.2$ for two circular cylinders and about 4 two plates). The observed discontinuity (a switching phenomenon and bistable nature of the flow between plates) results in two values of the drag coefficient. This results from the mutual interference of the vortices on the adjacent sides of the vortex streets. The bistable nature of the flow may be avoided by increasing the size of one of the cylinders. The sum of the bistable high and low drag is often less than twice the drag of the single cylinder. For two plates in side-by-side arrangement,

the said sum may be about 10 percent larger than twice the drag of the single plate. This increase strongly depends on the width of the flow field relative to the total width of the bodies, i.e., on the blockage ratio. For relatively large blockage, the flow is forced through the openings between the cylinders rather than around the total configuration. Consequently, the use of ordinary shielding and blockage factors for groups of cylinders is meaningless. Experiments must be conducted in channels or tunnels with very small blockage in order to obtain valid force-transfer coefficients. There is at present no means to separate the flow interference effects from the blockage effects for groups of cylinders.

Additional work with tube arrays in steady flows has been reported by a number of people [7 - 14]. Ross [15] conducted large scale wave tank tests for the case of one cylinder on each side of the test cylinder in the range of critical Reynolds numbers. His results appear to indicate that the wave force increases significantly only when the spacing between two cylinders is less than about one diameter.

The foregoing studies, conducted mostly in steady flows, show that the sum of the individual drag forces for isolated cylinders is often greater than the total force acting on the array as long as the local boundaries do not constrain the flow. They further show that the results obtained from the tandem and side-by-side arrangements cannot be generalized to predict the combined interference resulting from the staggered arrangement.

Gibson and Wang [16] carried out two different experiments to determine the added mass of a series of tube bundles. The bundles consisted of tubes of uniform diameter d arranged either in a square configuration or a circular configuration. In the first series of experiments, they towed the model of a pile cluster under linear acceleration. In the second series, they have vibrated the model at its own natural frequency. For both cases, they have calculated the added mass through the use of the measured force and acceleration and plotted them as a function of the 'solidification ratio' defined by $\Sigma d_i / \pi D$ where D is the pitch diameter of the bundle. Their results have shown that the added mass increases sharply after the solidification ratio reaches the value of 0.4 to 0.5. Beyond this value, the volume enclosed rather than the volume displaced by the structure becomes important. This result is disputed [17] and the results of both series of tests are no more applicable to separated wavy or oscillatary flows about tube bundles than those predicted from the potential theory with or without diffraction effects.

Relatively few studies have been carried out with oscillating tube bundles [18, 19]. Bushnell [19] determined the interference effects on the drag and transverse forces acting on a single member of a two-cylinder configuration through the use of a pulsating water tunnel. He did not evaluate the drag and inertia coefficients through the use of a suitable method, e.g. Fourier averaging. Instead, he picked out the maximum force values which occurred in each

half cycle and averaged them over ten consecutive values so as to obtain a mean maximum force for each flow direction. The results have shown that the presence of neighboring cylinders significantly affects the forces on an individual cylinder of an array and the interference effect increases with increasing relative flow displacement. The maximum drag force on shielded cylinders was reduced relative to an exposed cylinder by up to 50 percent. Bushnell has suggested that a design using a high Reynolds number single-cylinder drag coefficient applied throughout the array would have an extra margin of safety against maximum drag loading due to interference effects. The transverse force could be 3 to 4 times larger for interior array positions than that for a single cylinder. Thus, a cylinder array, such as a riser, supported at regular intervals may exhibit very complex dynamic behavior. Some of the members between supports may undergo violent transverse oscillations.

It is evident from the foregoing that there is very little systematic data for tube bundles and two cylinder interference. In view of this fact is was decided to carry out experiments with two bundle configuration consisting of 12 and 9 outer tubes, respectively. Subsequent to this investigation a detailed study of the interference effects of two cylinders in harmonic flow was undertaken.

III. EXPERIMENTAL EQUIPMENT AND PROCEDURES

A. OSCILLATING FLOW TUNNEL

Experiments were carried out in a large U-shaped oscillating water tunnel (see Figure 3). It has been used extensively at this institution over the past 6 years [20]. Only salient features, most recent modifications, as well as the adaptation for this work, are briefly described here.

The length of the tunnel has been increased from 30 feet to 35 feet and its height from 16 feet to 24 feet. Previously, a butterfly-valve arrangement at the top of one of the legs was used to initiate the oscillations. In 1978, the tunnel was modified so that the oscillations could be generated and maintained indefinitely at the desired amplitude. For this purpose the output of a 2 HP fan was connected to the top of one of the legs of the tunnel with a large pipe. A small butterfly valve, placed in a special housing between the top of the tunnel and the supply line, oscillated harmonically at a frequency equal to the natural frequency of the oscillations in the tunnel. The oscillation of the valve was perfectly synchronized with that of the flow through the use of a feedback control system. The output of a pressure transducer (sensing the instantaneous acceleration of the flow) was connected to an electronic speed-control unit coupled to a DC motor oscillating the valve plate. The circuit maintained the period of oscillations of the valve within 0.001 seconds. The fluid oscillated with a period of 6.000 seconds.

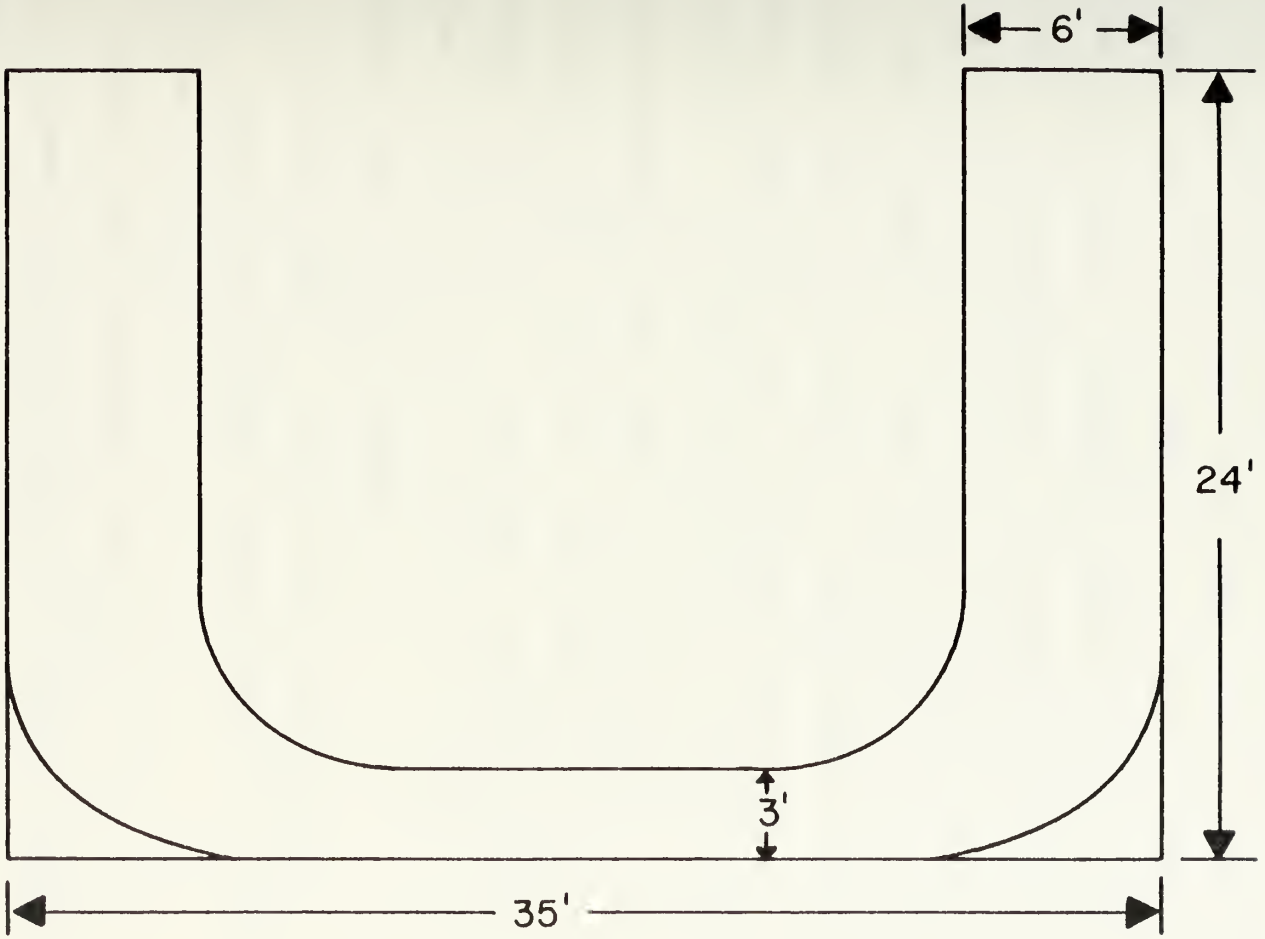

Fig. 3 U-shaped oscillating water tunnel

6'
24'
32'

The amplitude of oscillations was varied by constricting or enlarging an orifice at the exit of the fan. The flow oscillated at a given amplitude as long as desired.

Two identical force transducers, one at each end of the cylinder, were used to measure the instantaneous in-line and transverse forces. A special housing was built for each gage so that it can be mounted on the tunnel window and rotated to measure either the in-line or the transverse force alone.

The calibration of the each gage was accomplished by hanging loads in the middle of the cylinder after setting both gages to sense only the transverse force (here in the vertical direction). Repeated calibrations have shown that (a) the gages were absolutely linear up to 500 pounds; (b) the gages yielded the same signal for loads applied either upward or downward; and that (c) the gages, together with the electronic system to which they are attached, were capable of sensing loads as small as 0.02 pounds.

The displacement, velocity, and acceleration of the fluid in the tunnel were obtained through the use of several methods described in [20].

The data were recorded in analog form and then digitized and processed through the use of an HP9845 computer-digitizer system.

B. TEST BODIES

The tube bundles were made of aluminum rods and mounted between two circular stainless steel plates. Two configurations were chosen for test purposes. These configurations

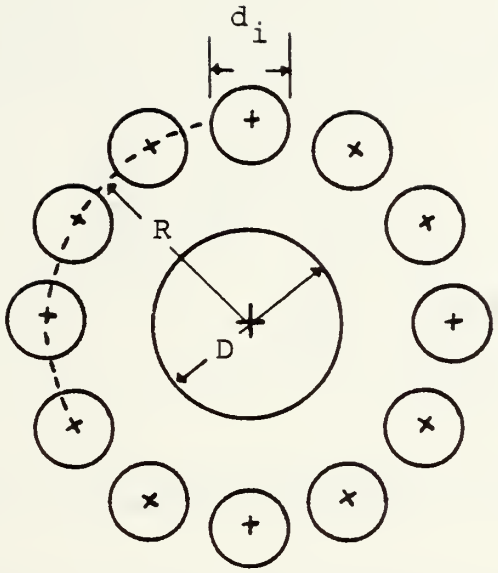

$D = 1.7917"$

$d_i = 0.750"$

$R = 2.937"$

$\frac{d_i}{D} = 0.4186$

$\frac{2R}{D} = 3.278$

$\frac{d_i}{2R} = 0.1277$

Fig. 4a Riser 1 configuration

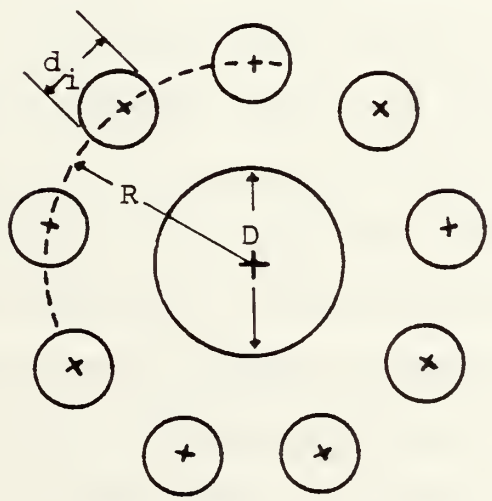

Fig. 4b Riser 2 configuration

roughly correspond to the most commonly used riser shapes in the off-shore industry. Figures 4a and 4b show the two riser configurations together with their characteristic dimensions.

The two cylinder configuration was arranged in a similar manner (see Figure 5). The active cylinder was mounted on the

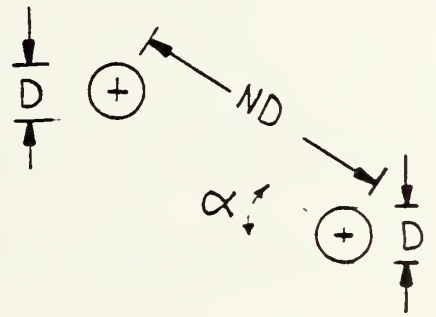

Fig. 5 General arrangement of two cylinders

force transducer as described previously. The passive cylinder spanned the entire test section and was rigidly mounted on the tunnel walls. Both cylinders were smooth and 3 inches in diameter. The angle α was varied from zero to 90 degrees in 30 degree increments. The N in cylinder spacing ND was varied from 1.5 to 3.5. The in-line and transverse forces acting on the active cylinder were measured and analyzed in terms of the appropriate lift coefficients and the drag and inertia coefficients through the use of the Fourier analysis. The details of the definition of the various force transfer coefficients are described in the following.

IV. FORCE TRANSFER COEFFICIENTS

A. TUBE BUNDLES

The in-line force, based on Morison's equation is written as

$$F = -0.5\rho C_d U_m^2 L \Sigma D_i \quad |\cos\omega t|\cos\omega t + 0.25\pi\rho L C_m \Sigma D_i^2 U_m \omega \sin\omega t \tag{1}$$

in which U_m is the maximum velocity in a given cycle. Denoting

$$D_a = \Sigma D_i \qquad D_e^2 = \Sigma D_i^2$$

and inserting in equation (1), one has

$$\frac{F}{0.5\rho D_e L U_m^2} = -C_d \cdot \left(\frac{D_a}{D_e}\right) \cdot |\cos\omega t| \cdot \cos\omega t + \frac{\pi^2}{\left(\frac{U_m T}{D_e}\right)} \cdot C_m \cdot \sin\omega t \tag{2}$$

in which $T = 2\pi/\omega$.

For an oscillating flow represented by $U = -U_m \cos\omega t$ the averages of C_d and C_m are given by [20]

$$C_d = \frac{3}{4} \cdot \left(\frac{D_e}{D_a}\right) \int_0^{2\pi} \frac{F_m \cos \omega t}{\rho L D_e U_m^2} \cdot d\omega t \qquad (3)$$

and

$$C_m = \frac{2U_m T}{\pi^3 D_e} \int_o^{2\pi} \frac{F_m \cdot \sin \omega t}{\rho L D_e U_m^2} d\omega t \qquad (4)$$

in which F_m represents the measured force.

The lift coefficient is defined as

$$C_L = \frac{F_L}{0.5 \rho L D_e U_m^2} \qquad (5)$$

in which F_L represents the amplitude of the transverse force and L, the length of the cylinder.

The vortex shedding frequency for the entire bundle was expressed in terms of the Strouhal number defined by

$$St = \frac{f_v D_e}{U_m} = \frac{f_v T}{K}$$

in which f_v represents the frequency of vortex shedding; T, the period of flow oscillation; and K, the Keulegan-Carpenter number defined by

$$K = \frac{U_m T}{D_e}$$

B. TWO CYLINDER ARRANGEMENT

The in-line force acting on the active cylinder is not independent of the direction of the fluid motion because of the interference effect of the passive cylinder. In the interval $\pi/2<\omega t<3\pi/2$ the direction of flow is opposite to that in the interval $3\pi/2<\omega t<5\pi/2$. With this fact in mind Morison's equation was written as

$$\frac{F}{0.5\rho D\, U_m^2} = \frac{\pi^2 D}{U_m T} \cdot C_m \sin\omega t - C_d |\mathrm{Cos}\,\omega t| \mathrm{Cos}\,\omega t \qquad (6)$$

and C_m and C_d were determined from

$$C_{m1} = \frac{4 \cdot U_m \cdot T}{\pi^3 F} \int_{\pi/2}^{3\pi/2} \frac{F \cdot \mathrm{Sin}\,\omega t}{\rho U_m^2 LD}\, d(\omega t) \qquad (7)$$

$$C_{d1} = -\frac{3}{2} \int_{\pi/2}^{3\pi/2} \frac{F \cdot \mathrm{Cos}\,\omega t}{\rho U_m^2 LD} \cdot d(\omega t) \qquad (8)$$

$$C_{m2} = \frac{4 U_m T}{\pi^3 D} \int_{3\pi/2}^{5\pi/2} \frac{F . \mathrm{Sin}\,\omega t}{\rho U_m^2 LD} \cdot d(\omega t) \qquad (9)$$

and

$$C_{d2} = -\frac{3}{2} \int_{3\pi/2}^{5\pi/2} \frac{F \cdot \mathrm{Cos}\,\omega t}{\rho U_m^2 LD}\, d(\omega t) \qquad (10)$$

in which C_{m1} and C_{d1} represent the inertia and drag coefficients for the interval $\pi/2<\omega t<3\pi/2$; and C_{m2} and C_{d2}, the corresponding coefficients for the interval $3\pi/2<\omega t<5\pi/2$. In general these two sets of in-line force coefficients are not identical accept when $\alpha=90^{o}$.

The evaluation of the transverse-force coefficients requires a distinction not only in the direction of flow but also in the direction of the transverse force. As the flow proceeds in a given direction the lift force acting on the active cylinder does not remain symmetrical primarily because of the proximity of the passive cylinder, situated asymmetrically relative to the direction of the flow. It is also recognized that the random nature of the vortex shedding does not allow a perfectly symmetric lift force even in the absence of any interference effects. Consequently, one must define four lift coefficients. In the interval $\pi/2<\omega t<3\pi/2$, one has (see Fig. 6a)

$$C_{L1} = \frac{F_{L1}}{0.5\rho U_m^2 \, DL}$$

$$C_{L2} = \frac{F_{L2}}{0.5\rho \cdot U_m^2 \, D \cdot L}$$

and in the interval $3\pi/2<\omega t<5\pi/2$, (see Fig. 6b)

$$C_{L3} = \frac{F_{L3}}{0.5\rho U_M^2 \, DL}$$

and

$$C_{L4} = \frac{F_{L4}}{0.5\rho U_m^2 \, DL}$$

where F_{L1} through F_{L4} are shown in Figures 6a and 6b.

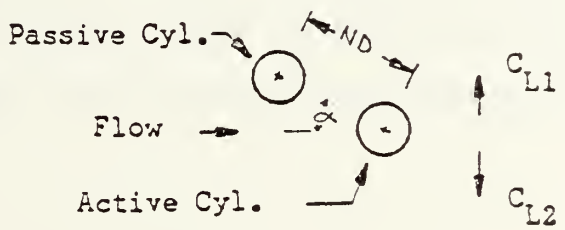

Fig. 6a Definition sketch for lift forces

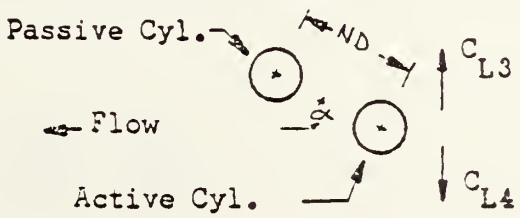

Fig. 6b Definition sketch for lift forces

The Strouhal number was defined in a manner similar to that previously described and evaluated through the use of

$$St_i = \frac{f_{vi} \cdot D}{U_m}$$

in which i = 1, .. .4, indicating the lift force directions shown in Figures 6a and 6b.

C. GOVERNING PARAMETERS

It has been shown previously [20] that the Fourier-averaged lift, drag, inertia coefficients for a smooth cylinder immersed in a harmonically oscillating flow depend on the Reynolds number and the Keulegan-Carpenter number. In other words

$$\{C_d, C_m, C_L\} = F_i \left(\frac{U_m D}{\nu} , \frac{U_m T}{D} \right)$$

In terms of a frequency parameter β defined by

$$\beta = \left(\frac{U_m D}{\nu}\right) / \left(\frac{U_m T}{D}\right) = \frac{D^2}{\nu T}$$

one has

$$\{C_d, C_m, C_L\} = F_i \left(\frac{D^2}{\nu T}, \frac{U_m T}{D}\right)$$

For the two cylinder arrangement one has to introduce two additional parameters namely, the angle α of the line joining the center of the two cylinders and the relative distance between the cylinders. Thus, all the force-transfer coefficients cited previously depend on the Keulegan-Carpenter number, Reynolds number (or the frequency parameter), the angle α, and the relative distance factor N (see Figure 5). Thus one has

$$C_i(\text{a coefficient}) = F_i(K, \beta, \alpha, N)$$

V. DISCUSSION OF RESULTS

A. TUBE BUNDLES

The drag and inertia coefficients for the two riser configurations are shown in Figures 7a and 7b as a function of the Keulegan-Carpenter number for constant values of β. The drag coefficient decreases gradually with increasing K. The inertia coefficient increases with increasing K and reaches values as large as 6. The use of the potential flow theory for unseparated flow yielded [21] an average inertia coefficient C^*_m=2.17 for the two configurations. C^*_m was defined by

$$C^*_m = (\Sigma C_{mi} D_i^2)/\Sigma D_i^2$$

The comparison of C^*_m with that obtained experimentally has shown that some fluid mass is entrapped within the array and that neither the potential theory nor the diffraction analysis can adequately describe the behavior of the complex separated flow through the bundle.

A comparison of the Figures 7a and 7b shows that the drag and inertia coefficents as defined here are nearly independent of the particular arrangement and the number of tubes comprising the bundle.

Experiments with different tube arrangements [21] have shown that the force coefficients are independent of the Reynolds number within the range of Reynolds and Keulegan-Carpenter numbers reported herein.

The reason for the dependence of C_d and C_m on K is thought to be the dependence of the interaction of the wakes of the outer and inner pipes. The vortices in the wake of a given cylinder loose about 70 percent of their strength within 10 cylinder diameters. Thus, for small values of K, the vortices generated by a small tube at the center front of the bundle arrive at the central tube as weak vortices. Consequently, each tube behaves more or less as if it were independently subjected to a turbulent harmonic flow. As K increases, not only the turbulence level but also the interaction between the wakes of the various cylinders increases. There is a certain amplitude of oscillation beyond which neither the interaction of the wakes nor the increase of the turbulence level affects the overall force acting on the bundle. A comparison of the total drag force acting on the bundle with the sum of the drag forces acting on each cylinder in isolation in harmonic flow (at the corresponding K and Re values appropriate to each tube) shows that the former is about 10 percent smaller.

The lift coefficients, as given by Eqn. (5), for the two riser configurations are shown in Figures 7c and 7d. Apparently, both configurations yield nearly identical lift coefficients. As will be seen later the rapid decrease of the lift coefficient

with increasing K is in conformity with that for a single cylinder. As the Keulegan-Carpenter number increases, each member of the bundle sheds an increasing number of vortices with different strengths and frequencies.

Furthermore the shielding or proximity effect of the tubes results in a highly confused vortex system. This in turn decreases the coherence of the regular vortex shedding, resulting in very low lift coefficients. Evidently, a greater understanding of the lift force requires the determination of the lift force acting on each member individually and the consequence of tube proximity.

B. DRAG AND INERTIA COEFFICIENTS FOR THE TWO CYLINDER ARRANGEMENT

The drag and inertia coefficients for N=1.5, N=2, N=2.5, and N=3.5 (only for $\alpha=0$) and for $\alpha=0^{\circ}$, $\alpha=30^{\circ}$, $\alpha=60^{\circ}$, and $\alpha=90^{\circ}$ are shown in Figures 8 through 20. Each figure represents either the drag or the inertia coefficient for two different flow directions. For example, Figure 8a shows the drag coefficients C_{d1} and C_{d2} for $\alpha=0^{\circ}$ and N=1.5. The coefficients C_{d1} is for the flow directed from passive towards active cylinder. The coefficient C_{d2} is for the flow directed from the active towards the passive cylinder. In addition, included in each figure is the drag or inertia coefficient for the single cylinder of the same size.

Figure 8b shows the inertia coefficients C_{m1} and C_{m2} for $\alpha=0^{\circ}$ and N=1.5. The coefficients C_{m1} and C_{m2} are related to the flow direction in the same manner as the coefficients C_{d1} and C_{d2}.

Figures 8a, 9a, 10a, and 11a show that for the tandem arrangement corresponding to $\alpha=0^{o}$ the drag coefficient C_{d2} is always larger than C_{d1}. The difference between the two drag coefficients decreases with increasing N (larger spacing). This finding is in conformity with the measurements reported by Zdravkovich [5] for the tandem arrangement in steady flow. For relatively small spacings (smaller N) the wake of the passive cylinder is highly turbulent. This causes earlier separation on the active cylinder and hence in smaller C_{d1} values. One may also express the same fact by stating that the active cylinder is shielded by the passive cylinder when the flow sees the passive cylinder first. As the spacing between the two cylinders increases, C_{d1} and C_{d2} gradually approach each other and single cylinder value. Even for N=3.5, C_{d2} is slightly larger than C_{d1} because of the aforementioned effect of turbulence in the wake of passive cylinder.

The inertia coefficients C_{m1} and C_{m2} for the tandem arrangement are shown in Figures 8b, 9b, 10b, and 11b. Unlike the drag coefficient, the inertia coefficient C_{m2} is always smaller than C_{m1}. This is not entirely unexpected. All drag and inertia evaluations for single cylinders in waves and harmonic flows have shown that [20] the drag and inertia coefficients follow opposite trends. In other words, when the drag coefficient increases the inertia coefficient decreases and vice versa. The reason for this is embedded in the formulation of the Morison's equation (See Eq. (1)). When the phase angle between the velocity and the maximum force

is small the total force is primarily due to the velocity-square dependent drag and the contribution of the inertial force is negligible. In fact such flows are termed drag-dominated flows. When the phase angle between the velocity and maximum force is large, the total force is primarily due to the acceleration-dependent inertia. Such flows are termed inertia-dominated flows. Thus, it is apparent that the drag and inertia coefficients should follow opposite trends.

As the relative spacing increases (See Fig. 11b) C_{m1} and C_{m2} approach each other. However, the difference between two coefficients remains relatively larger than that between C_{d1} and C_{d2}. The experimental fact is that the spacing between the two cylinders in tandem arrangements must be considerably larger than 3.5 diameters for the inertia coefficients to become independent of the proximity effects. It is also clear that structures in close proximity can cause relatively more significant changes in the inertia coefficient than in the drag coefficient.

Figures 8b, 9b, 10b, and 11b also show that the inertia coefficient for single cylinder (dashed lines) is nearly the same as C_{m2}. In other words, when the flow sees the active cylinder first the proximity effect on the inertia coefficient C_{m2} is negligible. It is also apparent that when the flow sees the passive cylinder first the inertia coefficient C_{m1} is considerably increased. The important conclusion to be reached on the basis of these results is that the inertia coefficient of a shielded cylinder may increase considerably

and the drag coefficient may decrease significantly.

The other extreme of the two cylinder arrangement is the side-by-side arrangement. The discussion of this case will be taken up next since the force coefficients for all other intermediate values of α follow trends intermediate to the tandem and side-by-side arrangements.

Figures 18a, 19a, and 20a show C_{d1} and C_{d2} for N=1.5, N=2, N=2.5 for the side-by-side arrangement. Several facts are immediately apparent from these figures. For spacings as small as 1.5 diameter the drag coefficients are not greatly incluenced by the proximity effects. Secondly, C_{d1} and C_{d2} are very close to that for the single cylinder. The slight difference in the lower range of Keulegan-Carpenter numbers may be attributed to the increased blockage in the tunnel and experimental uncertainty which was found to be about 5 percent. Experiments [5] with steady flows about the same type of two-cylinder arrangement have also shown that the proximity effects are negligible for spacings larger than about 1.5 diameter.

The inertia coefficients C_{m1} and C_{m2} shown in Figures 18b, 19b, 20b exhibit a somewhat different behavior. Even though they are nearly identical for any given spacing they are considerably larger than that for the single cylinder. Only for N=2.5 that they approach the single cylinder values.

The two other arrangements intermediate to those discussed above behave as would be expected. Both the drag and inertia coefficients shown in Figures 12 through 17 vary between the

cases for $\alpha=0^{\circ}$ and $\alpha=90^{\circ}$ and both gradually approach the corresponding single cylinder values. The conclusions regarding the effect of shielding remain valid for the intermediate arrangements.

C. LIFT COEFFICIENTS FOR THE TWO CYLINDER ARRANGEMENT

As in the case of drag and inertia coefficients, first the tandem arrangement, then the side-by-side arrangement, and finally, the intermediate arrangements will be discussed.

For the tandem arrangement $C_{L1}=C_{L2}$ and $C_{L3}=C_{L4}$ (See Figs. 6a and 6b). The coefficients C_{L1} or C_{L2} are shown in Figures 21-24 and the coefficients C_{L3} or C_{L4} are shown in Figures 25-28. Also shown in each figure is the lift coefficient for a single cylinder of the same size.

The data showed that the lift coefficient is strongly affected by the cylinder proximity, irrespective of the direction of the flow. For Keulegan-Carpenter numbers larger than about 20 the lift coefficients C_{L1} and C_{L3} remain practically constant. Only for very small Keulegan-Carpenter numbers that C_{L1} and C_{L3} increase rapidly, in conformity with that for a single cylinder. The reason for this is that for Keulegan-Carpenter numbers near 10, at most two vortices are shed during a given half-cycle. These vortices do not travel 1.6 diameters in one direction as seen from the simple relation that $K=2\pi A/D$ where A is the amplitude of the flow oscillation. Consequently, the vortices shed from the active cylinder are only partially blocked by the passive cylinder for K smaller than about 10. Nevertheless, the effect of cylinder proximity is ever present as seen from a comparison of the data with

that for the single cylinder. As the spacing increases, the lift coefficients gradually approach that of the single cylinder as seen in the Figures 24 and 28.

In the case of side-by-side arrangement $C_{L1}=C_{L3}$ and $C_{L2}=C_{L4}$. The coefficients C_{L1} or C_{L3} are shown in Figures 29-31 and the coefficients C_{L2} or C_{L4}, in Figures 32-34. The lift coefficients for this particular arrangement have been measured for only N=1.5, N=2, and N=2.5.

As the flow oscillates about the cylinders arranged in side-by-side position, the blockage introduced by the proximity of the cylinders forces the fluid to flow above the top and below the bottom cylinder. In other words, the velocity on the extreme sides of the passive and active cylinder increases while the velocity between the two cylinders decreases. This in turn increases the pressure on the sides of the cylinders nearest each other and decreases the pressure on the opposite sides. Consequently, C_{L1} or C_{L3} should be smaller than C_{L2} or C_{L4}. A comparison of the Figures 29-31 with Figures 32-34 shows that C_{L1} or C_{L3} is in fact, always smaller than C_{L2} or C_{L4}. As the relative spacing increases all four coefficients gradually approach that for a single cylinder as seen from Figures 31 and 34. These results are in conformity with those obtained with steady flow about a side-by-side arrangement of circular cylinders. [5]

For arbitrary arrangements one must deal with four different lift coefficients, namely, C_{L1}, C_{L2}, C_{L3}, and C_{L4}. The coefficient C_{L1} is shown in Figures 35-37 for $\alpha=30^{\circ}$ and

for N=1.5, N=2, and N=2.5. Similarly; C_{L2} is shown Figures 38-40; C_{L3}, in Figures 41-43; and finally, C_{L4}, in Figures 44-46. The corresponding lift coefficients for $\alpha=60^{\circ}$ arrangement is shown in Figures 47-58.

A comparison of Figures 35-37 with Figures 38-40 shows that C_{L1} is always larger than C_{L2}. The reason for this is that the vortices shed from the passive cylinder pass over the top of the active cylinder and thereby reduce the pressure at the top of the active cylinder. The coefficients C_{L1} and C_{L2} gradually approach that for a single cylinder as the spacing increases.

When the flow first sees the active cylinder, C_{L3} remains relatively larger than C_{L4} because of the presence of the vortices near the top of the active cylinder which were shed during the previous half cycle. As the spacing between the two cylinders increases both C_{L3} and C_{L4} rapidly approach the lift coefficient for a single cylinder.

For $\alpha=60^{\circ}$ arrangement all four lift coefficients are practically unaffected by the cylinder proximity even for a spacing as small as 1.5 diameters and they are nearly equal to that of an isolated cylinder. Evidently, the effect of cylinder-cylinder proximity on the lift coefficient for a harmonically oscillating flow is confined to relatively small spacings and angular positions.

The frequency of the lift force oscillations has been expressed in terms of the Strouhal number and evaluated for all cylinder arrangements. The results have shown that the

Strouhal number remains constant at an average value of about 0.2. The only exception to that was the case corresponding to $\alpha=30^{\circ}$ and N=1.5.

Figures 59 and 60 show the Strouhal number as a function of K for $\alpha=0^{\circ}$ and N=1.5. As N increased the Strouhal numbers for the two flow directions rapidly approached each other and a mean value of 0.2.

Figures 61 and 62 show the Strouhal number for $\alpha=90^{\circ}$ and N=2. Once again the lift coefficients for the two directions of flow are identical and gradually approach a value of about 0.2. In the case of $\alpha=30^{\circ}$, the wakes interfere in an asymmetric manner and the Strouhal number shows a strong dependence on the Keulegan-Carpenter number. Figures 63-68 show the Strouhal number as a function of K for various values of N for $\alpha=30^{\circ}$. Apparently, the Strouhal number decreases from values as large as 0.4 to about 0.15 as K increases. For spacings larger than about two diameters Strouhal number decreases to about 0.2.

VI. CONCLUSIONS

An extensive investigation of the forces acting on tube bundles and arrangements of two cylinders has warranted the following conclusions:

1. Experiments with two particular riser configurations have shown that the inertia coefficient is considerably larger than that predicted by the potential theory and shows that some fluid mass is entrapped within the bundle as a consequence of the solidification of the tube configuration.
2. For tandem arrangement of two cylinders the drag and inertia coefficients depend on both the Keulegan-Carpenter number and the relative spacing of the cylinders. As the amplitude of flow oscillation becomes comparable or smaller than the gap between the two cylinders, the drag and inertia coefficients gradually approach those corresponding to an isolated cylinder, i.e., the wakes of the two cylinders do not interfere with each other.
3. The drag and inertia coefficients for the side-by-side arrangement exhibit a similar behavior. For a relative spacing larger than about 2.5 diameters, the cylinders behave as if they were independent.
4. The quantification of the lift force for an arbitrary arrangement requires four different lift coefficients,

depending on the direction of the flow and the direction of the force. These coefficients have been evaluated and it has been shown that the effect of cylinder-cylinder proximity is confined to relatively small spacings and angular positions.

5. The Strouhal number for practically all two-cylinder arrangements remained nearly constant at about 0.2. Only in the case of 30° orientation did the strong asymmetric interference of the cylinder wakes result in a Keulegan-Carpenter-number dependent Strouhal number, ranging from 0.4 to 0.2. However, as the spacing increased the Strouhal number again approached a mean value of 0.2.

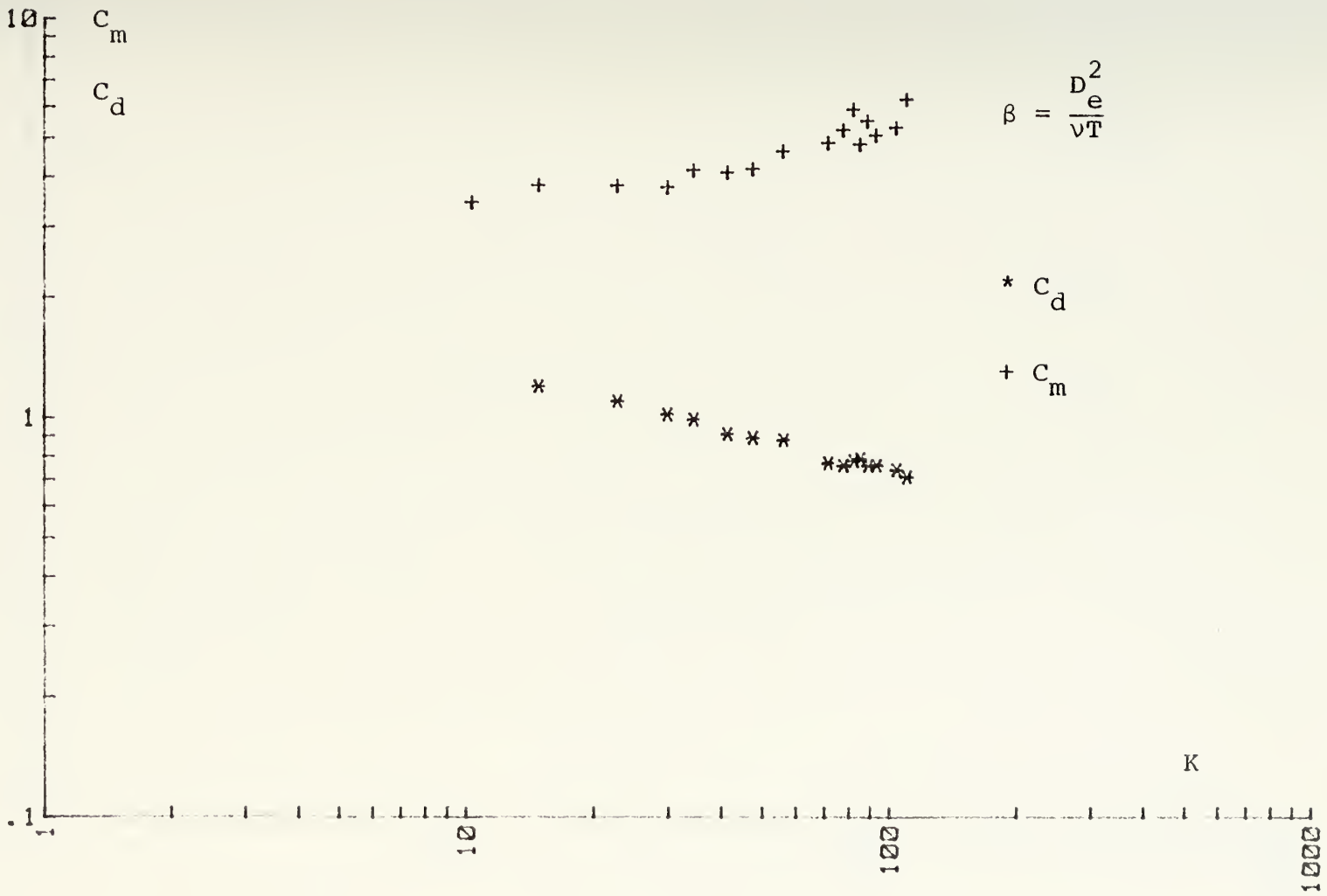

Fig. 7a C_m and C_d versus K for riser 1

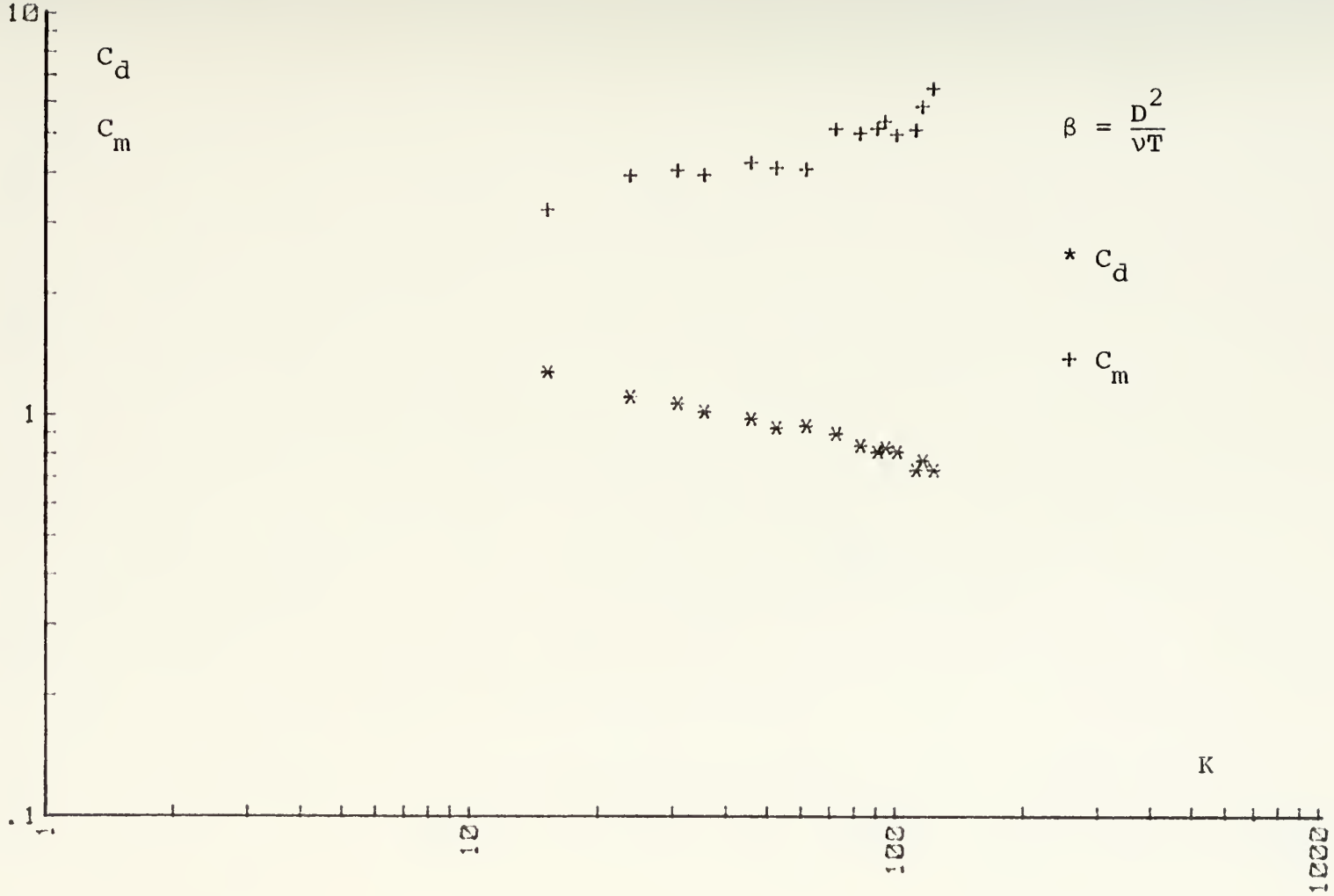

Fig. 7b C_m and C_d versus K for riser 2

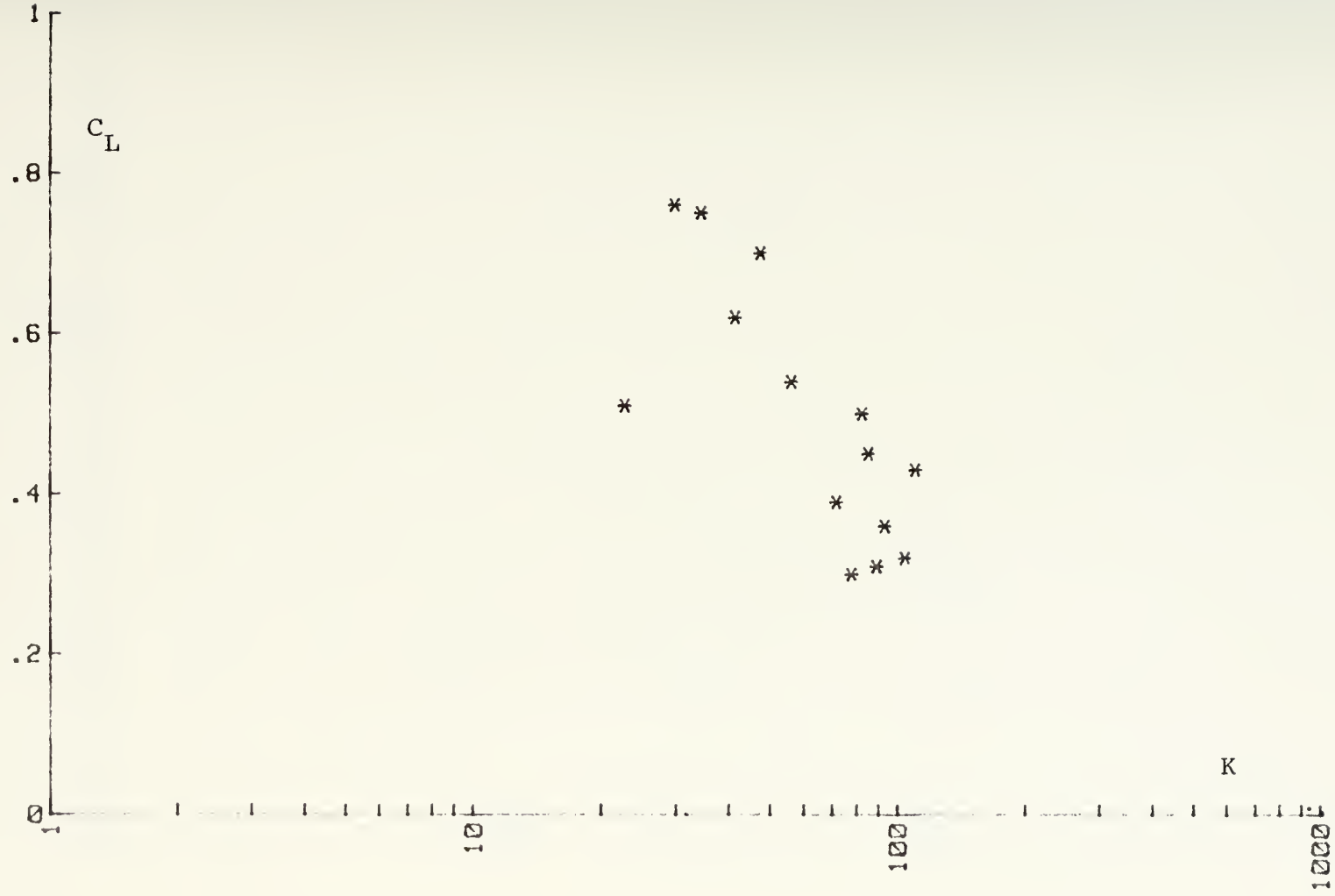

Fig. 7c C_L vs K for riser 1

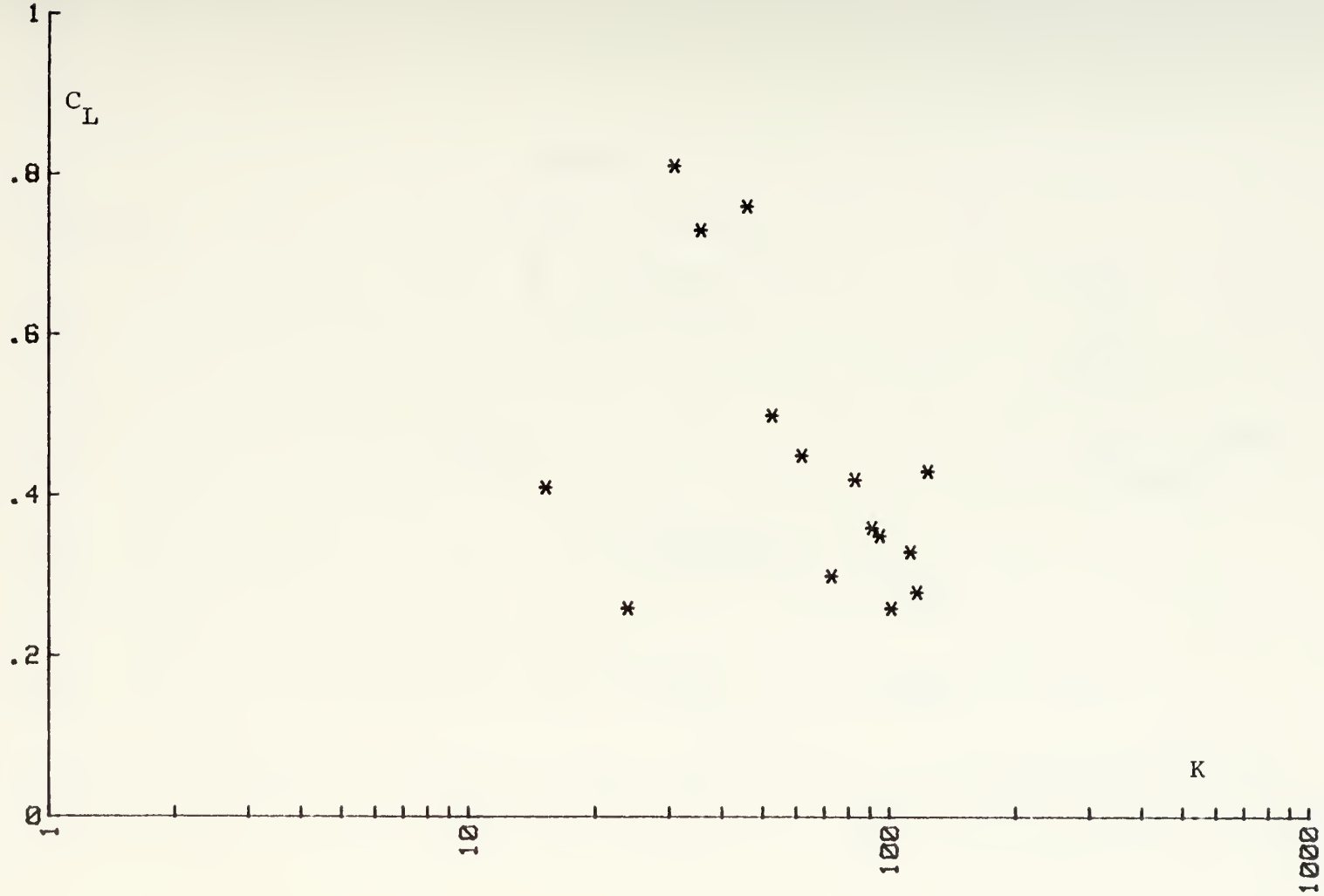

Fig. 7d C_L vs K for riser 2

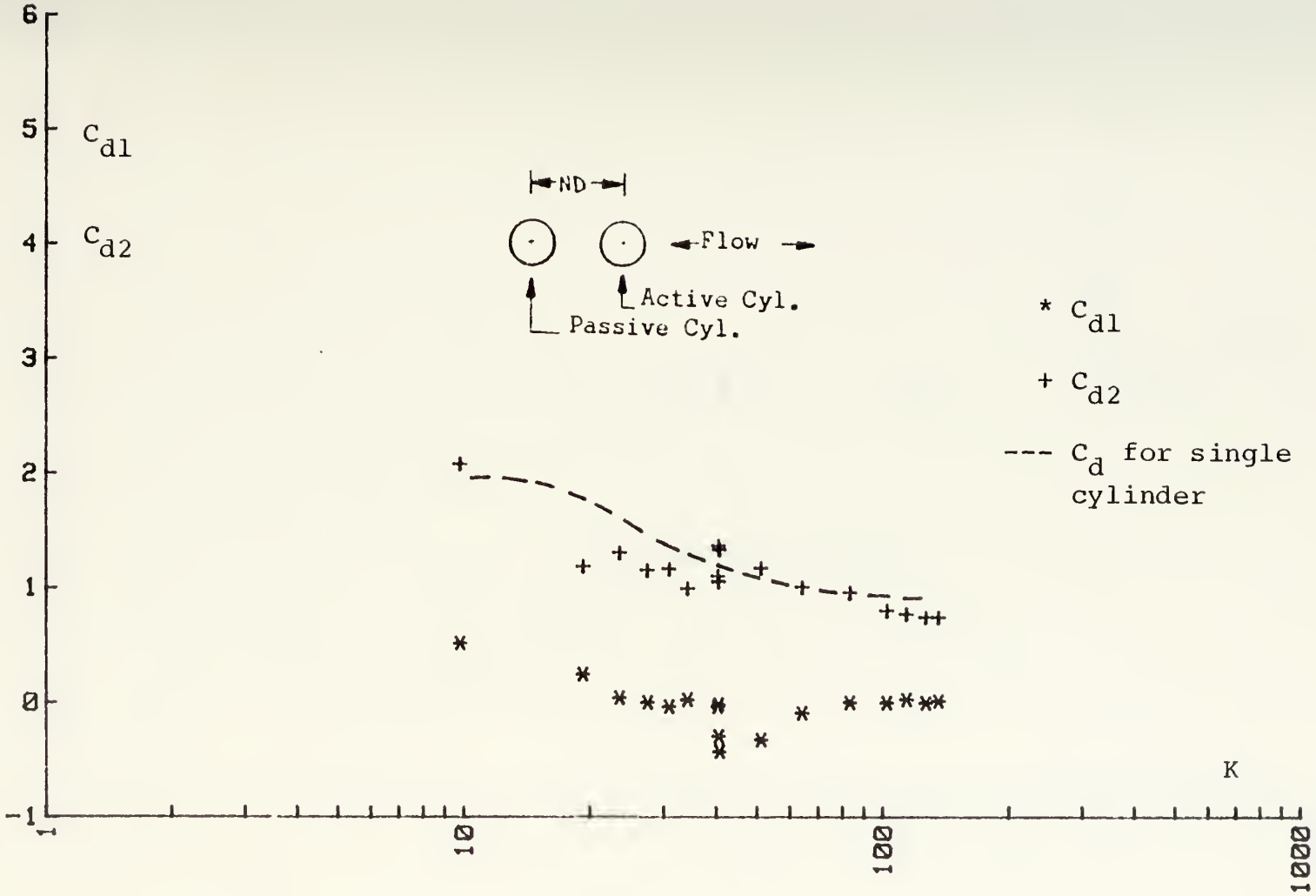

Fig. 8a C_{d1} and C_{d2} versus K for N=1.5 and $\alpha=0^o$

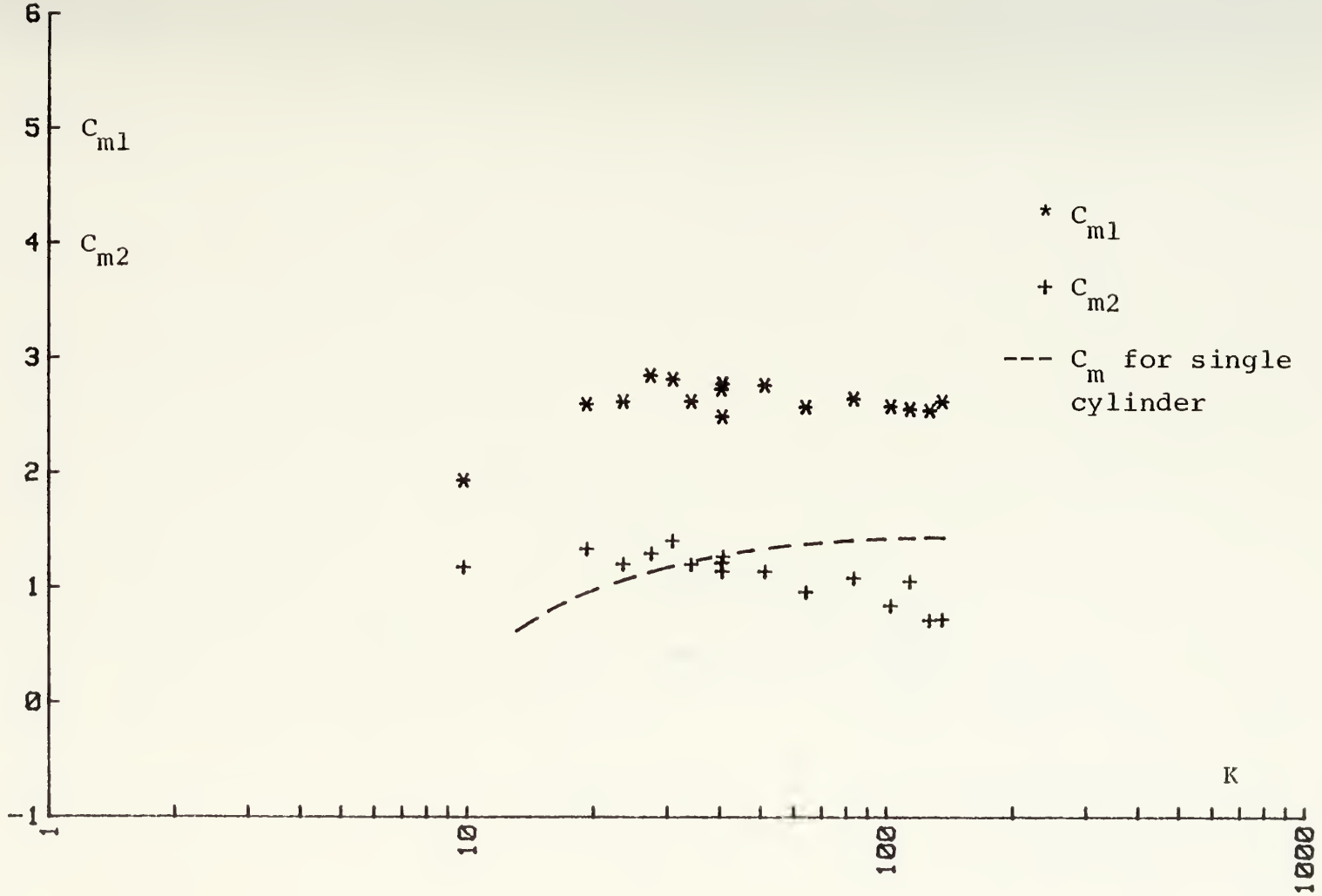

Fig. 8b C_{m1} and C_{m2} versus K for N-1.5 and $\alpha=0^{\circ}$

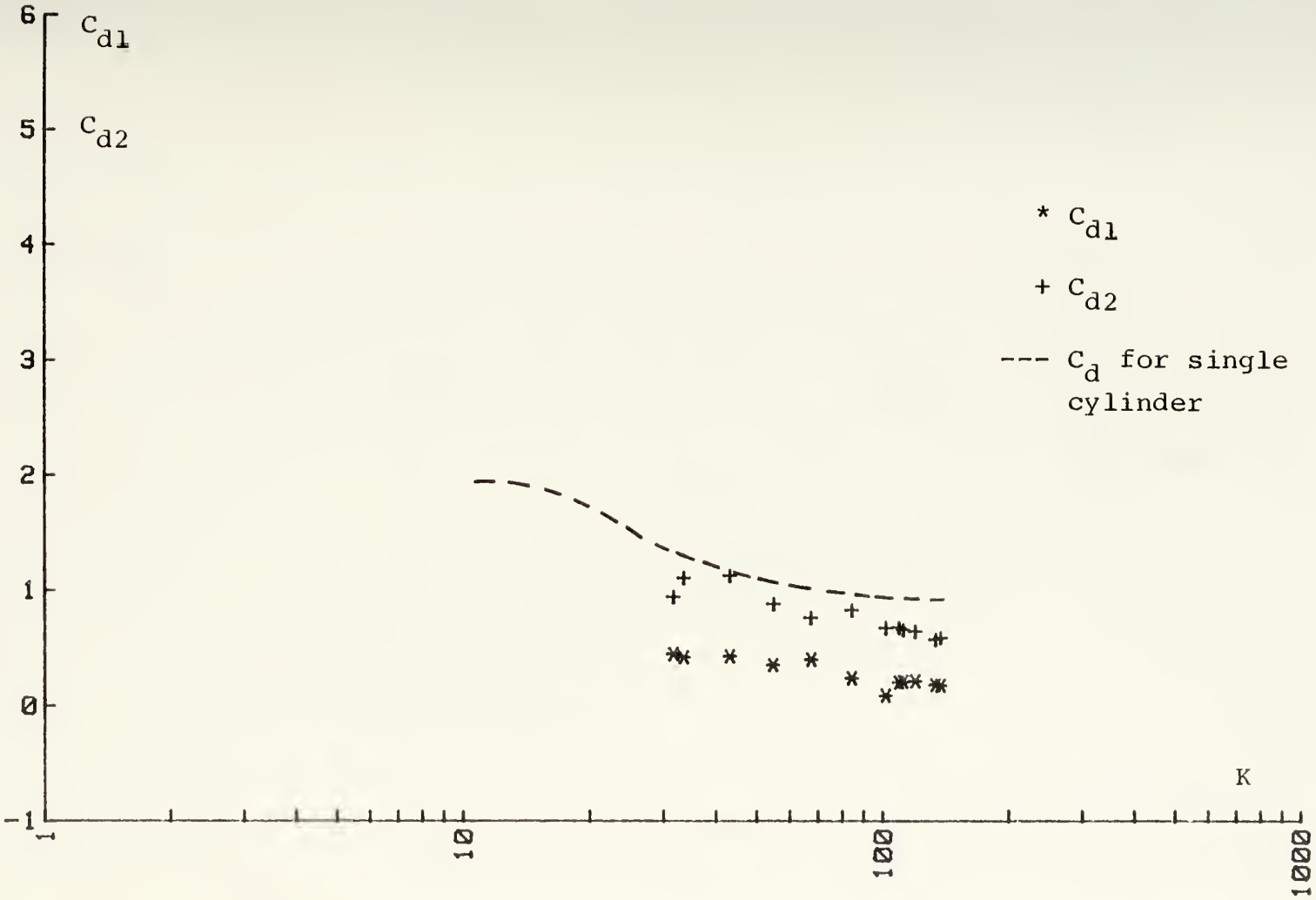

Fig. 9a C_{d1} and C_{d2} versus K for N=2 and $\alpha = 0^{o}$

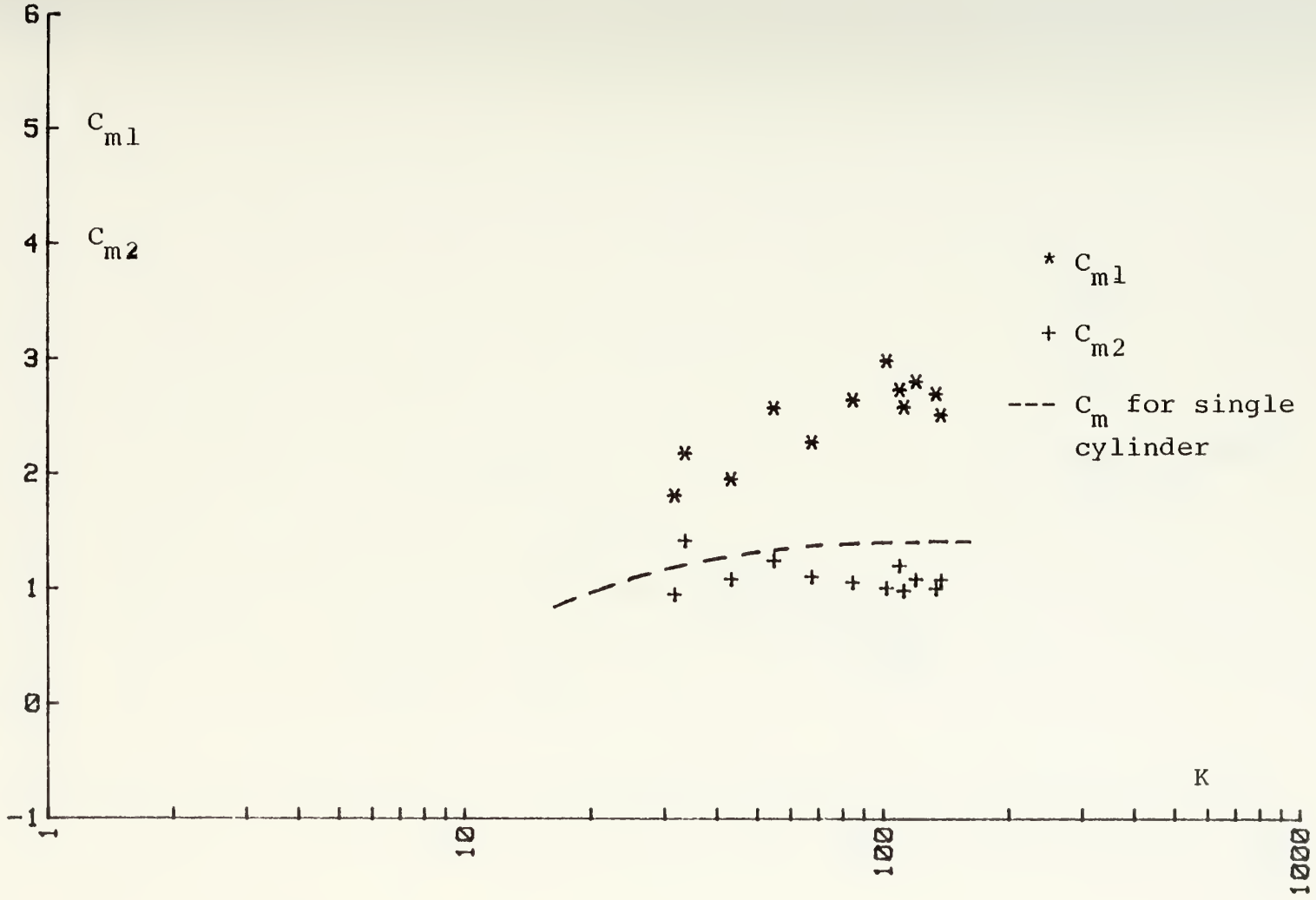

Fig. 9b C_{m1} and C_{m2} versus K for N=2 and $\alpha=0^{o}$

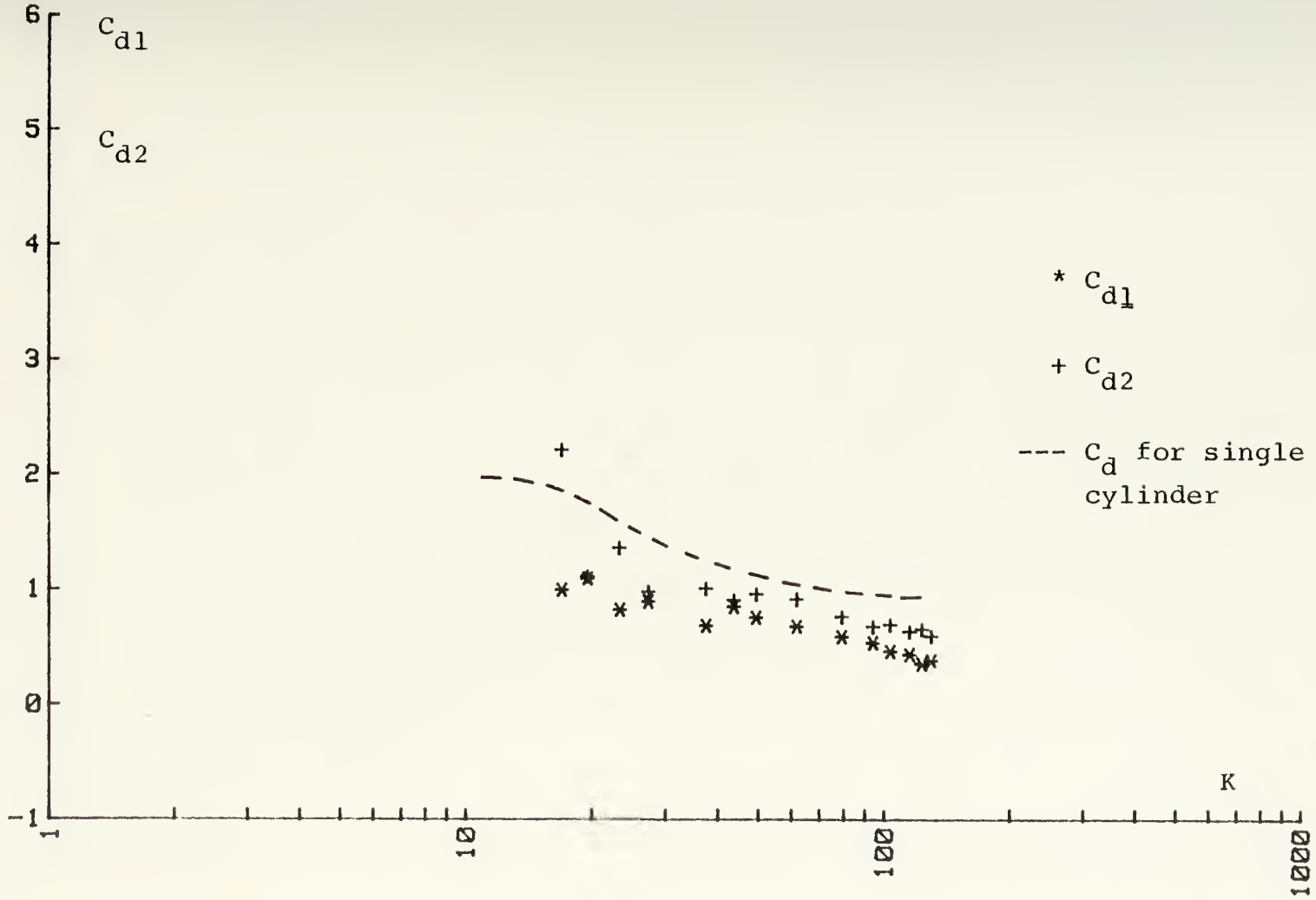

Fig. 10a C_{d1} and C_{d2} versus K for N=2.5 and $\alpha=0^{o}$

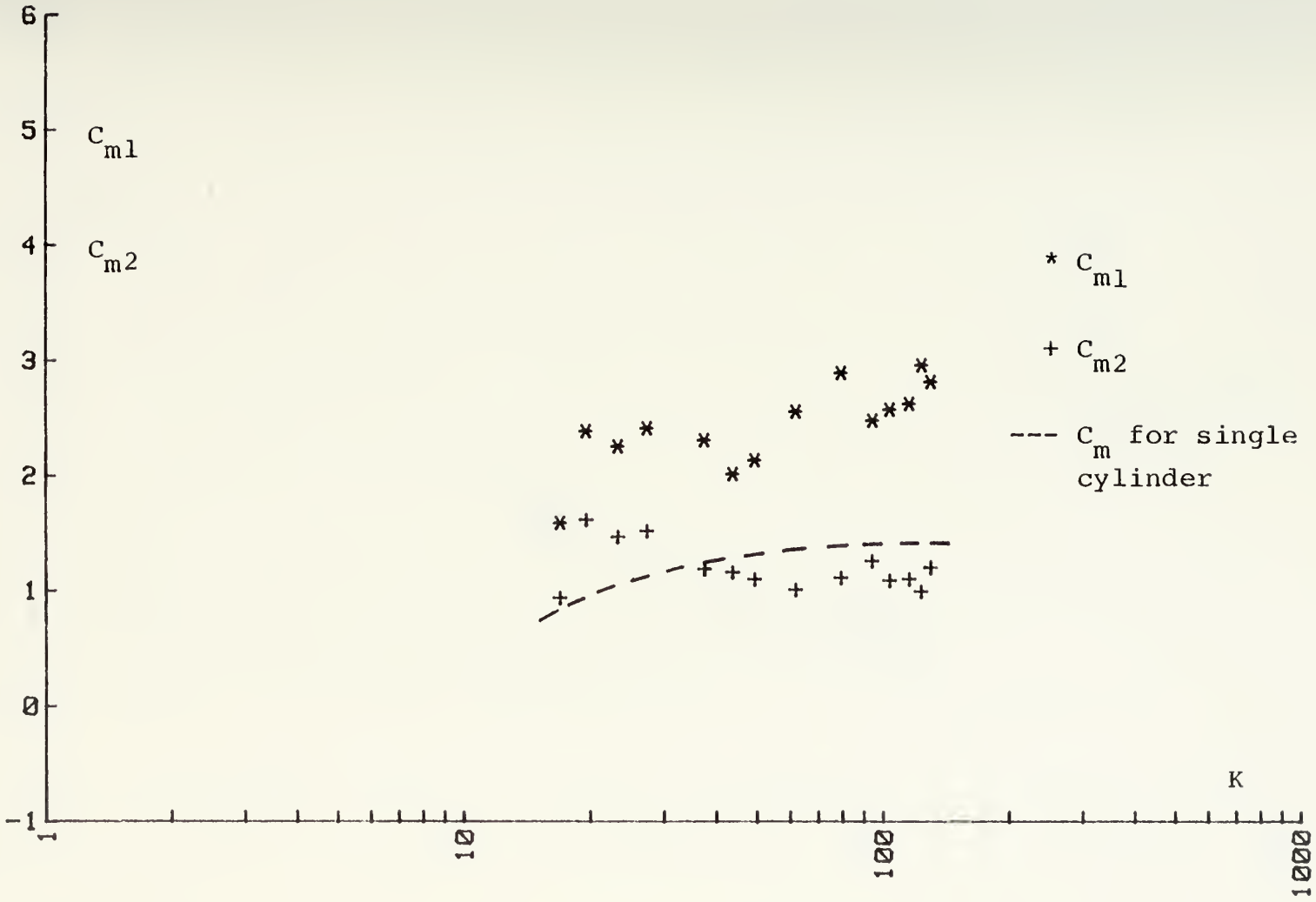

Fig. 10b C_{m1} and C_{m2} versus K for N=2.5 and $\alpha=0^{o}$

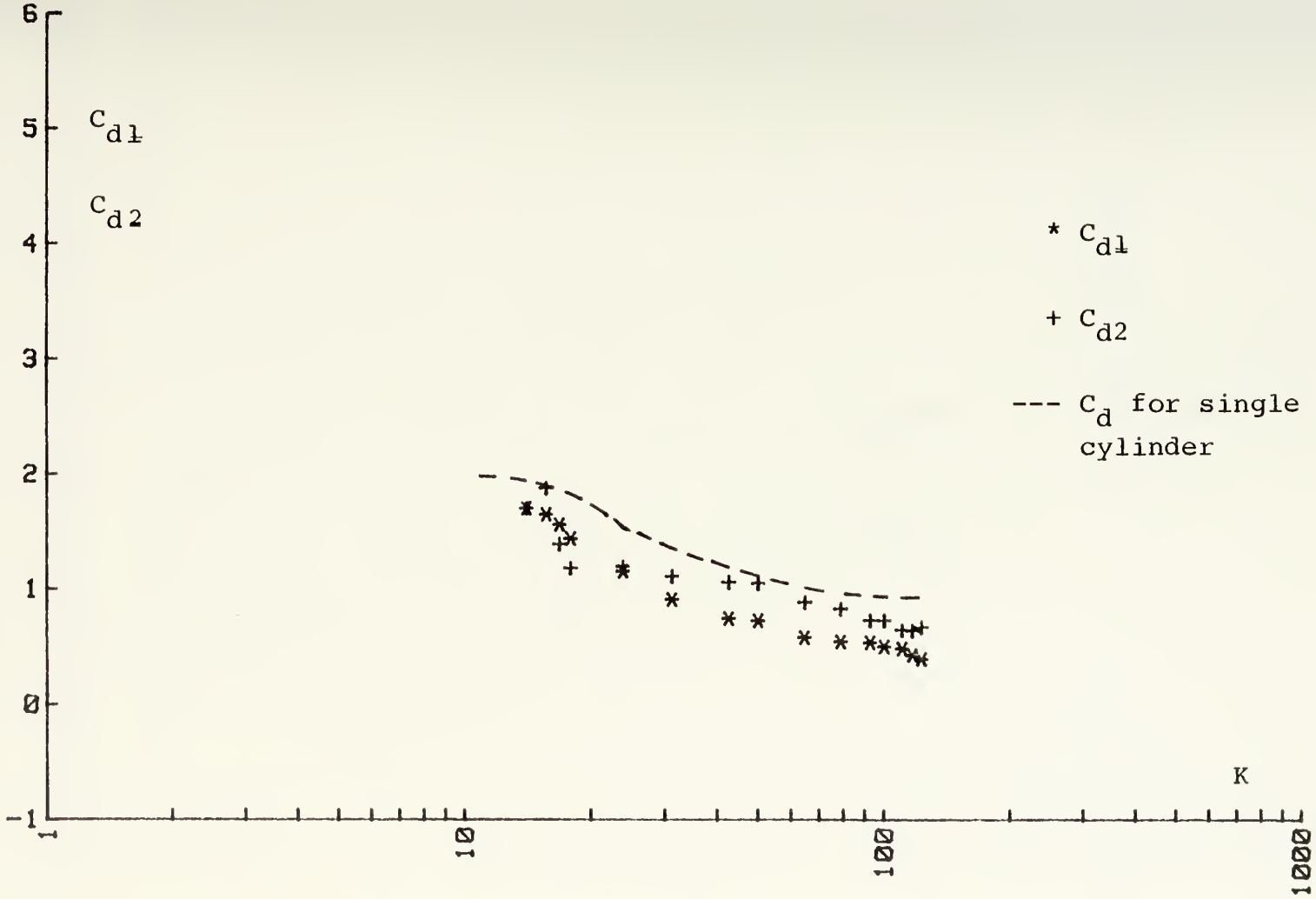

Fig. 11a C_{d1} and C_{d2} versus K for N=3.5 and $\alpha=0^{o}$

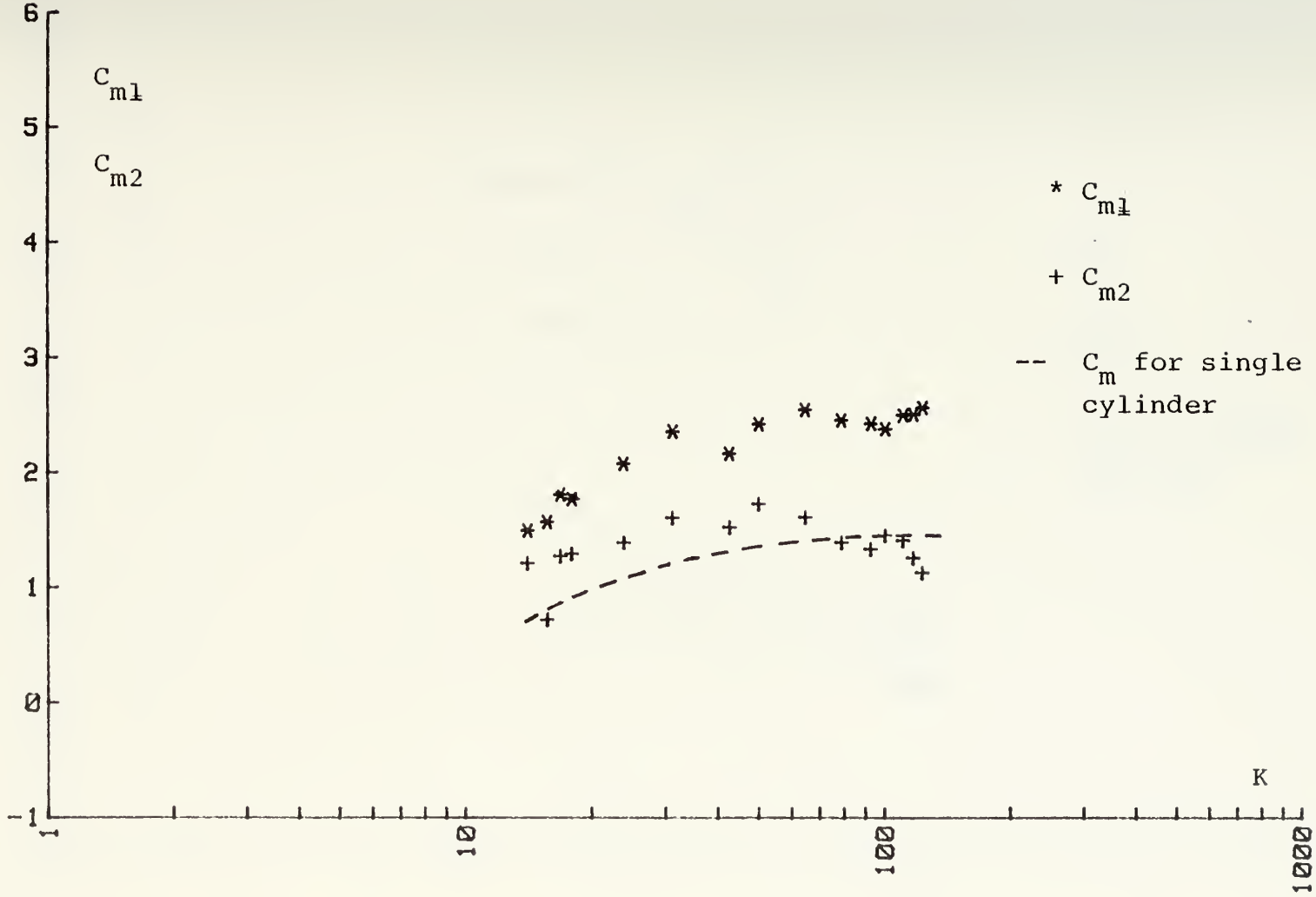

Fig. 11b C_{m1} and C_{m2} versus K for N=3.5 and $\alpha=0^{o}$

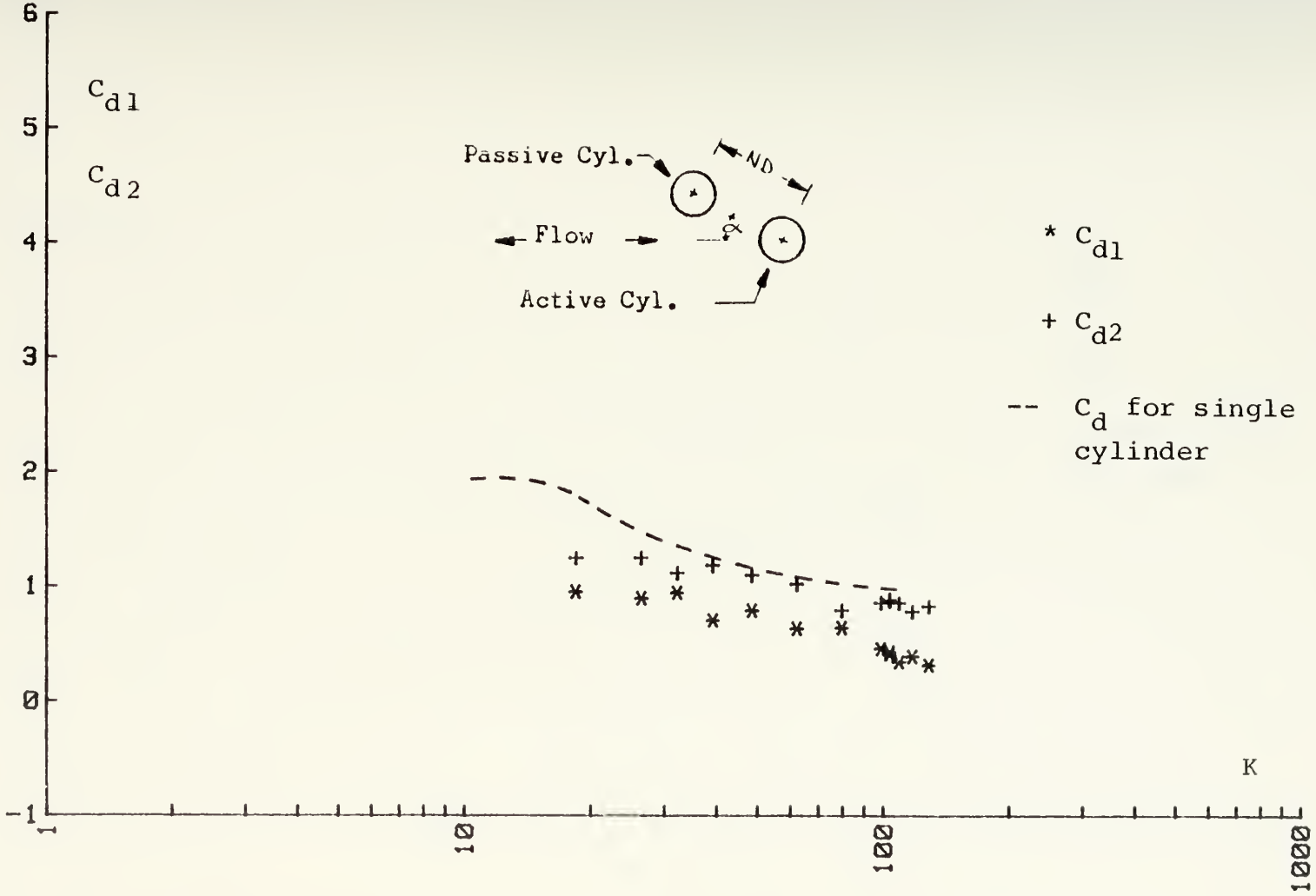

Fig. 12a C_{d1} and C_{d2} versus K for N=1.5 and $\alpha=30^{o}$

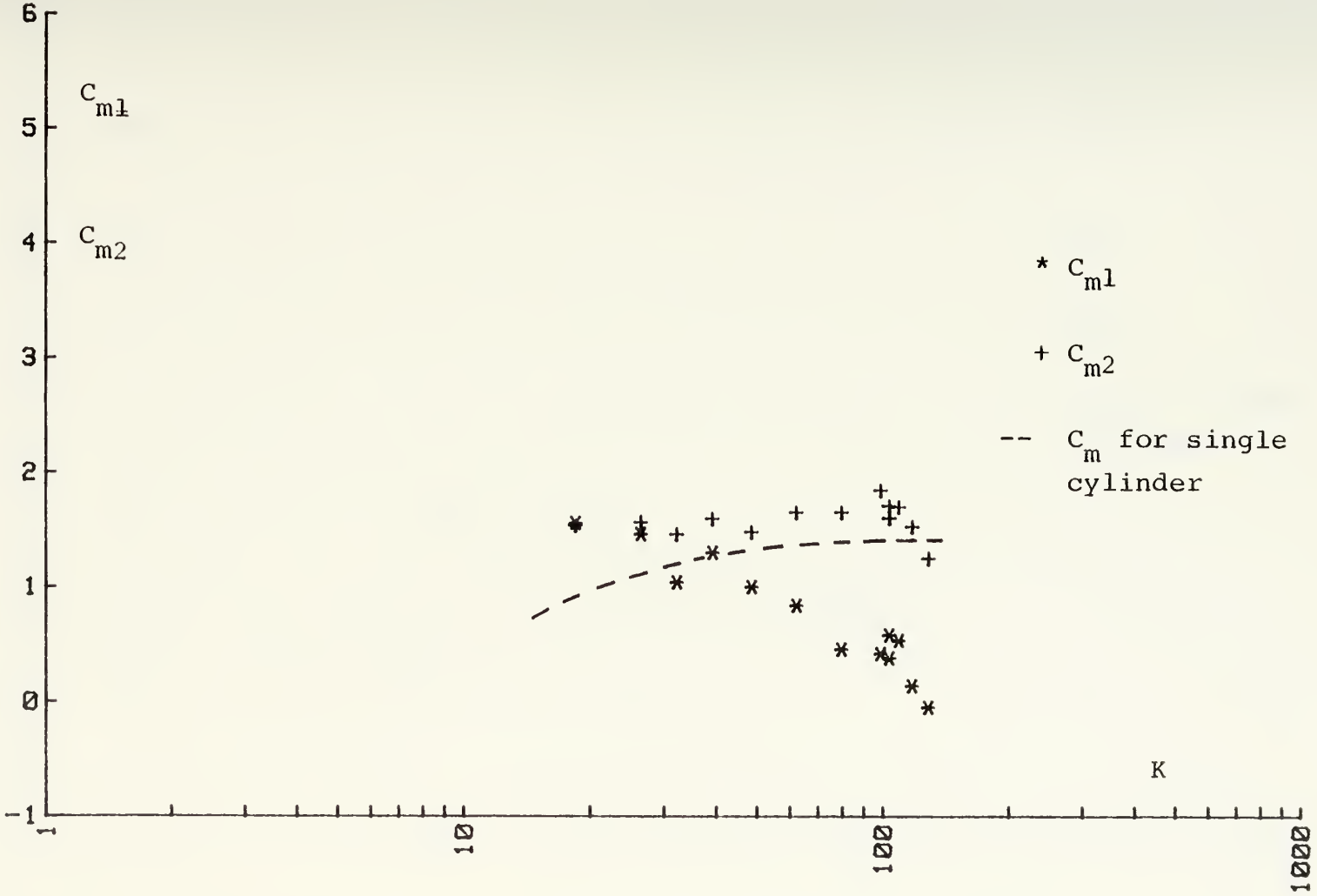

Fig. 12b C_{m1} and C_{m2} versus K for N=1.5 and $\alpha=30^{o}$

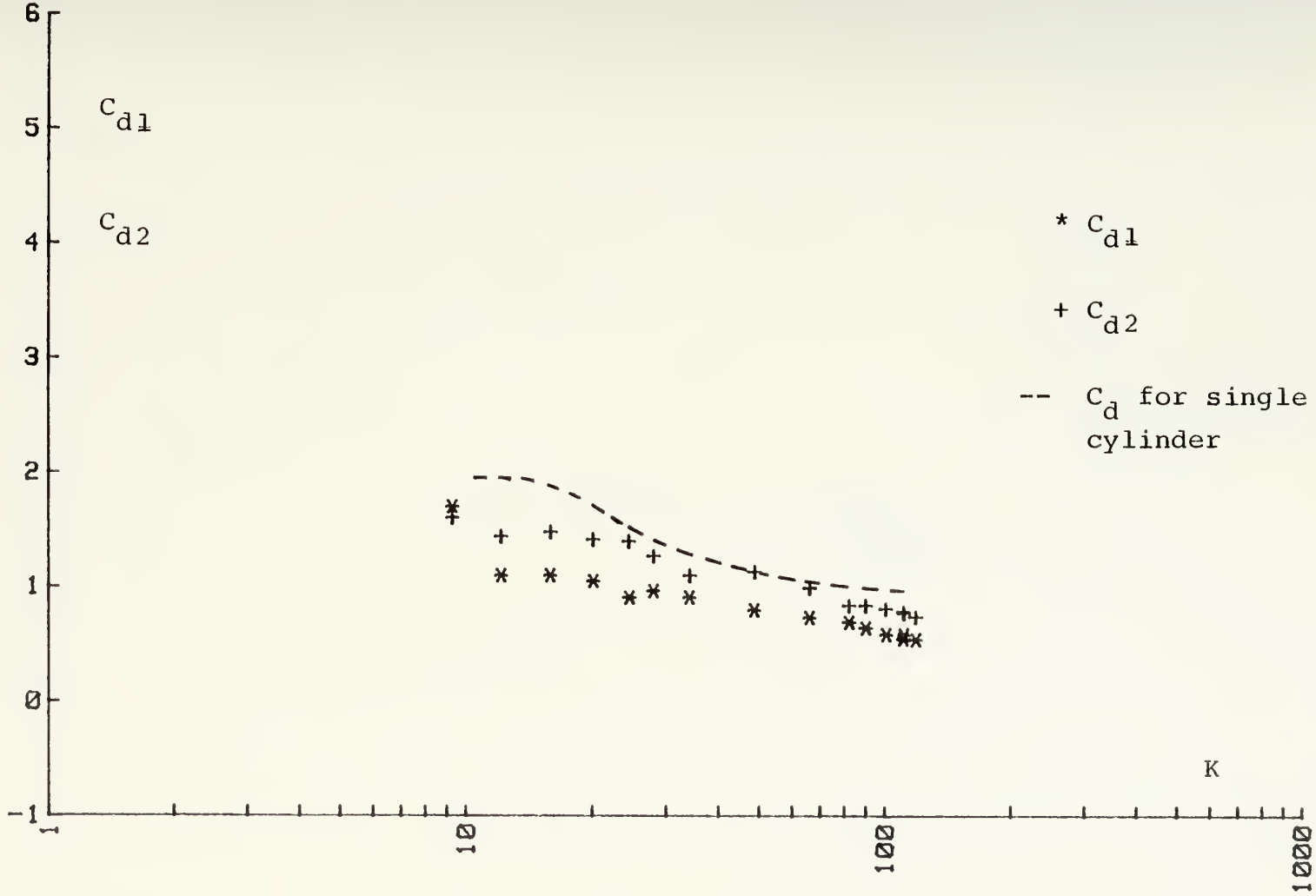

Fig. 13a C_{d1} and C_{d2} versus K for N=2 and $\alpha=30^{o}$

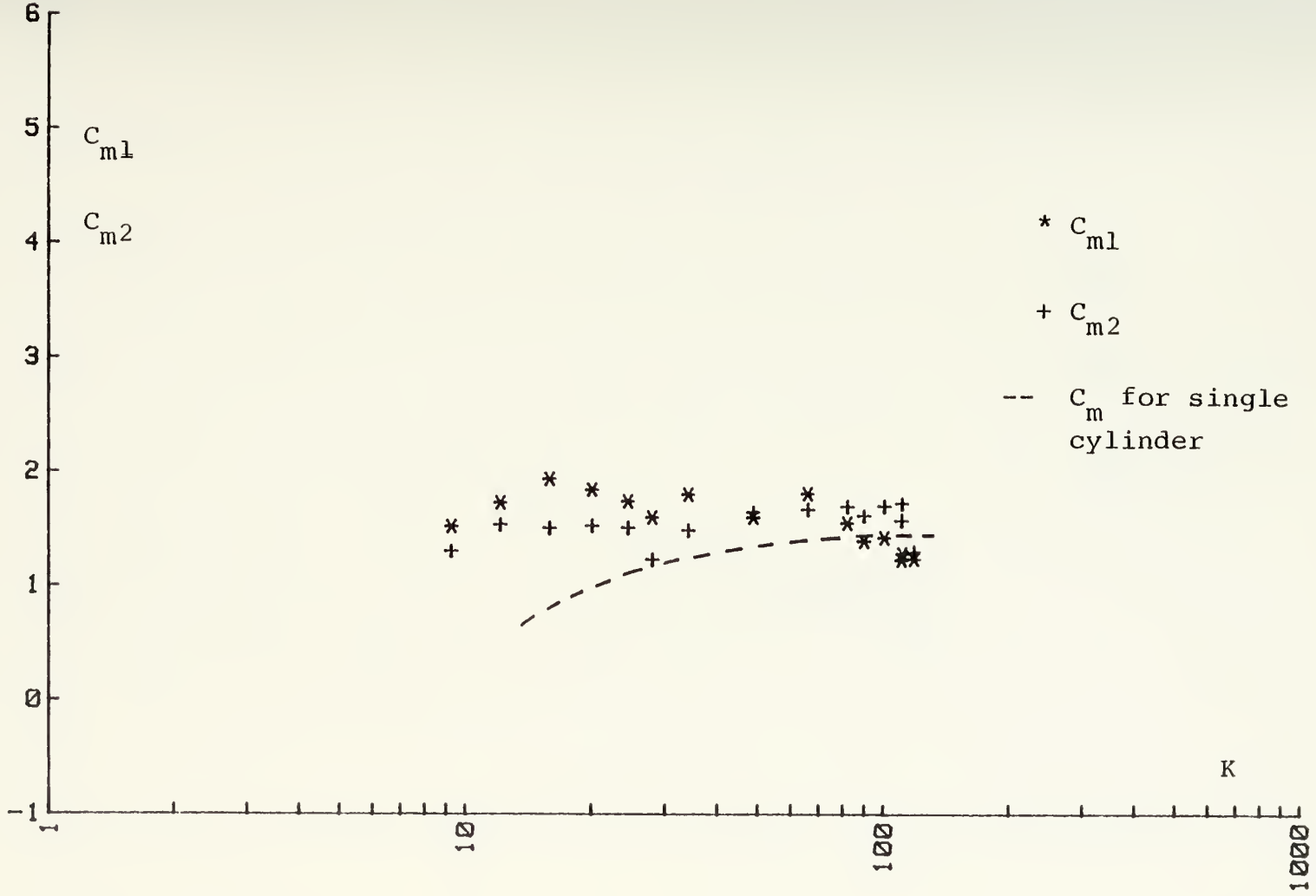

Fig. 13b C_{m1} and C_{m2} versus K for N=2 and $\alpha=30^{o}$

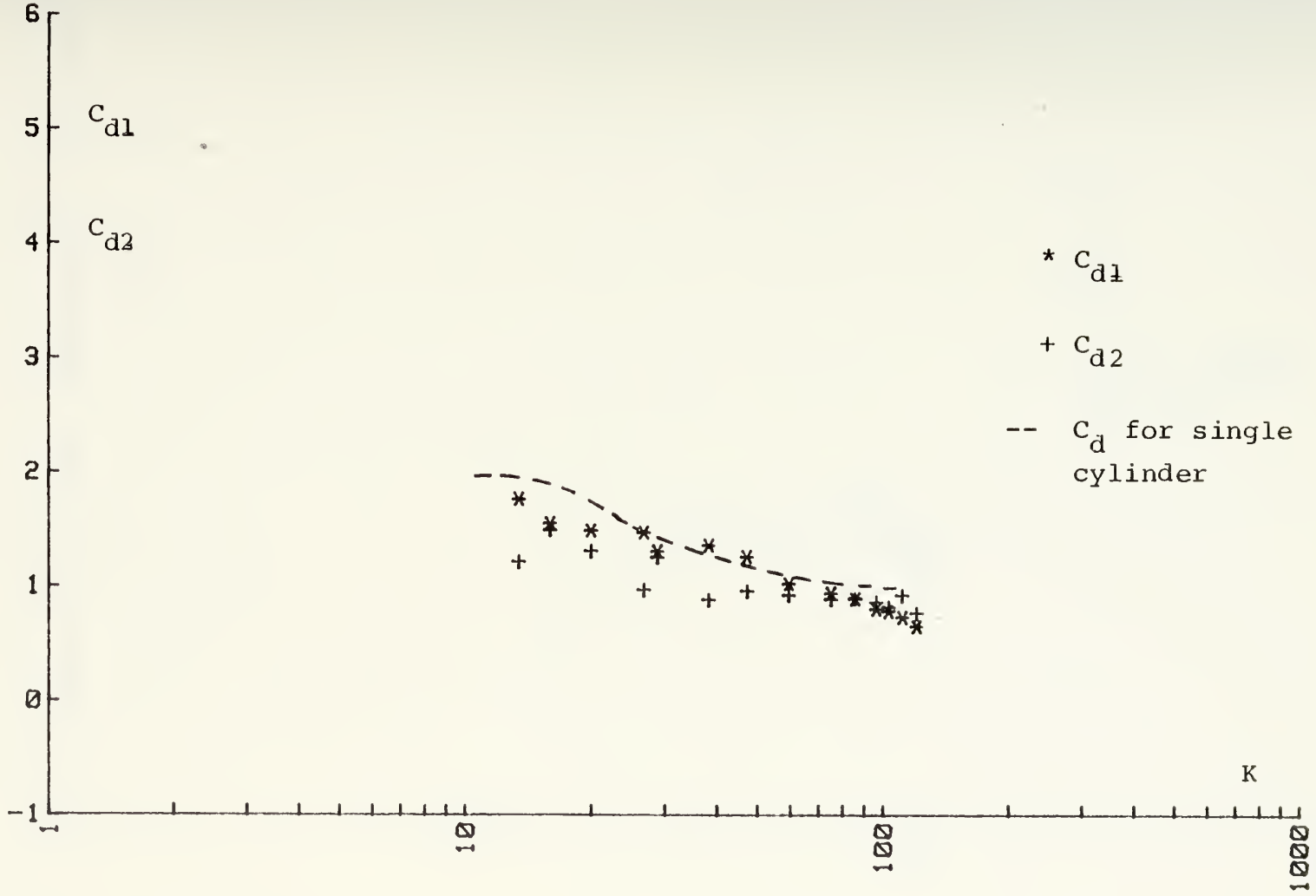

Fig. 14a C_{d1} and C_{d2} versus K for N=2.5 and $\alpha=30^{o}$

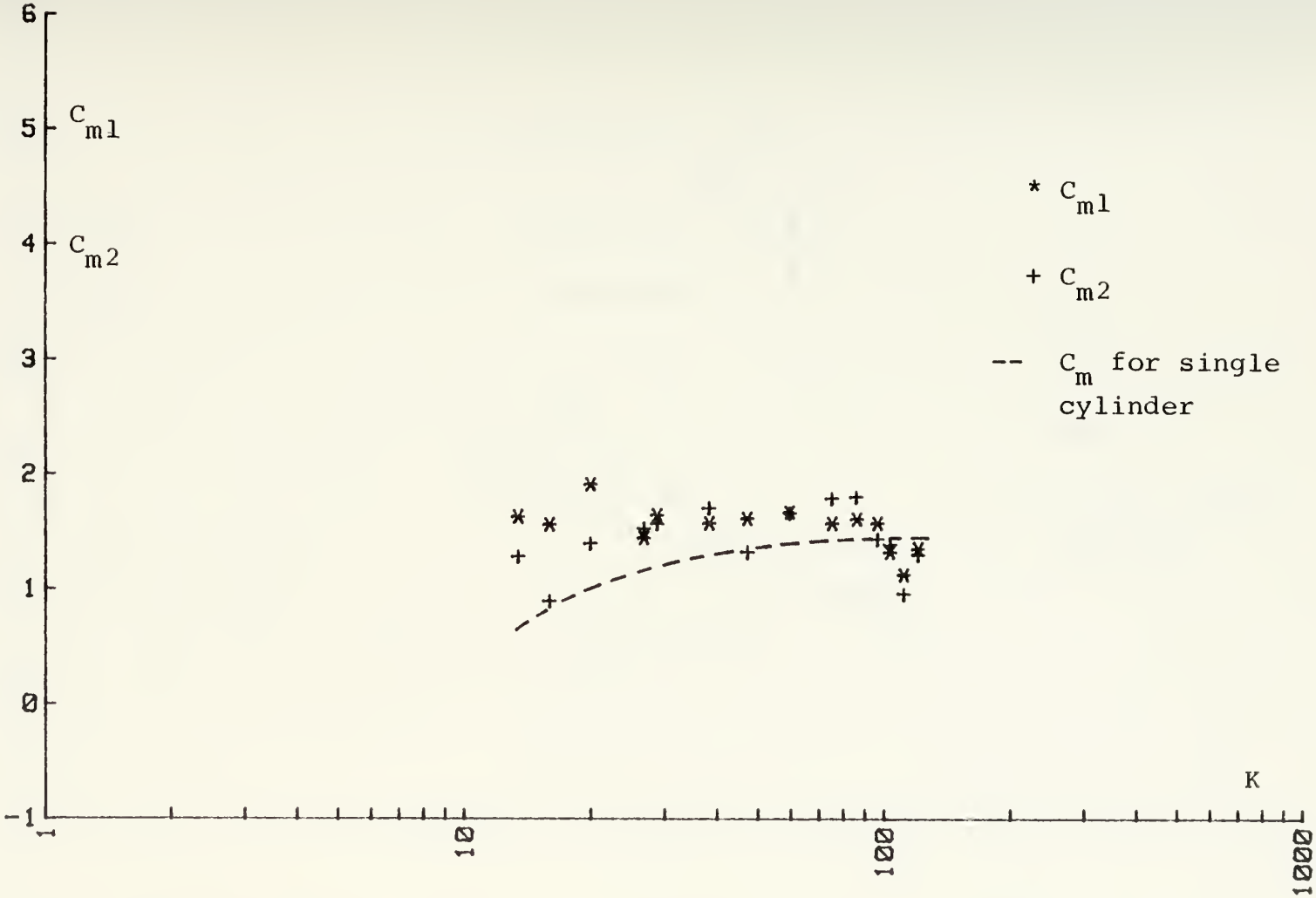

Fig. 14b C_{m1} and C_{m2} versus K for N=2.5 and $\alpha=30^{o}$

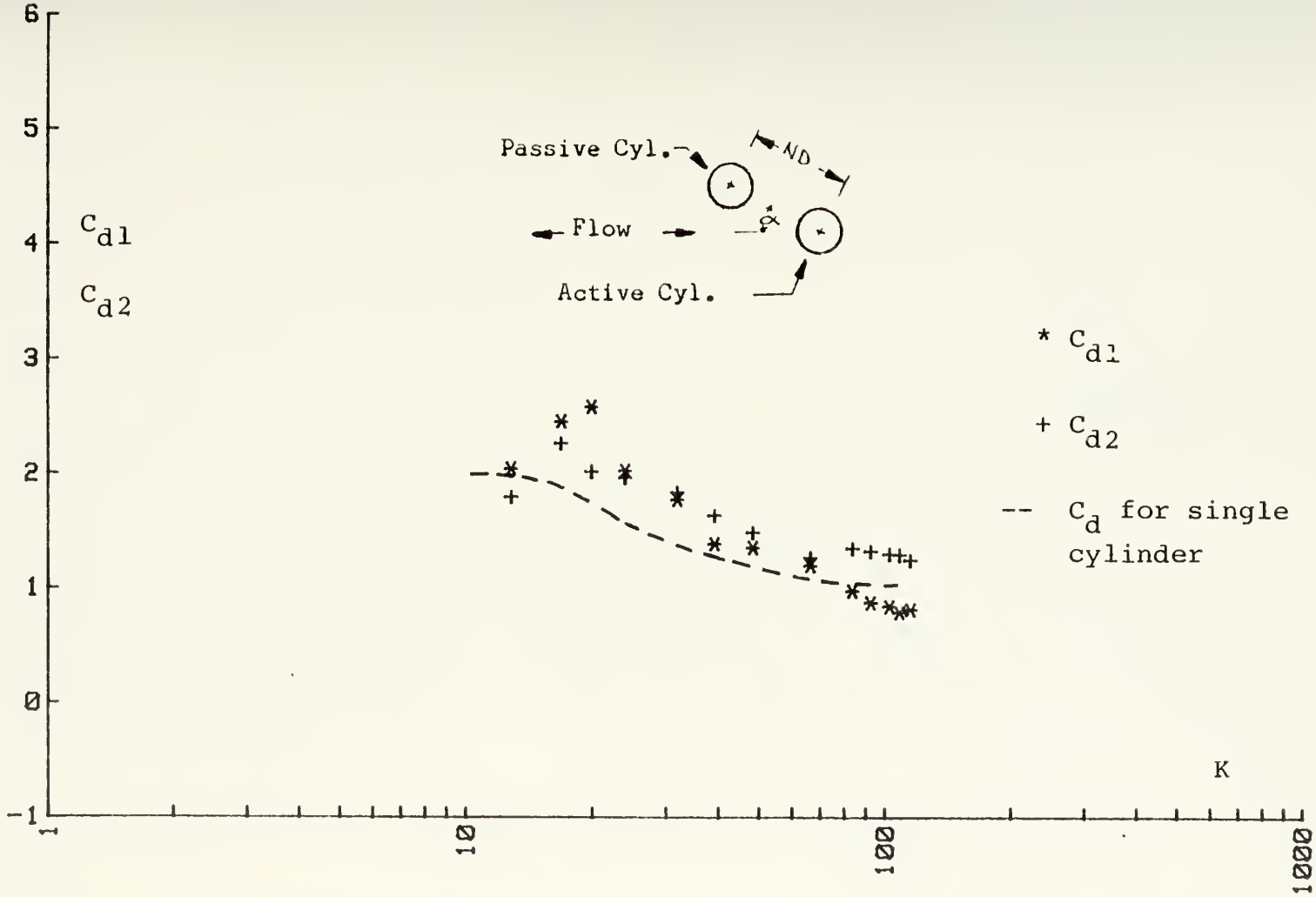

Fig. 15a C_{d1} and C_{d2} versus K for N=1.5 and $\alpha=60^{o}$

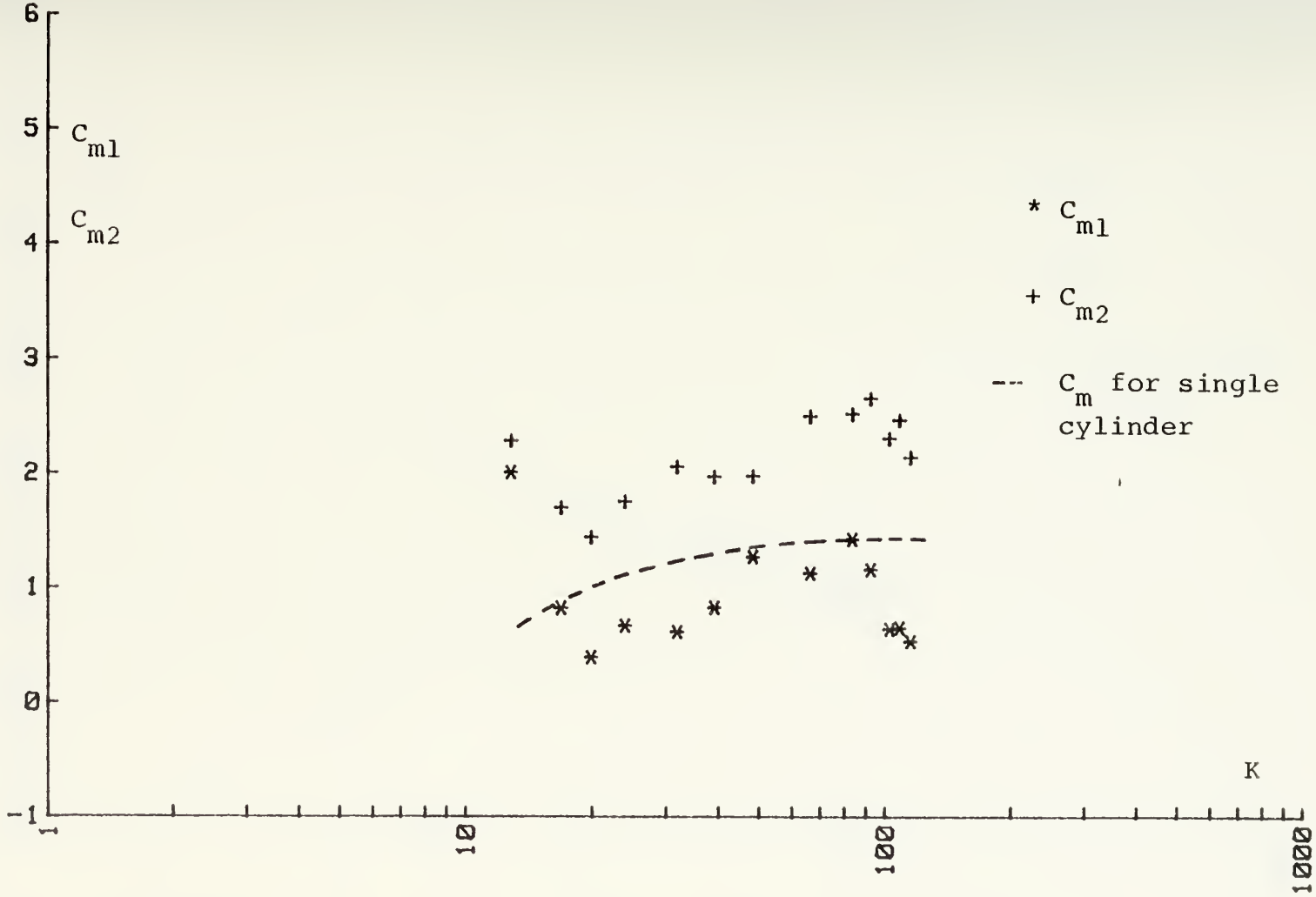

Fig. 15b C_{m1} and C_{m2} versus K for N=1.5 and $\alpha=60^{o}$

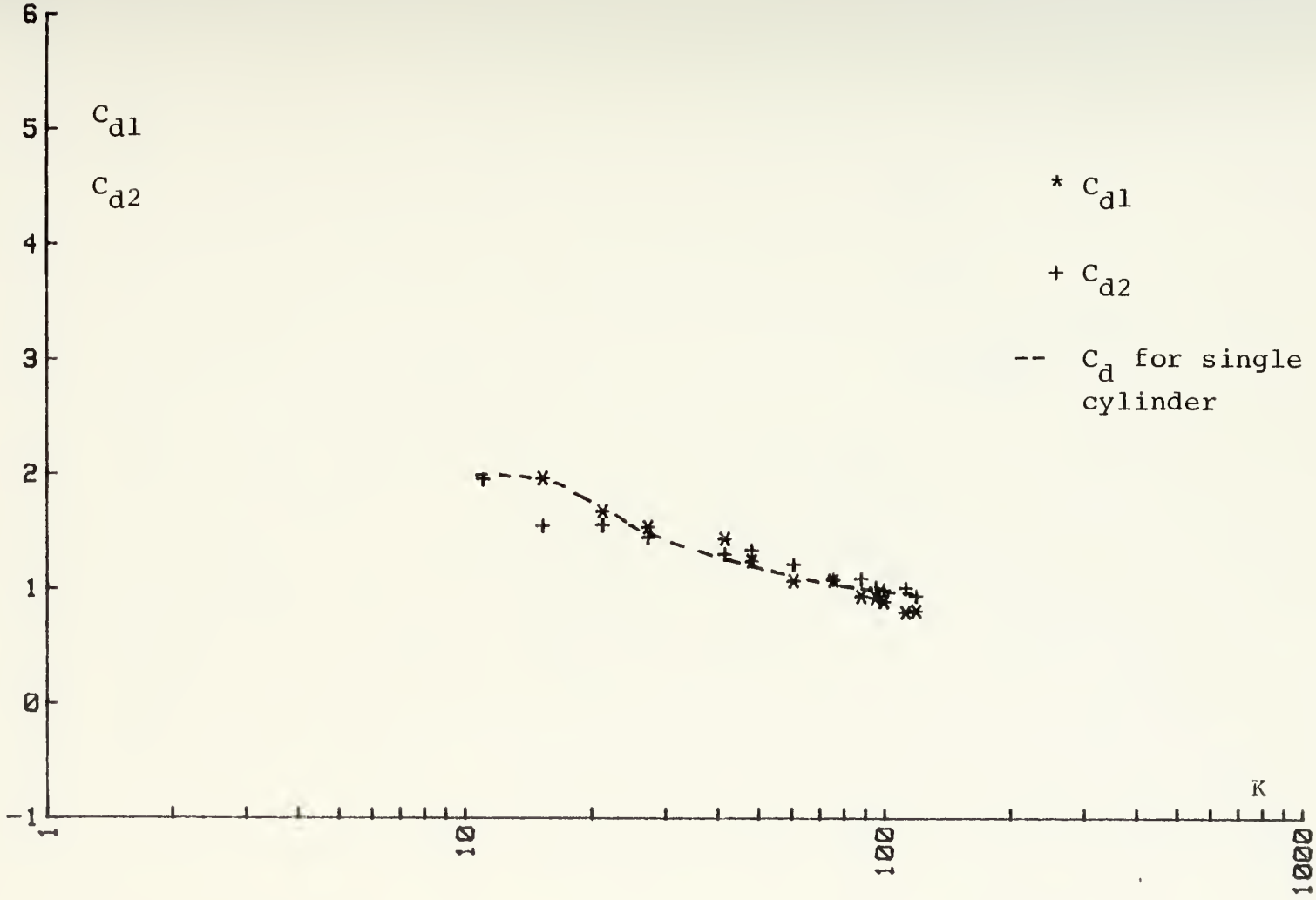

Fig. 16a C_{d1} and C_{d2} versus K for N=2 and $\alpha=60^{o}$

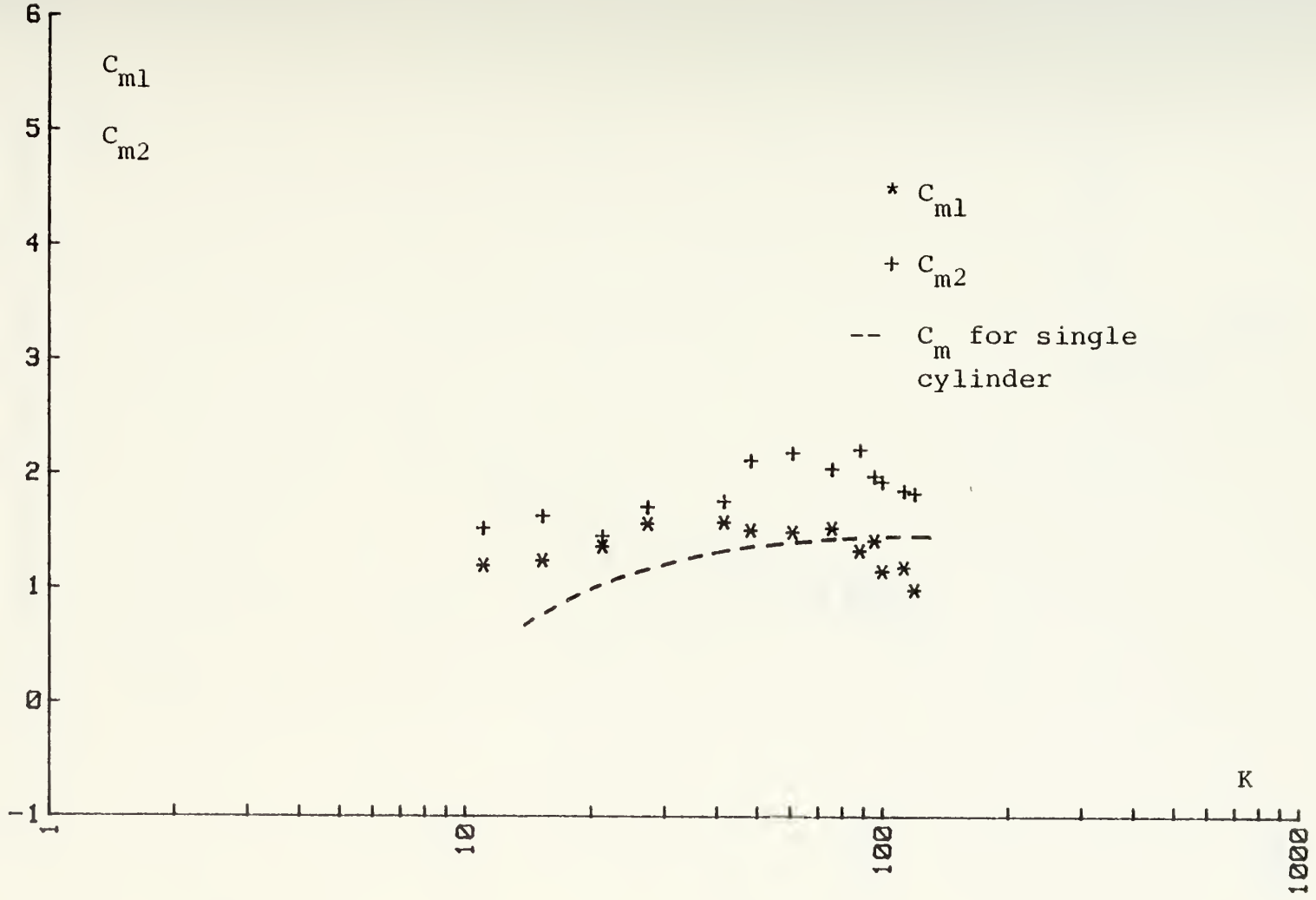

Fig. 16b C_{m1} and C_{m2} versus K for N=2 and $\alpha=60^{o}$

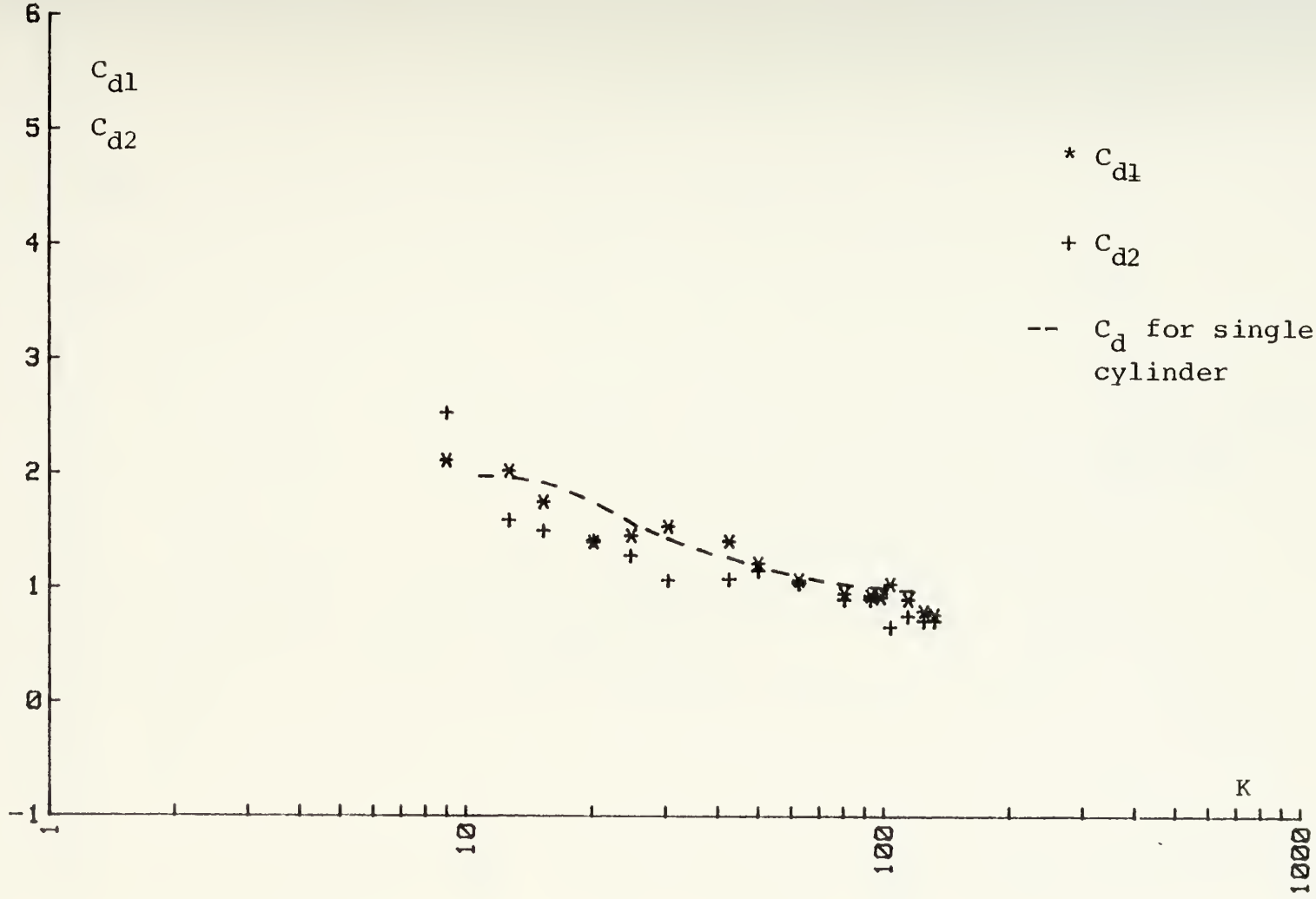

Fig. 17a C_{d1} and C_{d2} versus K for N=2.5 and $\alpha=60^{o}$

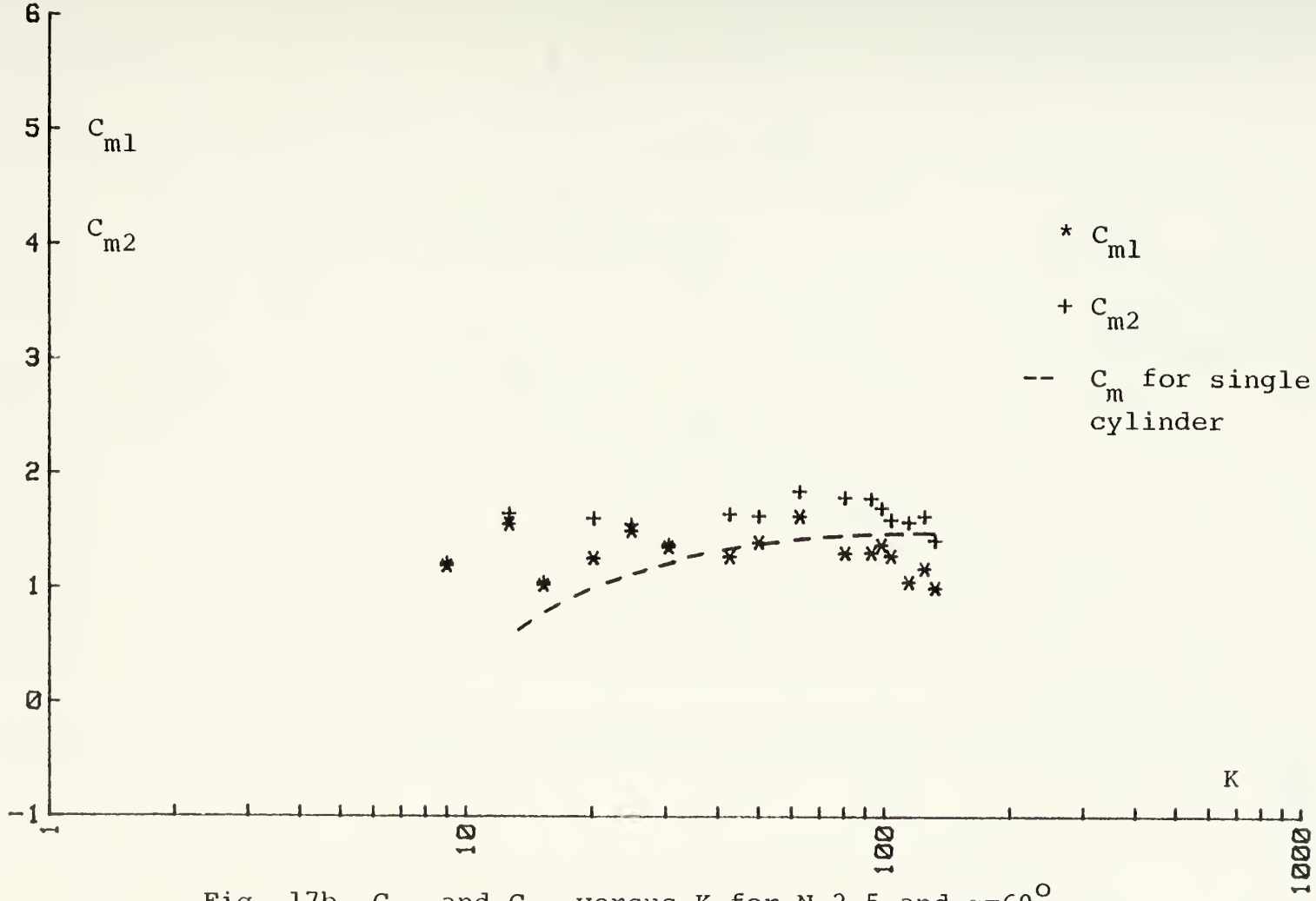

Fig. 17b C_{m1} and C_{m2} versus K for N-2.5 and $\alpha=60^{o}$

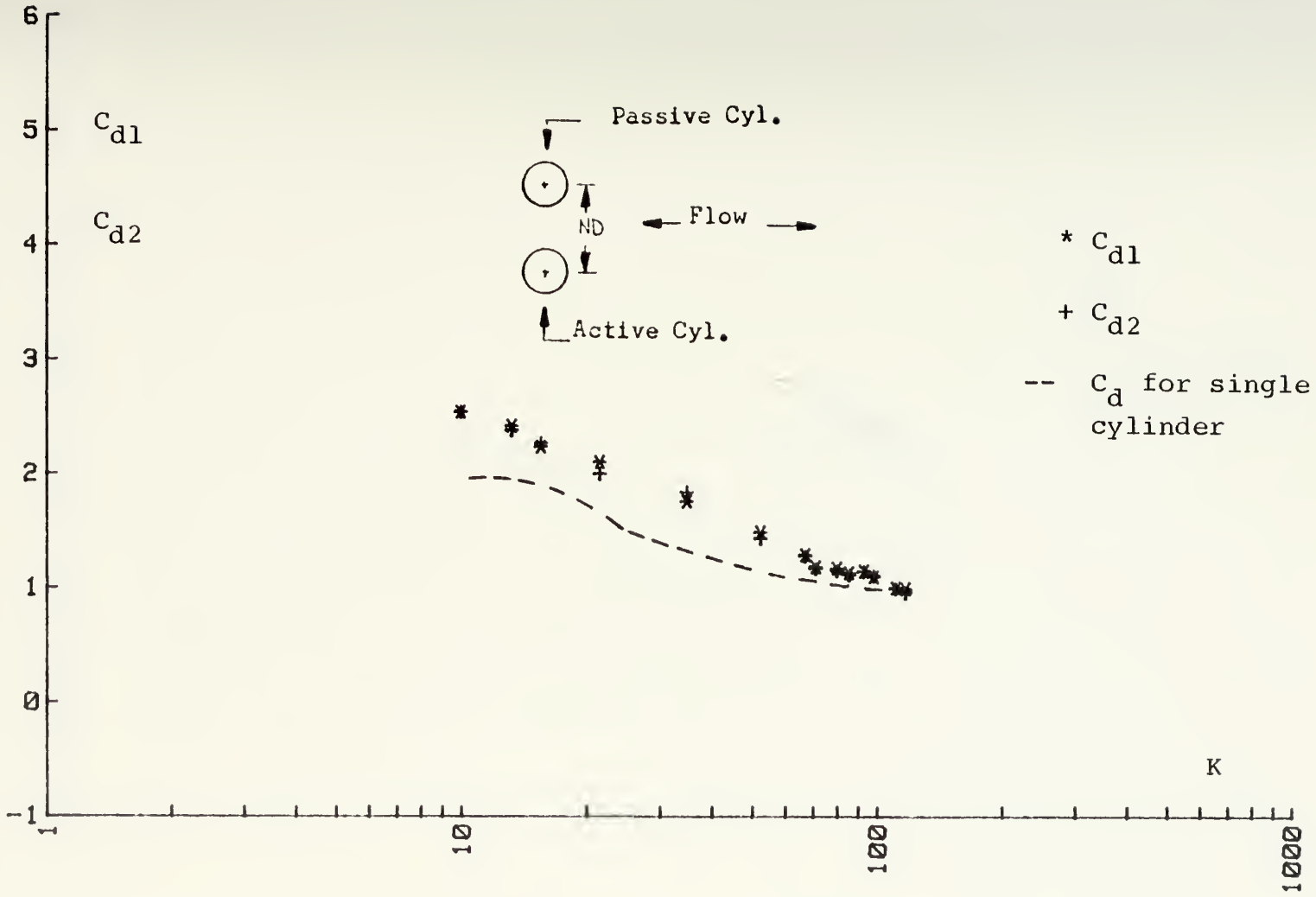

Fig. 18a C_{d1} and C_{d2} versus K for N=1.5 and $\alpha=90^{o}$

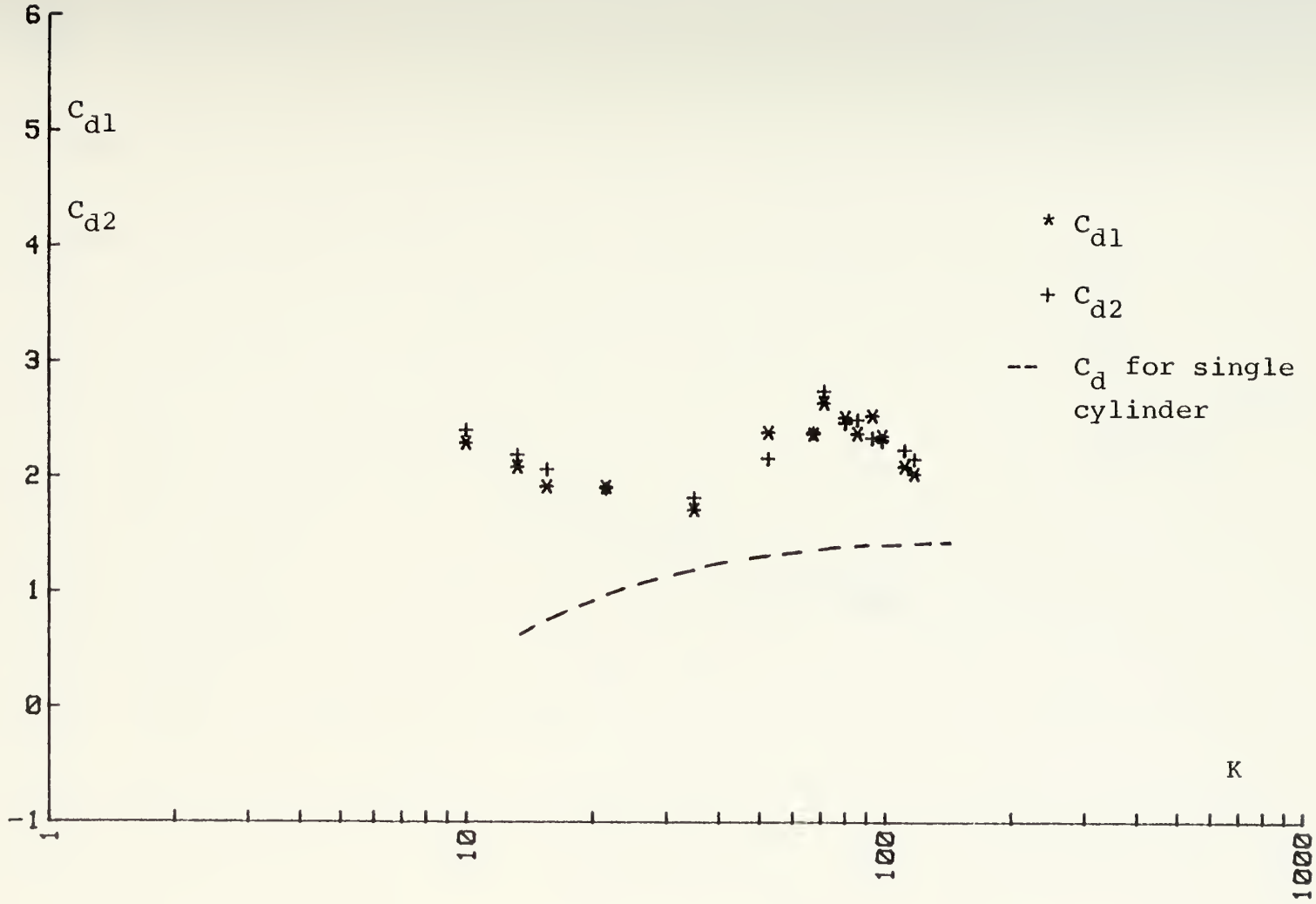

Fig. 18b C_{d1} and C_{d2} versus K for N=1.5 and $\alpha=90^{o}$

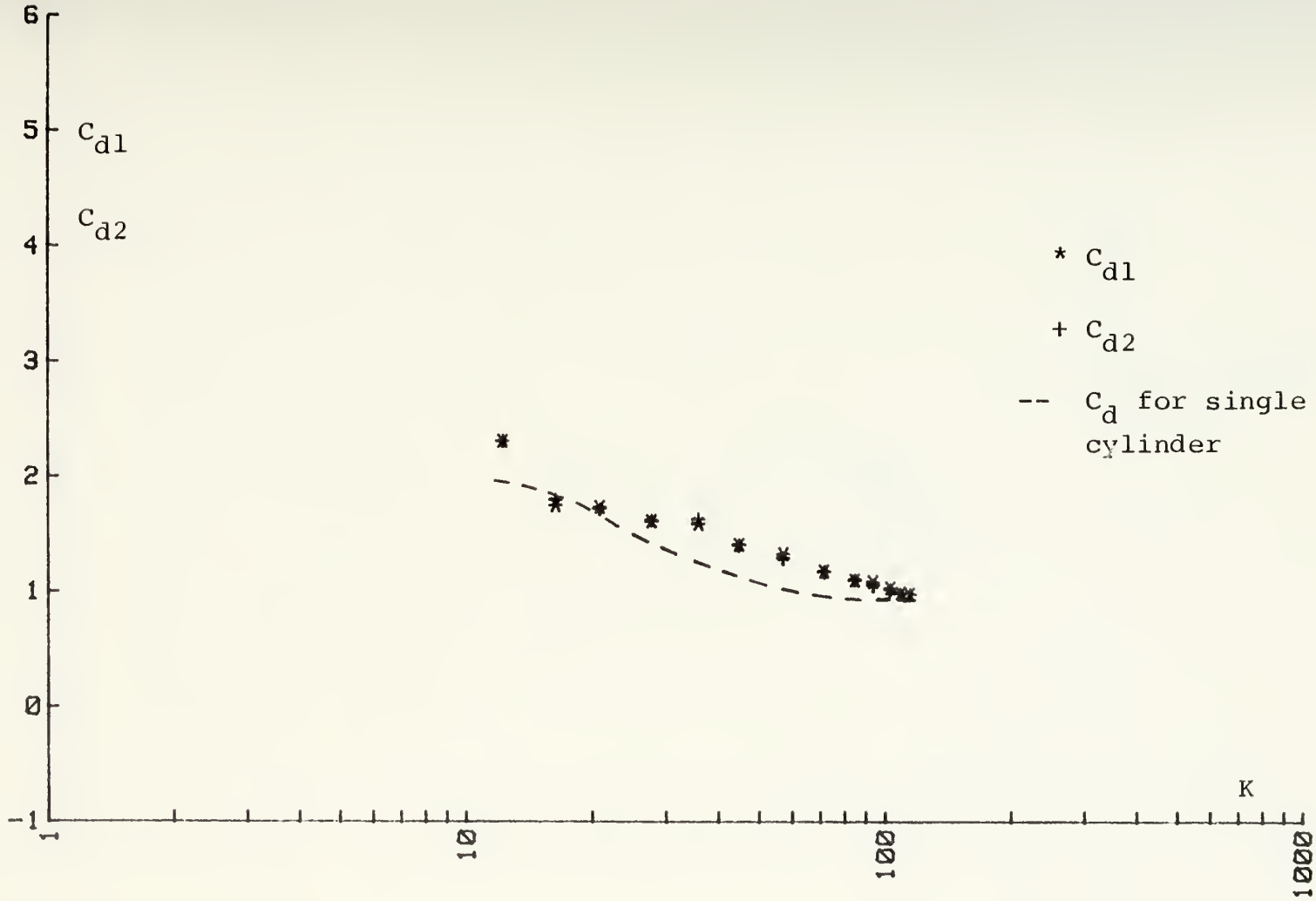

Fig. 19a C_{d1} and C_{d2} versus K for N=2 and $\alpha=90^{o}$

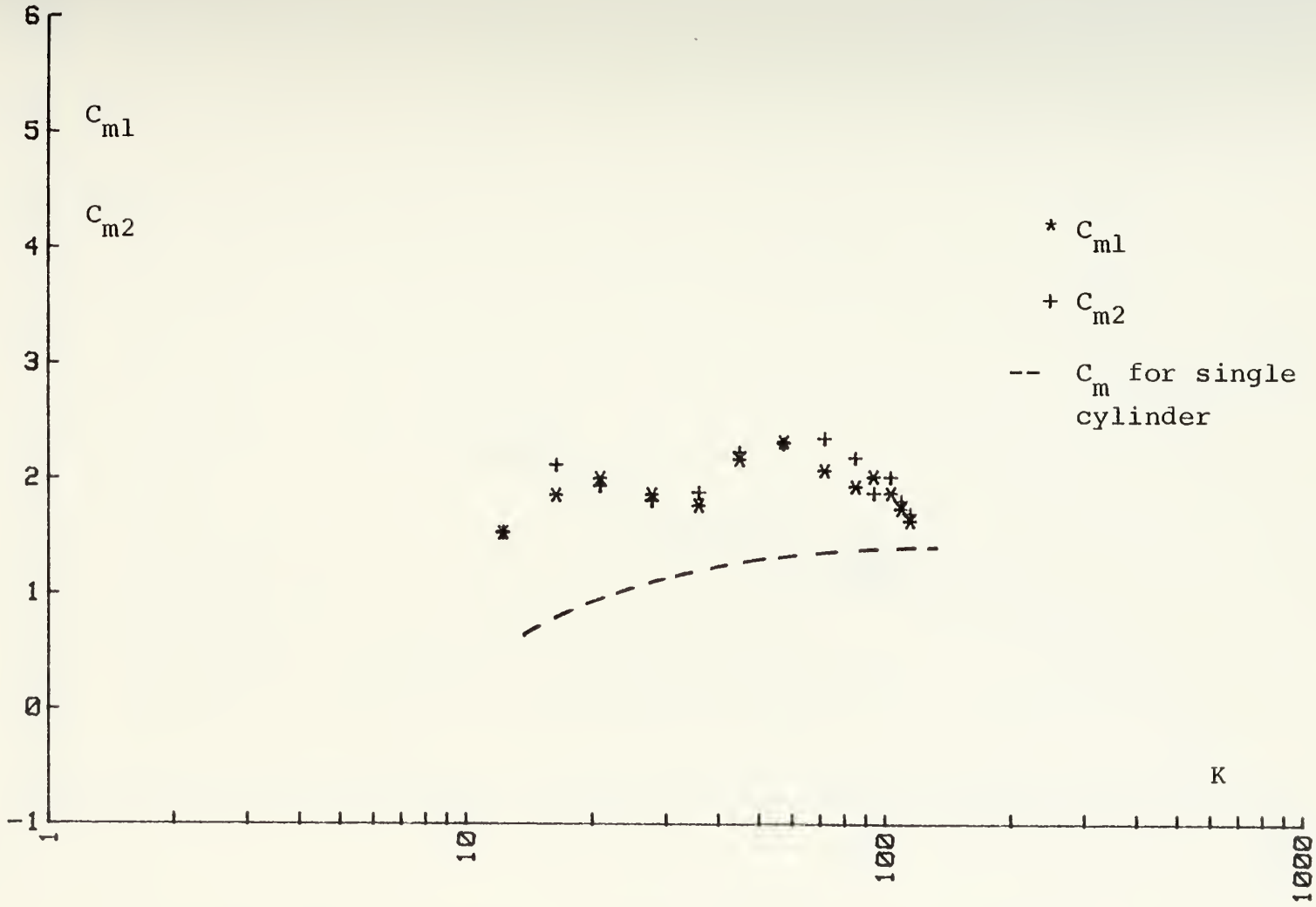

Fig. 19b C_{m1} and C_{m2} versus K for N=2 and $\alpha=90^{o}$

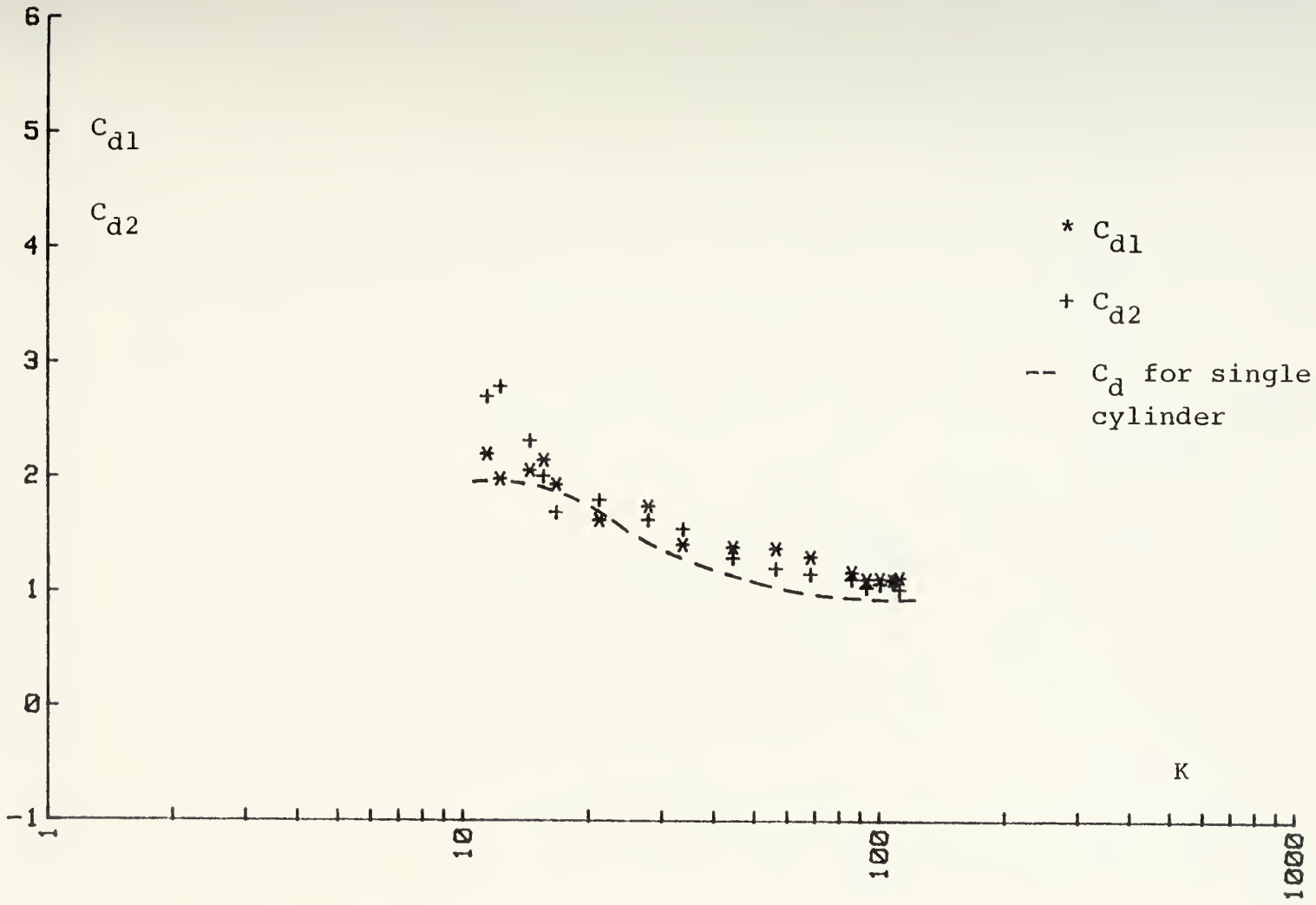

Fig. 20a C_{d1} and C_{d2} versus K for N=2.5 and $\alpha=90^{o}$

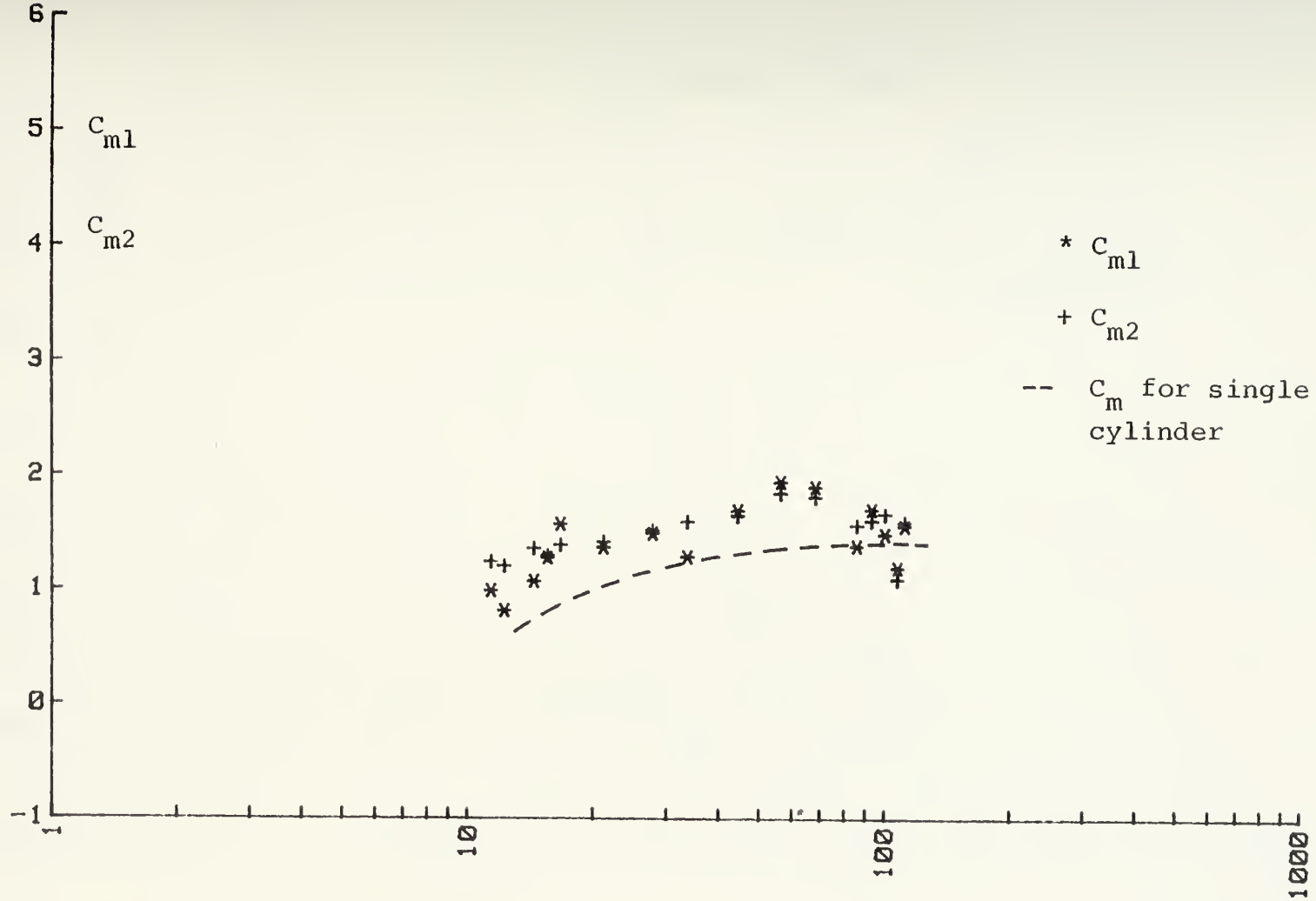

Fig. 20b C_{m1} and C_{m2} versus K for N=2.5 and $\alpha=90^{o}$

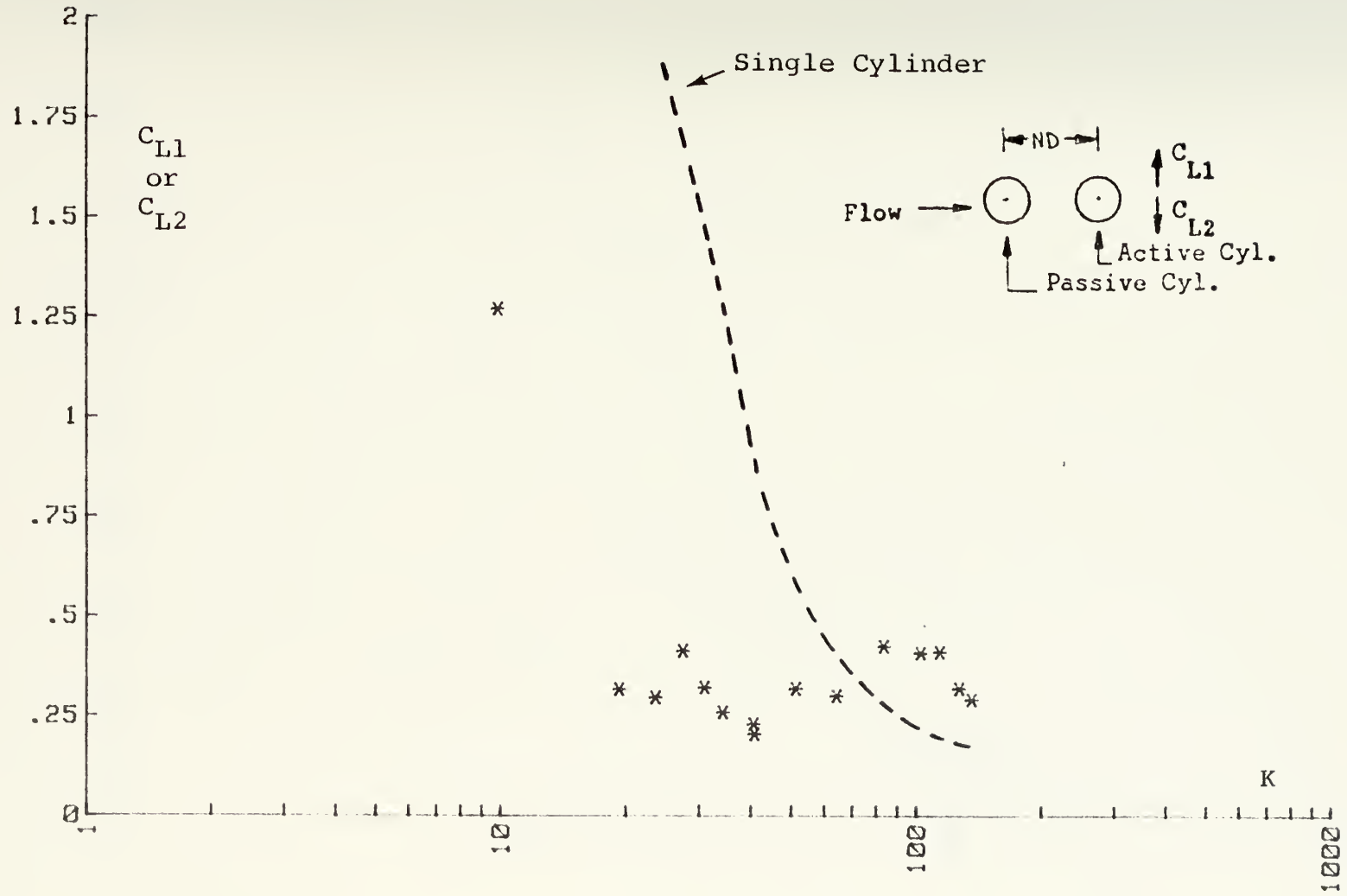

Fig. 21 C_{L1} or C_{L2} vs K for N=1.5 and $\alpha=0^{O}$

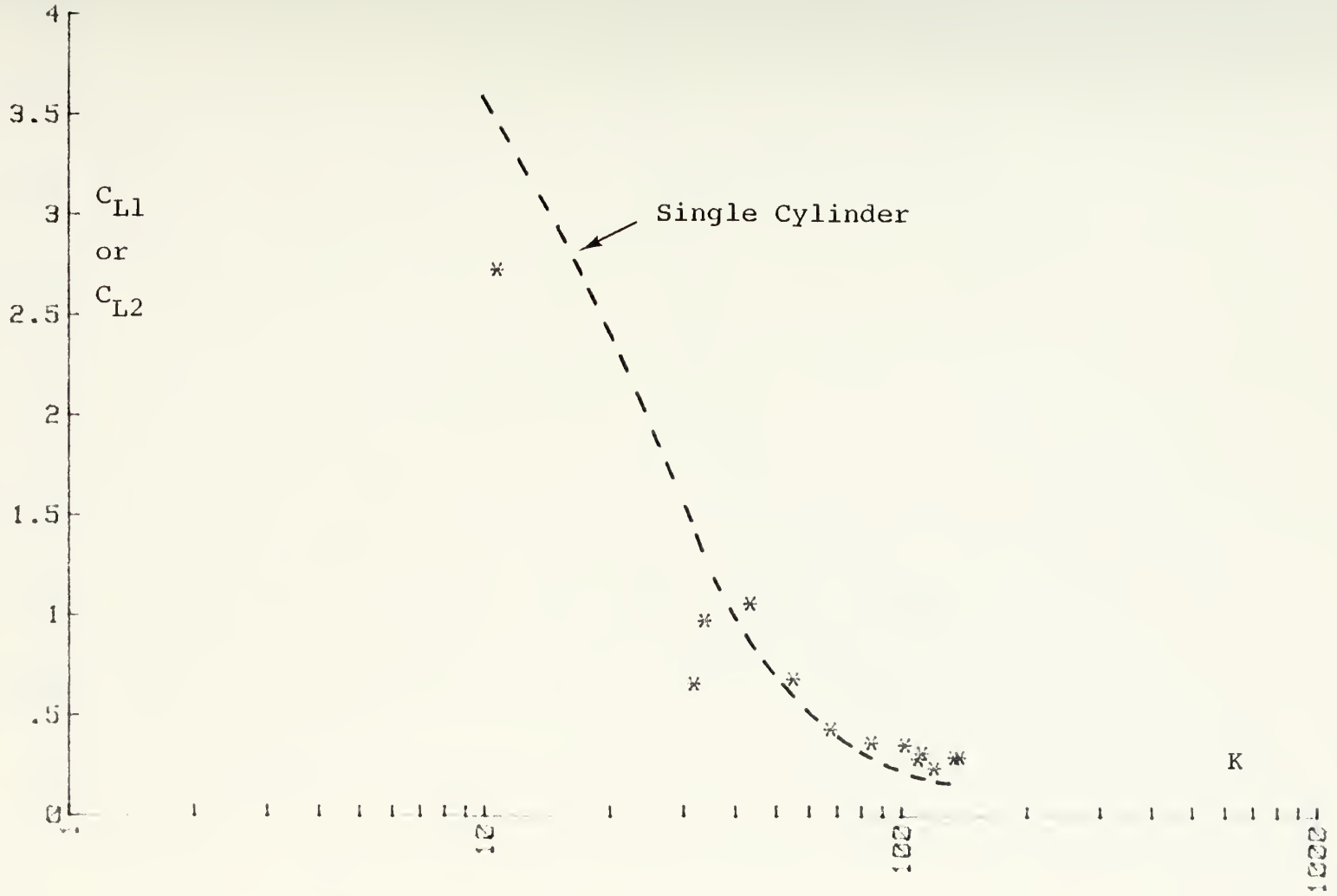

Fig. 22 C_{L1} or C_{L2} vs K for N=2 and $\alpha=0^{o}$

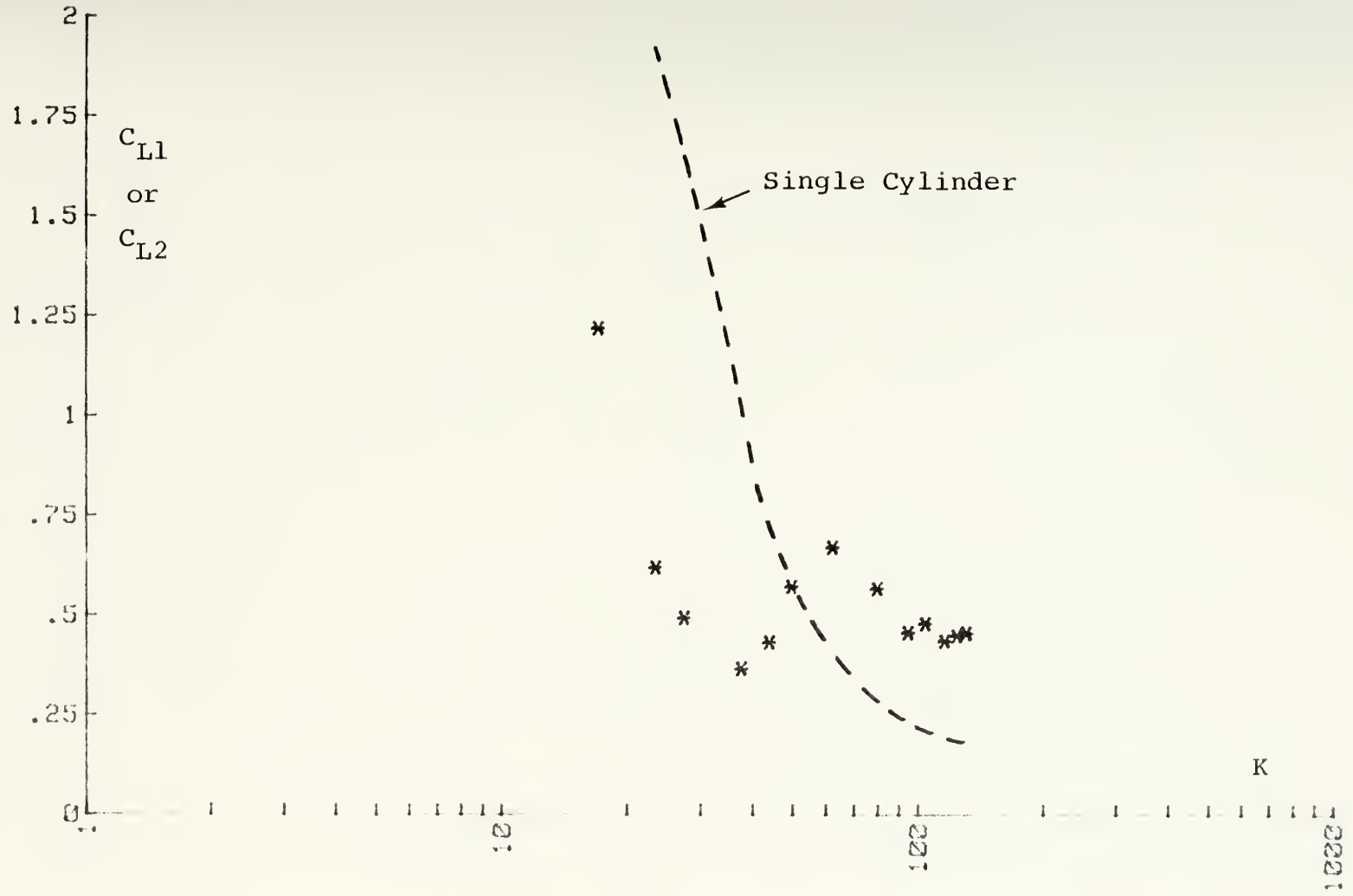

Fig. 23 C_{L1} or C_{L2} vs K for N=2.5 and $\alpha=0^{\circ}$

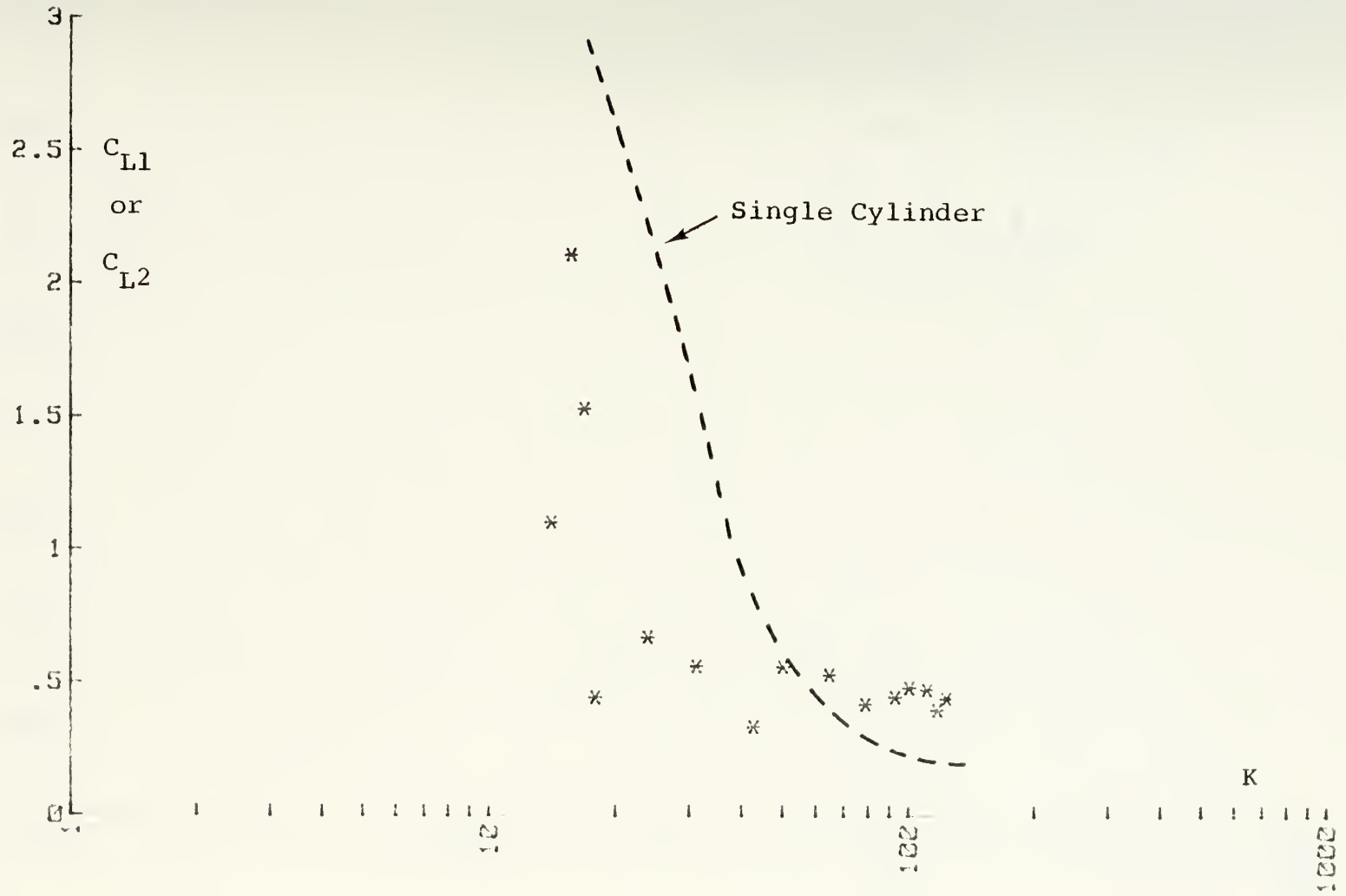

Fig. 24 C_{L1} or C_{L2} vs K for N=3.5 and $\alpha=0^{o}$

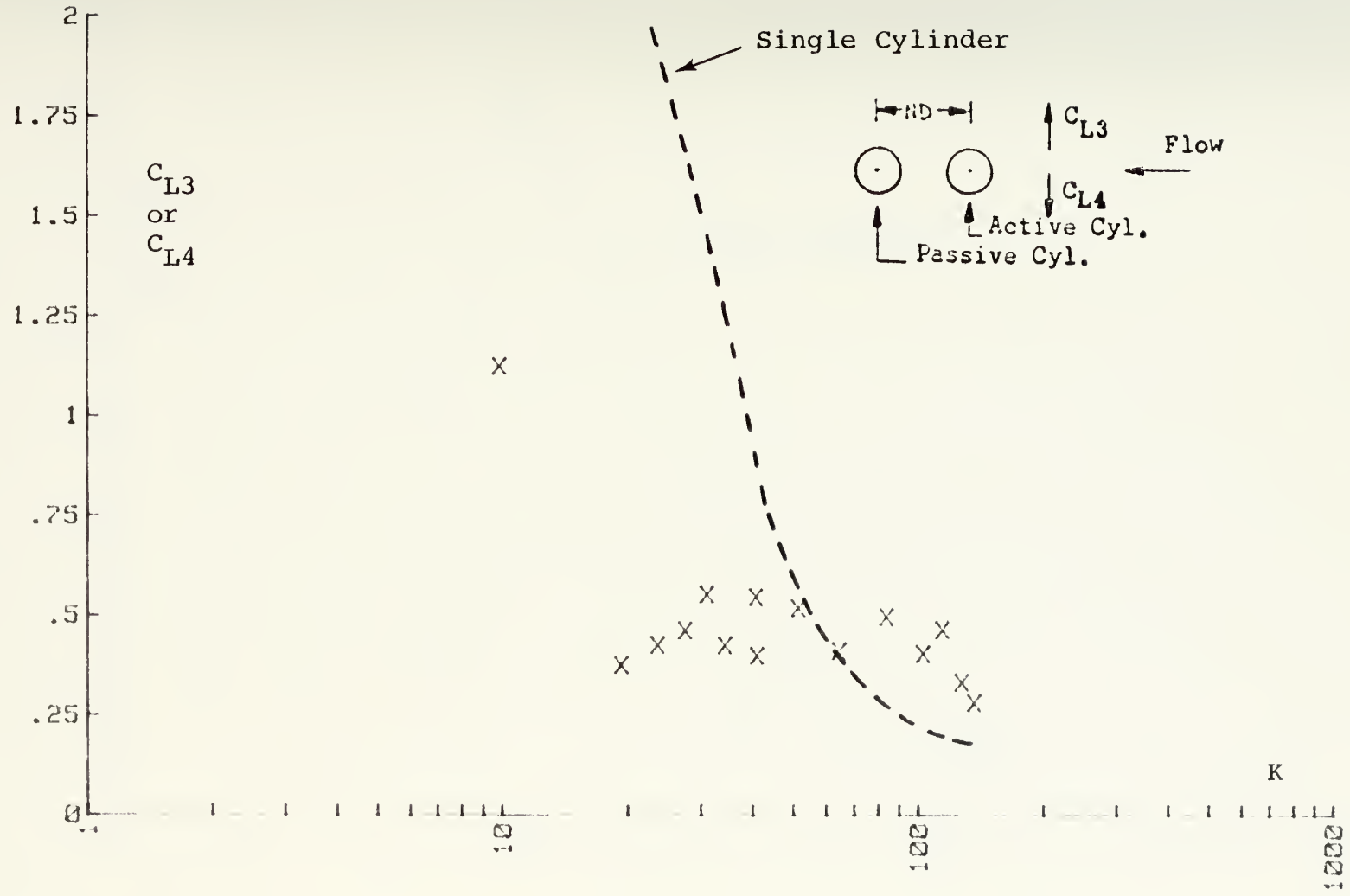

Fig. 25 C_{L3} or C_{L4} vs K for N=1.5 and $\alpha=0^{o}$

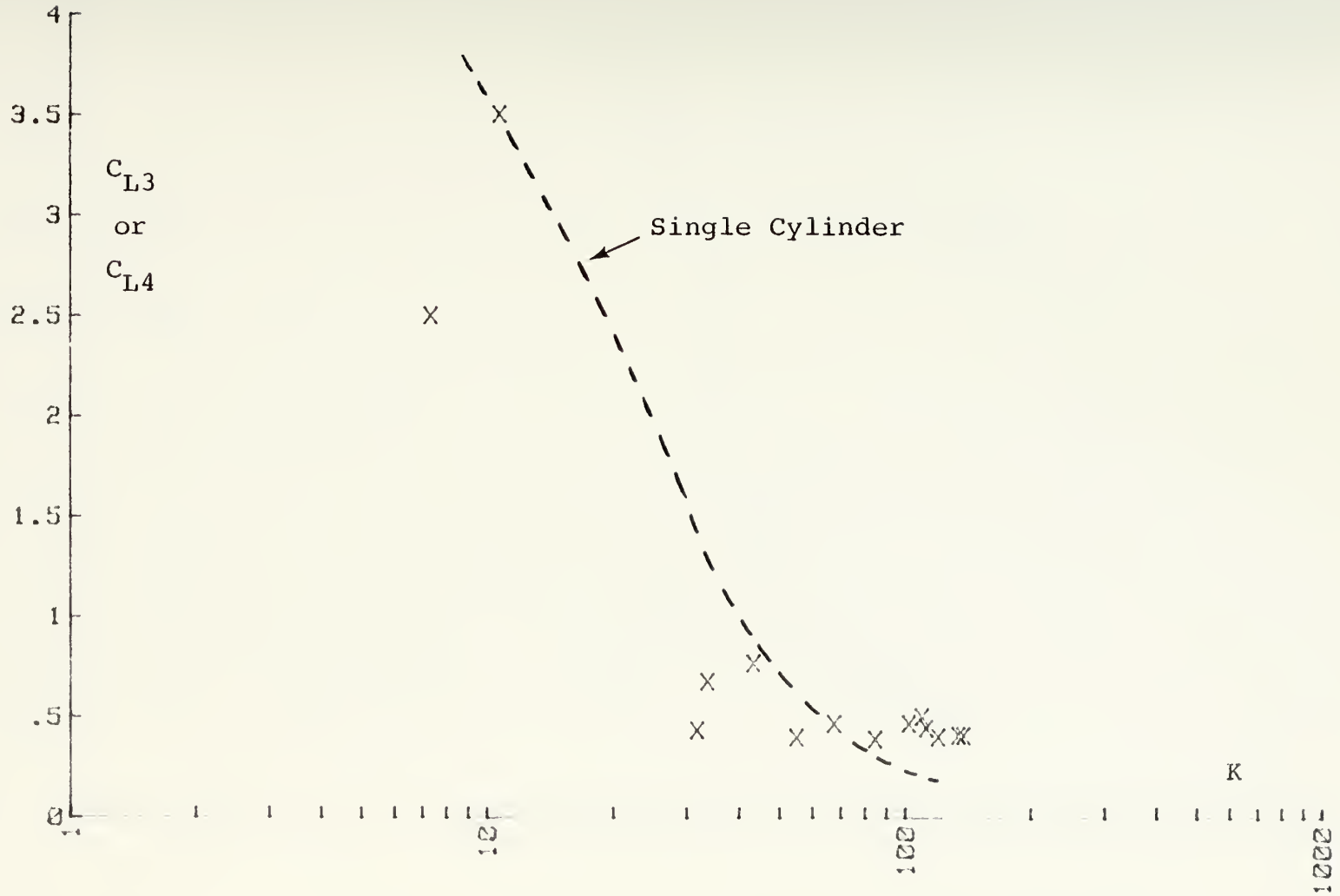

Fig. 26 C_{L3} or C_{L4} vs K for N=2 and $\alpha=0^{o}$

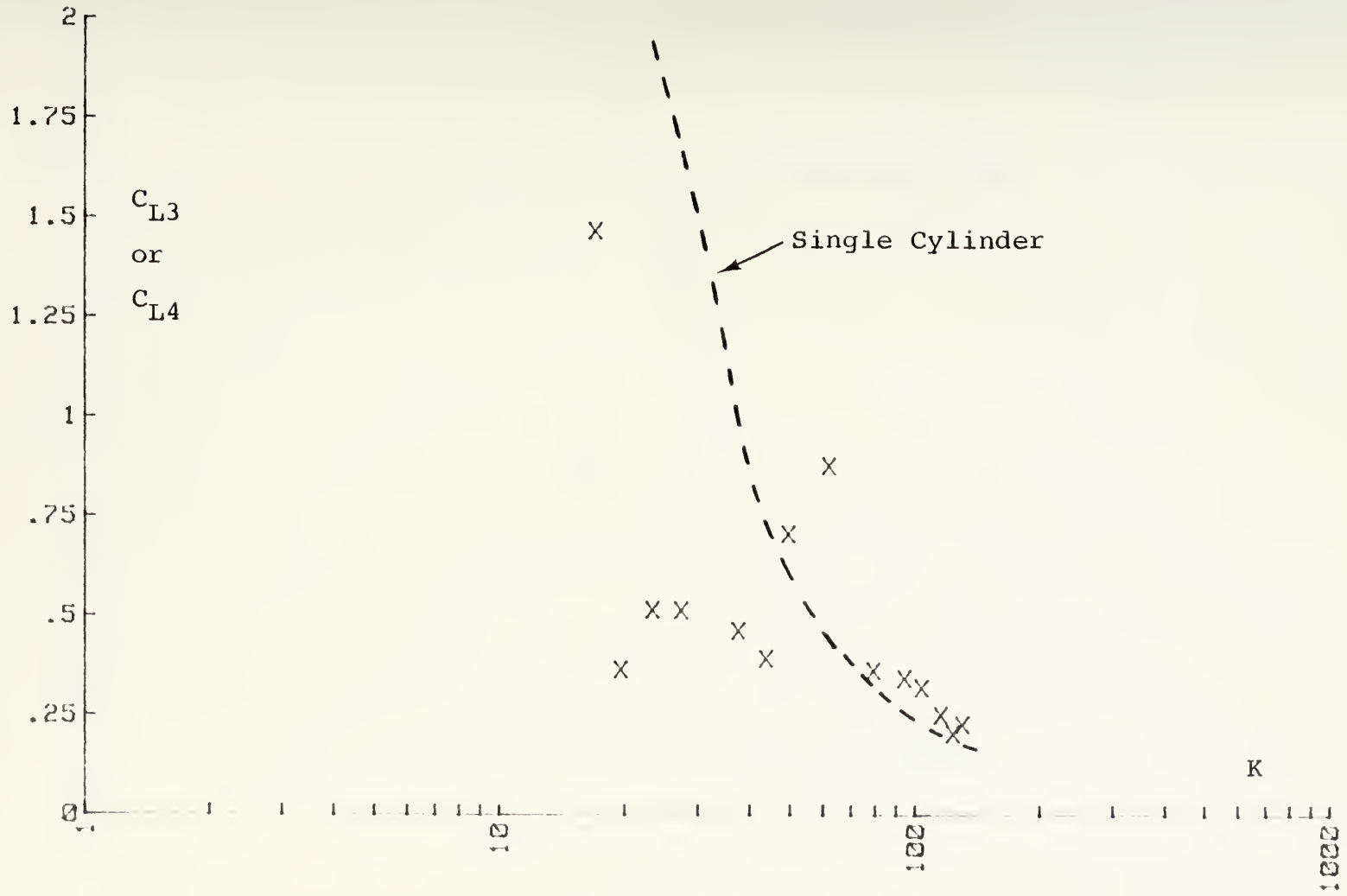

Fig. 27 C_{L3} or C_{L4} vs K for N=2.5 and $\alpha=0^{o}$

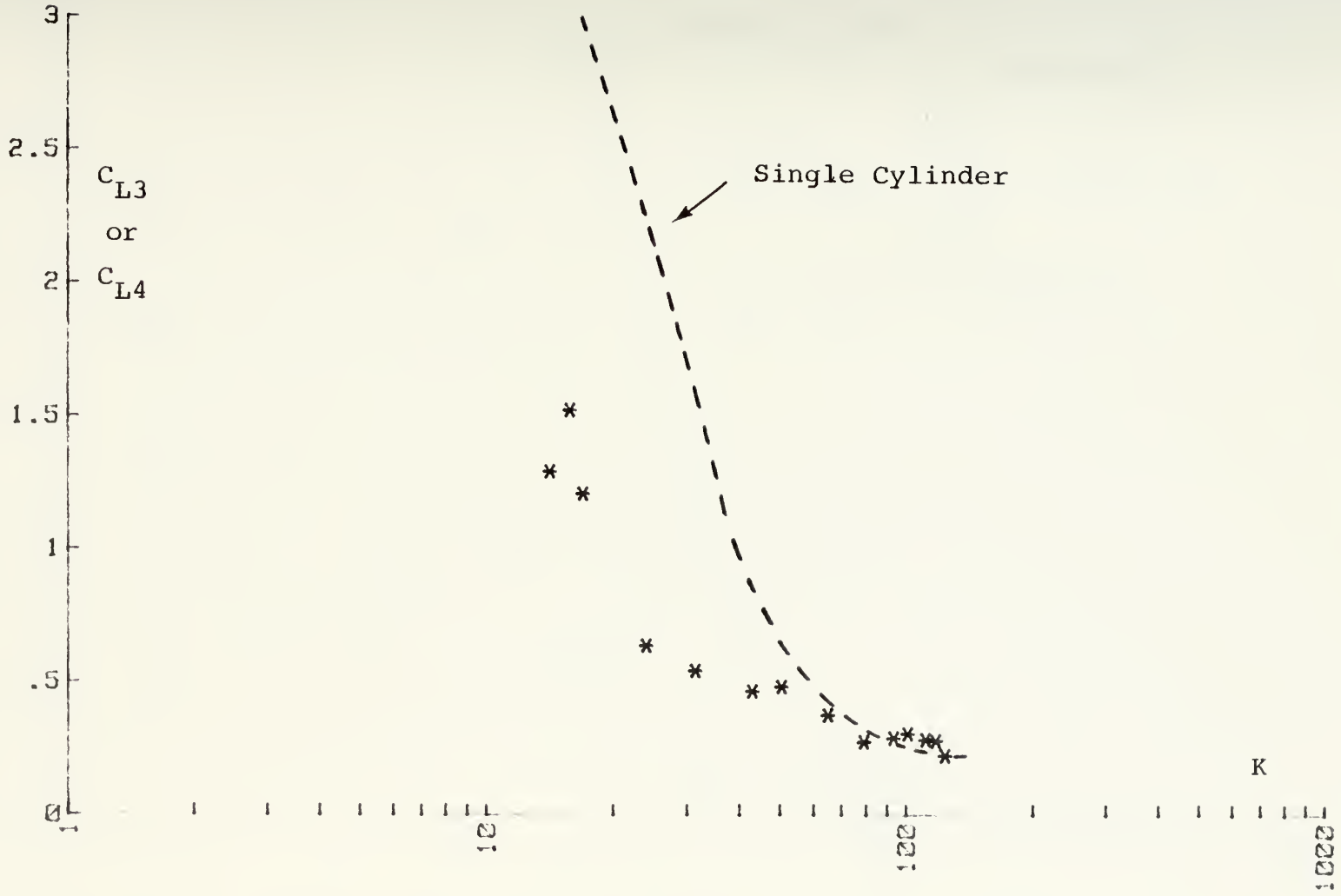

Fig. 28 C_{L3} or C_{L4} vs K for N=3.5 and $\alpha=0^{\circ}$

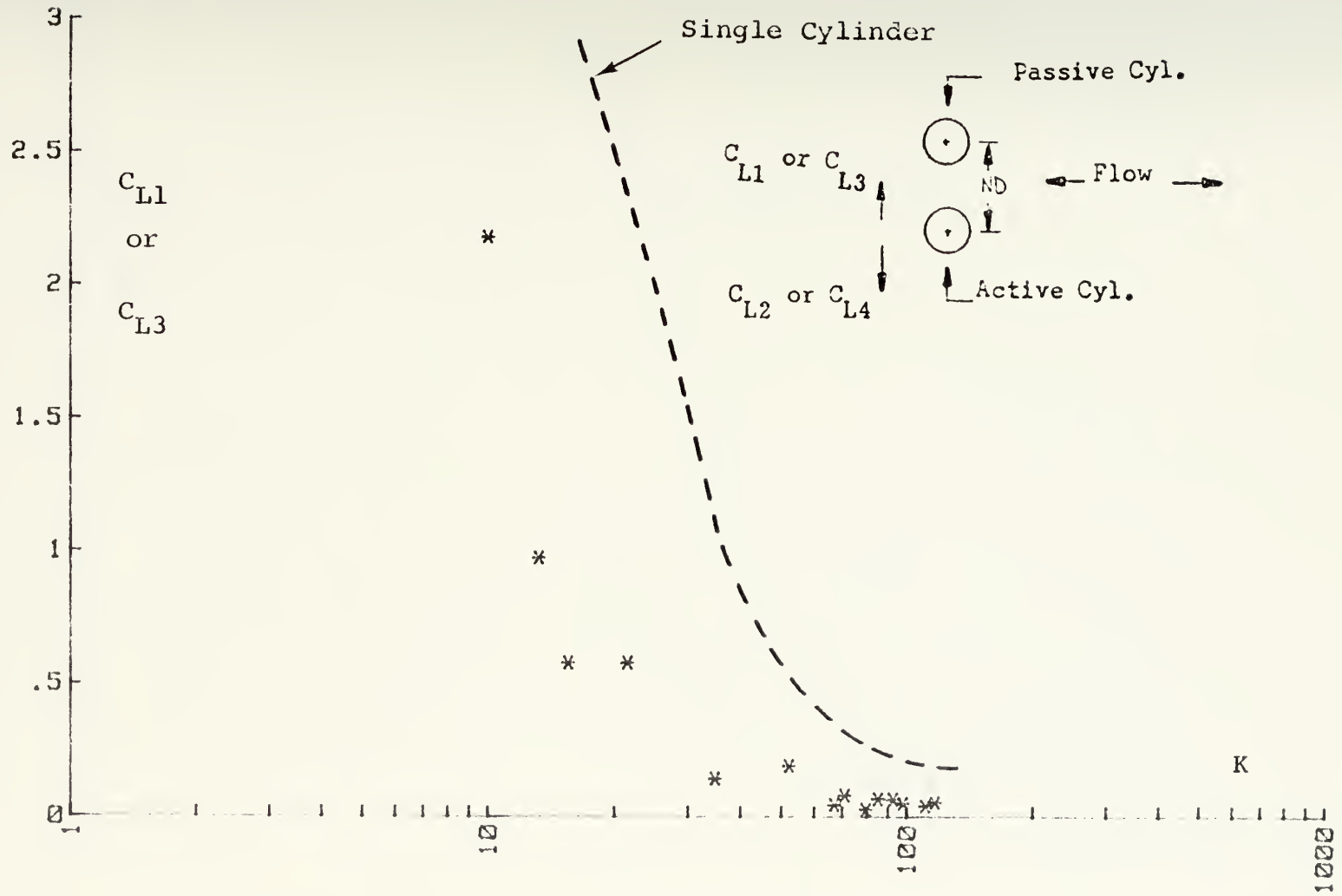

Fig. 29 C_{L1} or C_{L3} vs K for N=1.5 and $\alpha=90^{o}$

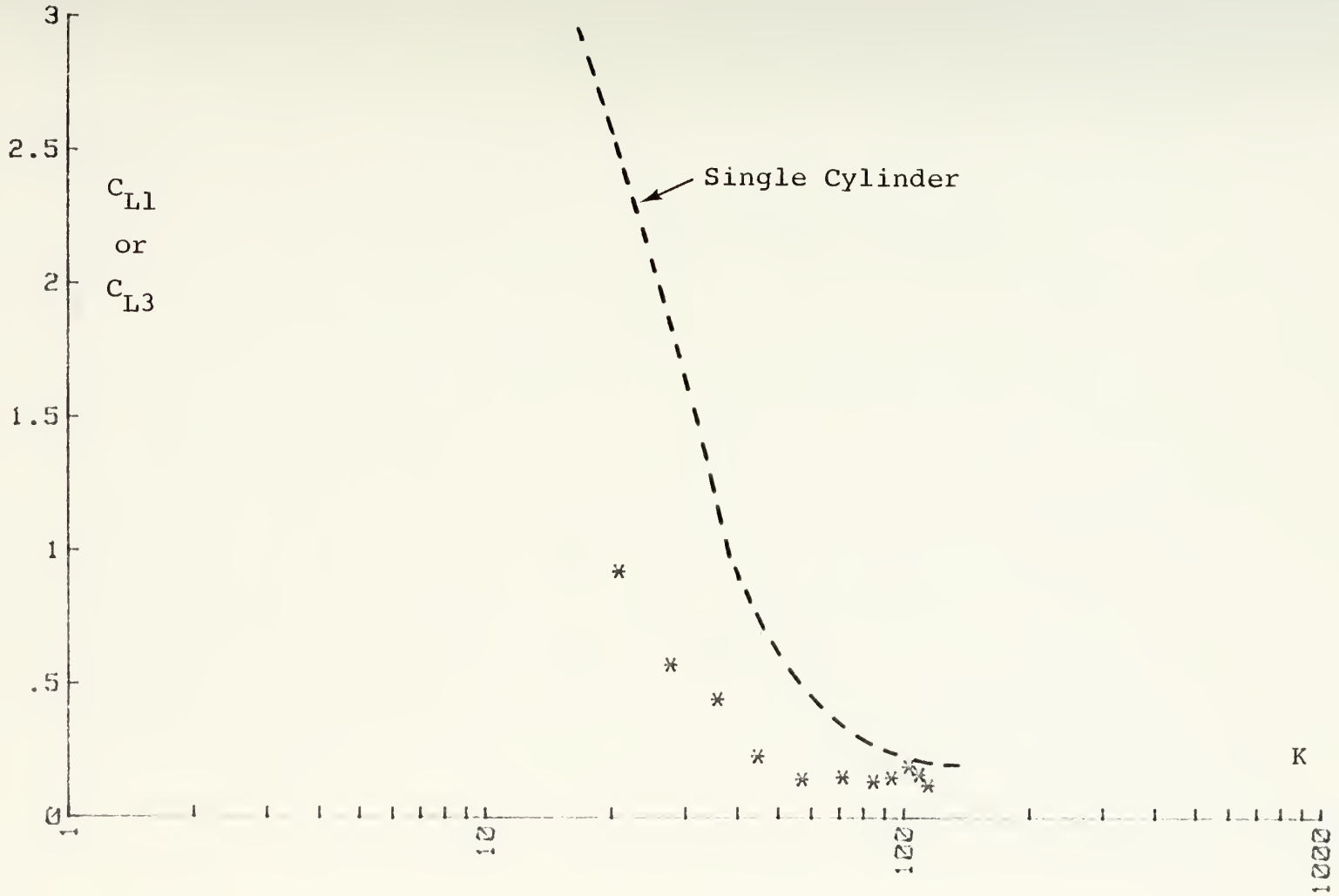

Fig. 30 C_{L1} or C_{L3} vs K for N=2 and $\alpha=90^{o}$

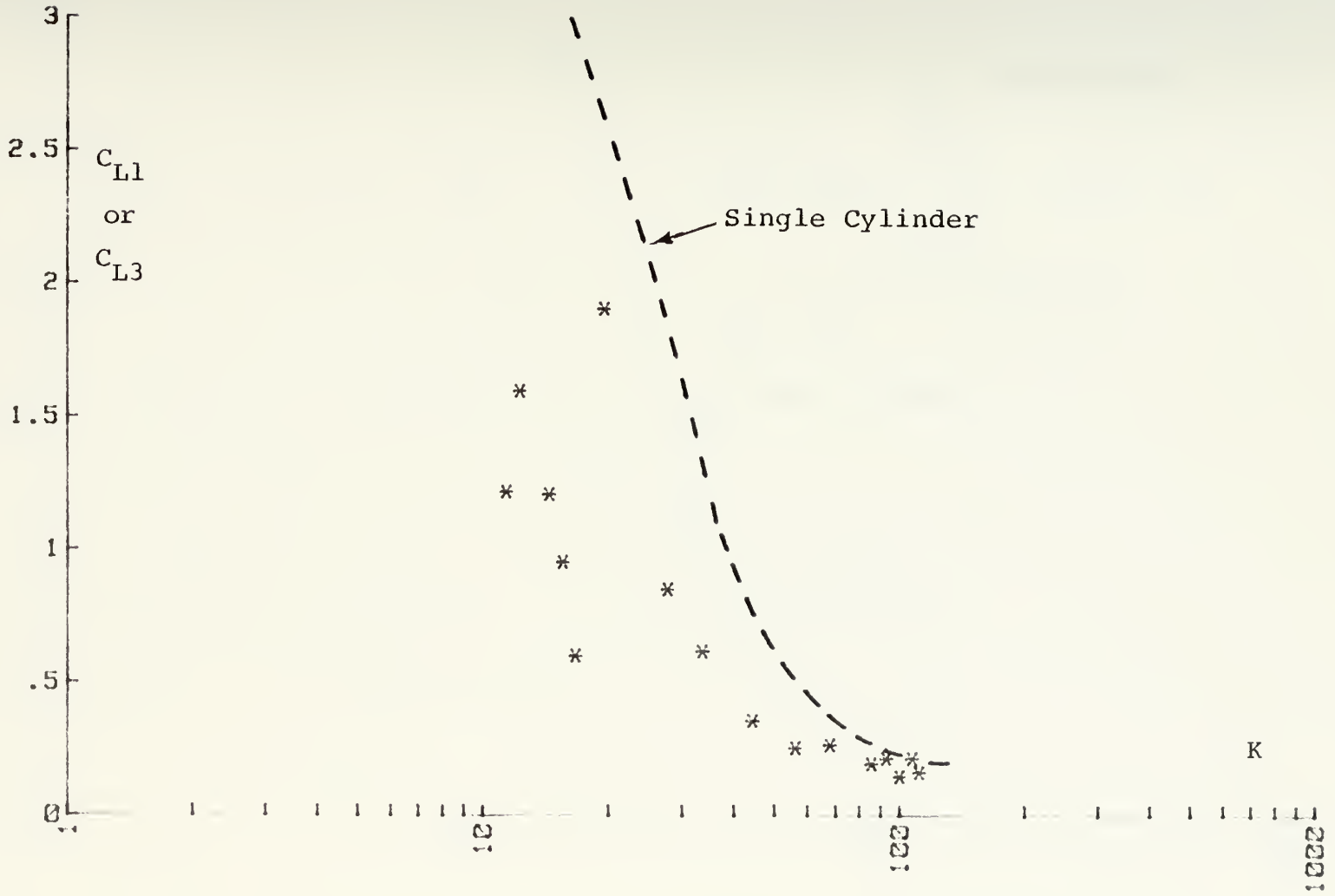

Fig. 31 C_{L1} or C_{L3} vs K for N=2.5 and $\alpha=90^{o}$

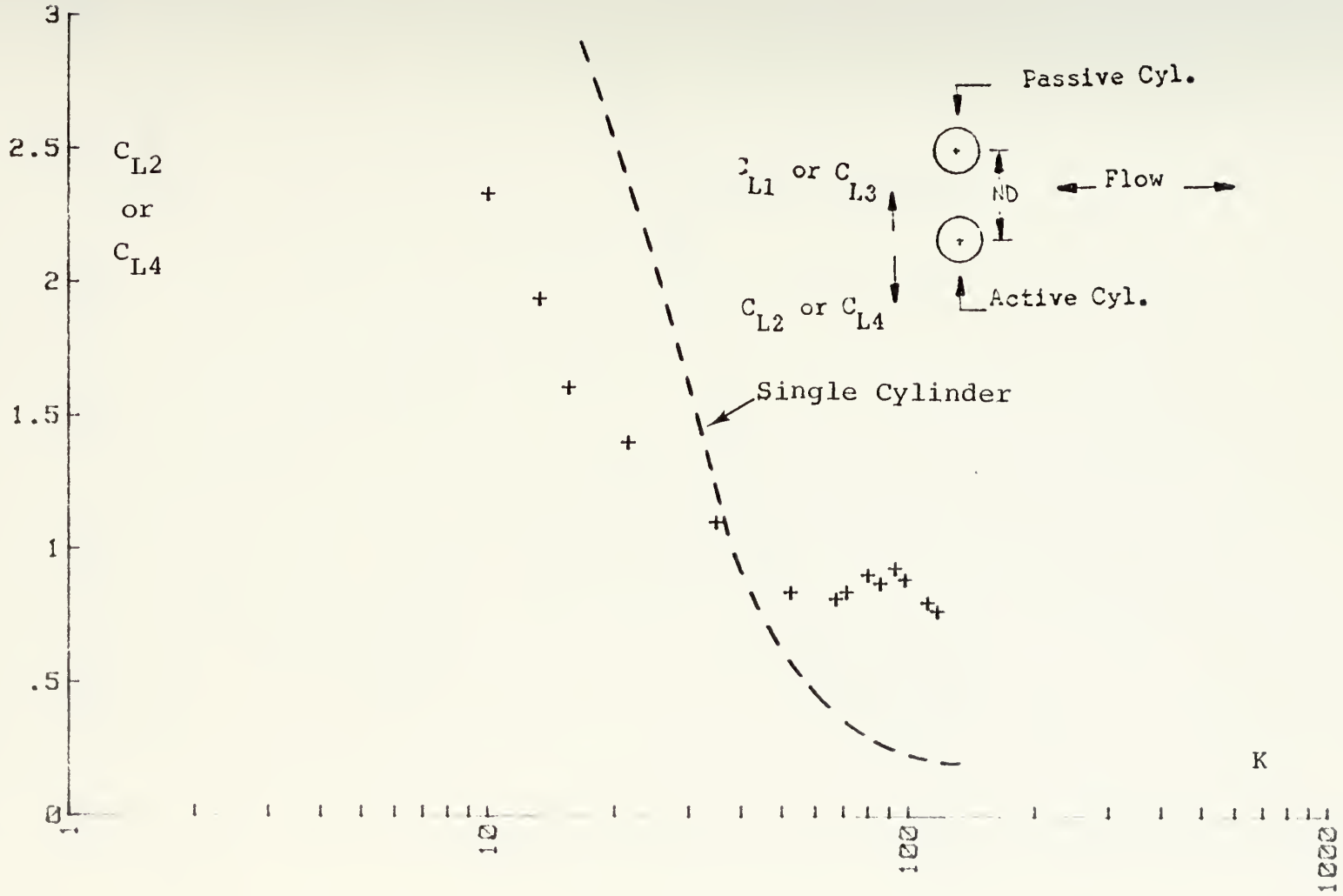

Fig. 32 C_{L2} or C_{L4} vs K for N=1.5 and $\alpha=90^{O}$

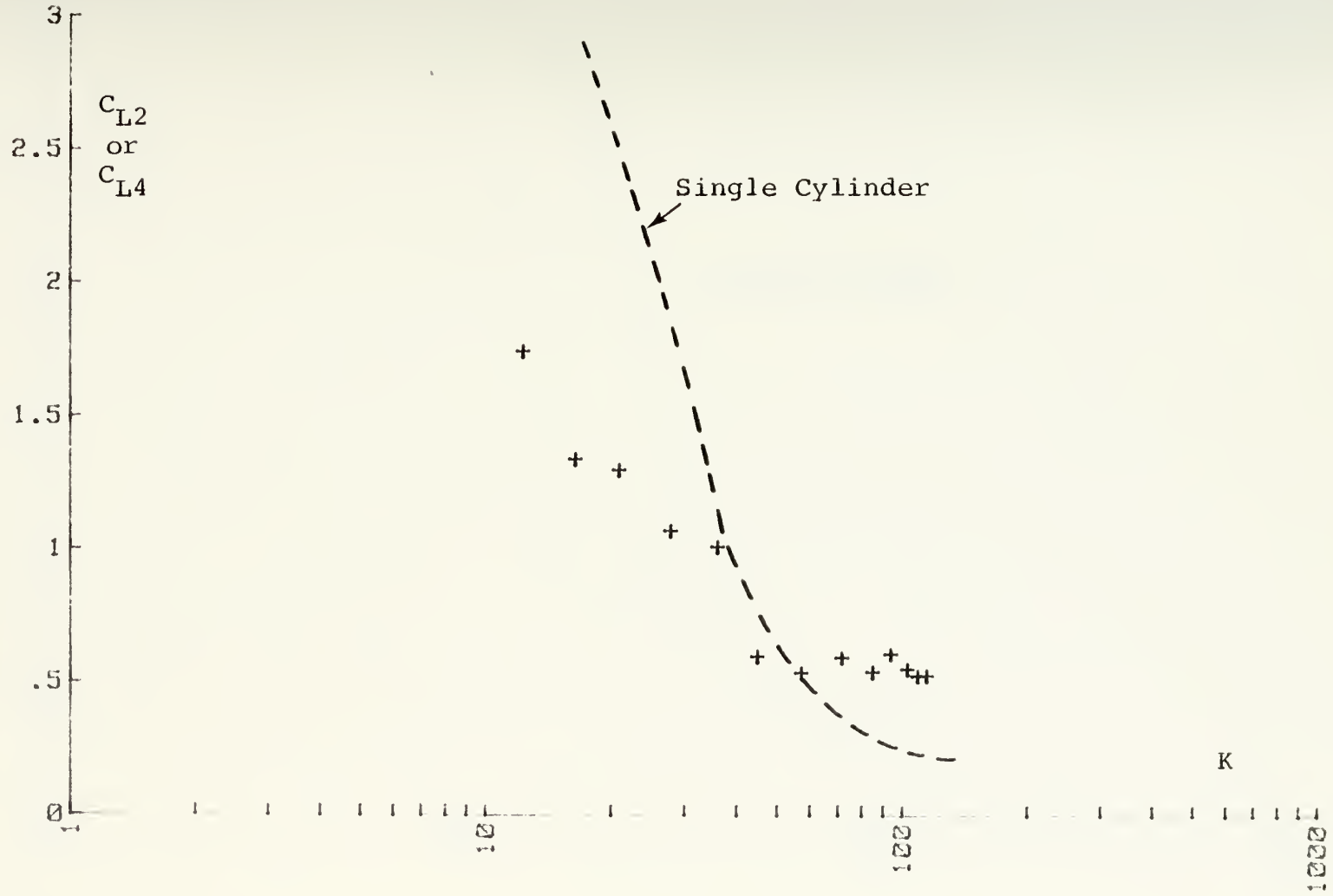

Fig. 33 C_{L2} or C_{L4} vs K for N=2 and $\alpha=90^{o}$

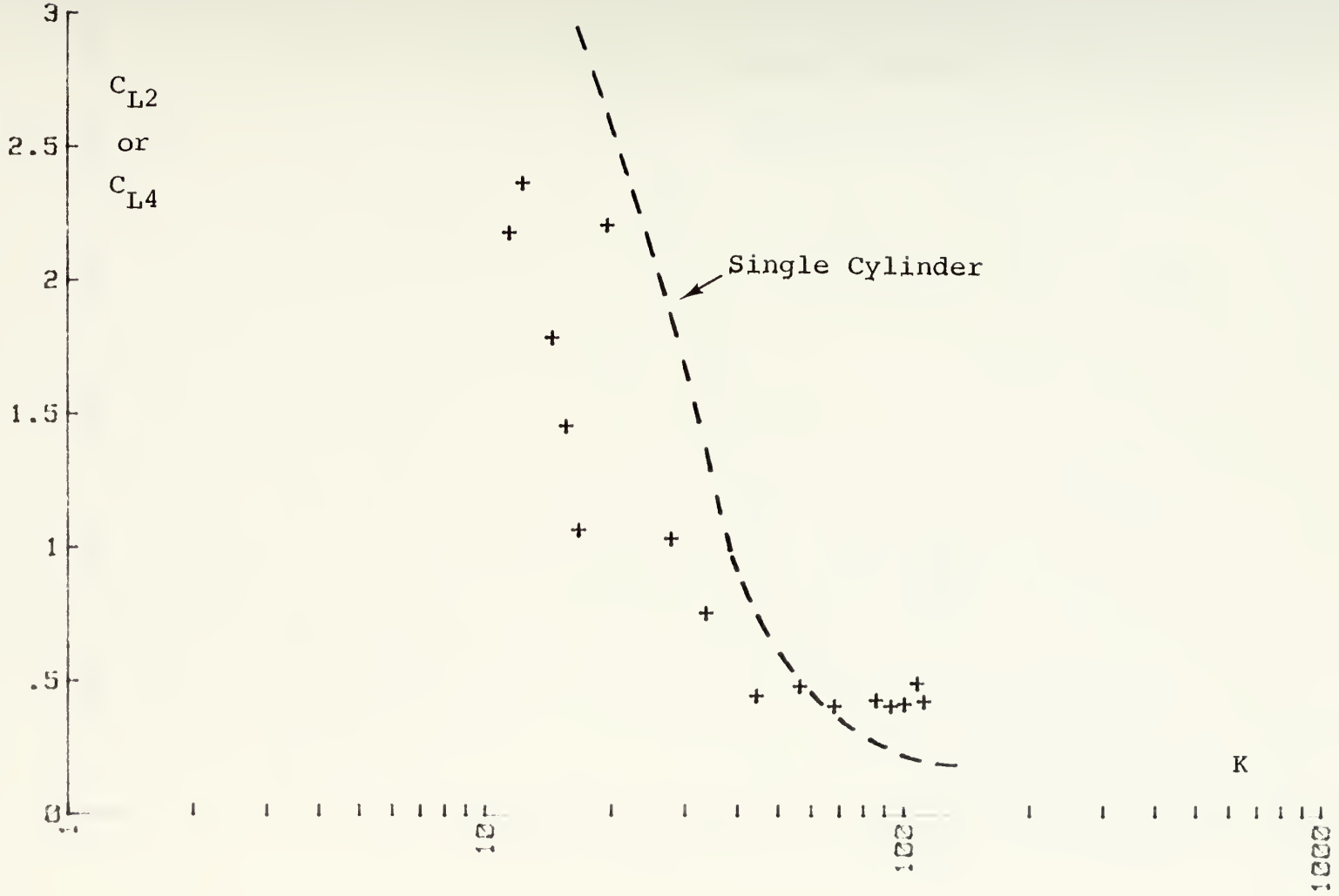

Fig. 34 C_{L2} or C_{L4} vs K for N=2.5 and $\alpha=90^{o}$

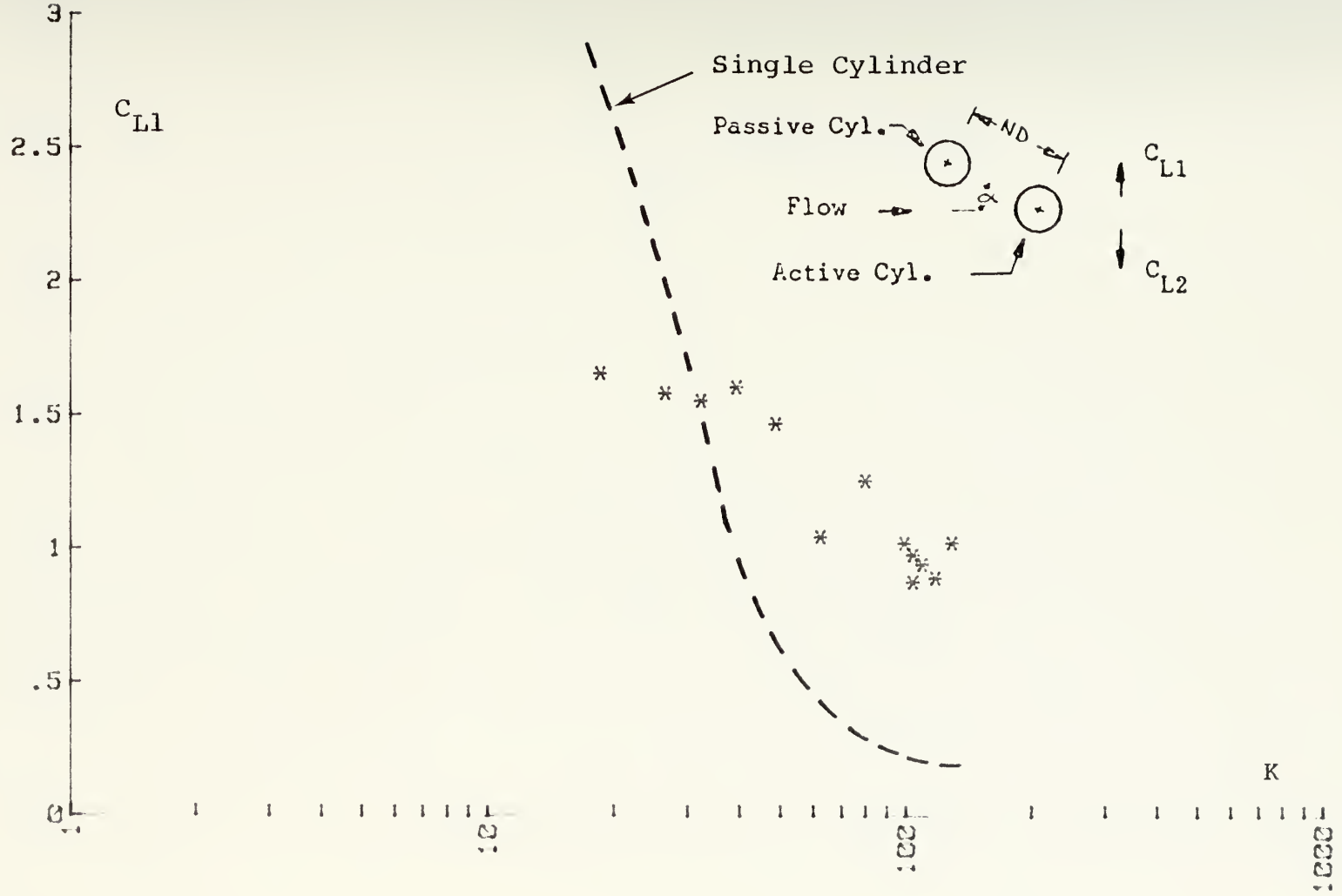

Fig. 35 C_{L1} vs K for N=1.5 and $\alpha=30^{o}$

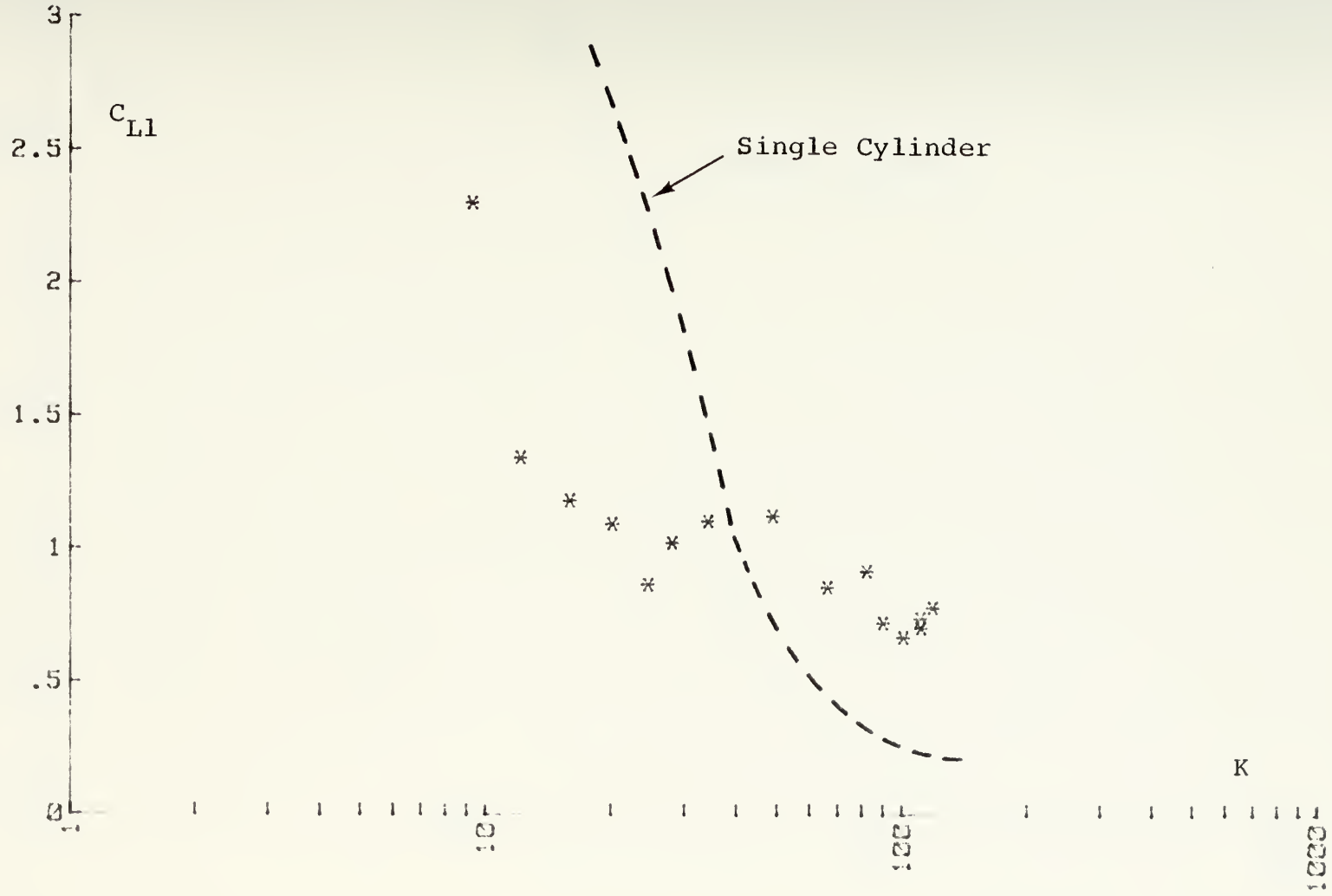

Fig. 36 C_{Ll} vs K for N=2 $\alpha=30^{o}$

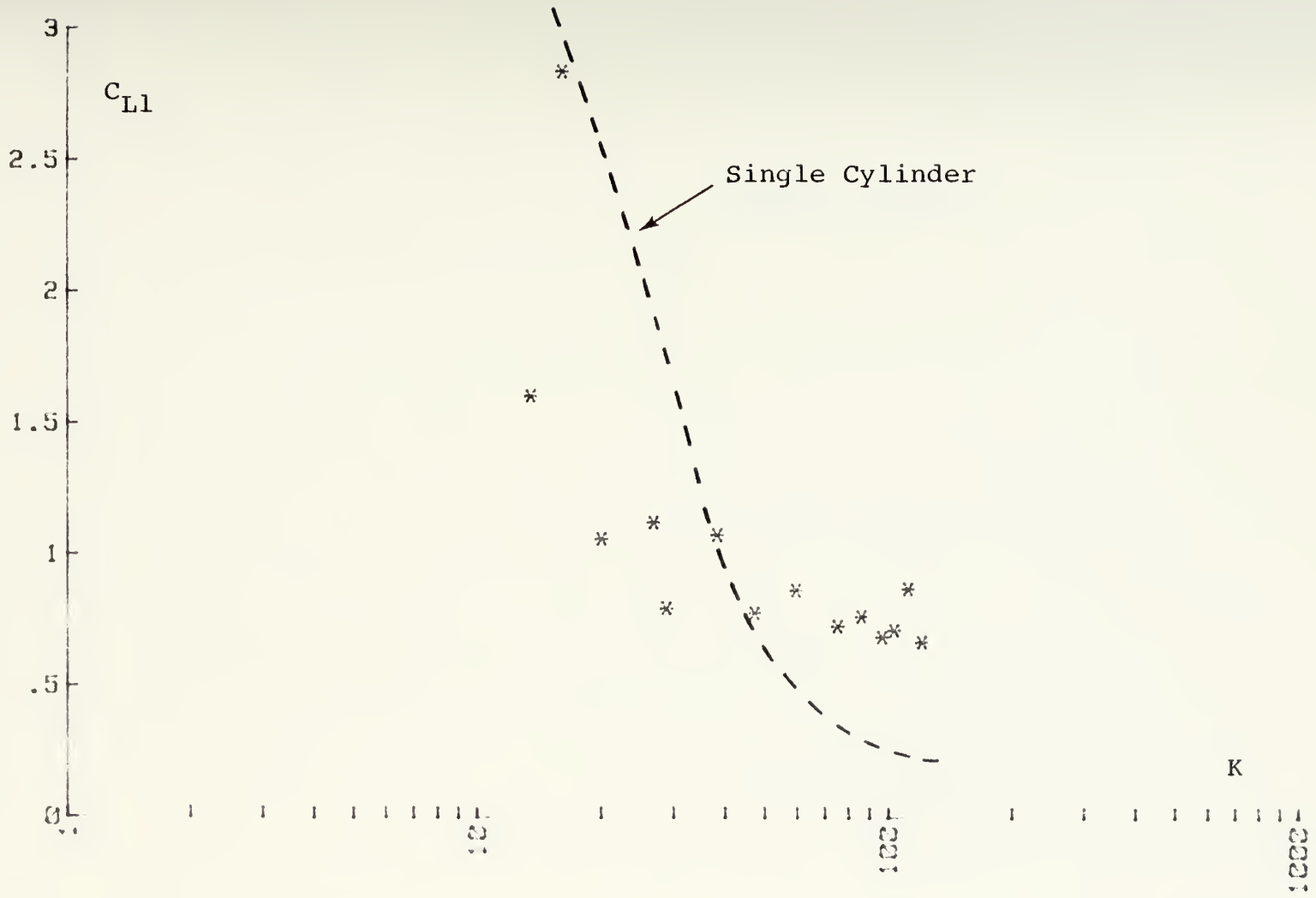

Fig. 37 C_{L1} vs K for N=2.5 and $\alpha=30^{o}$

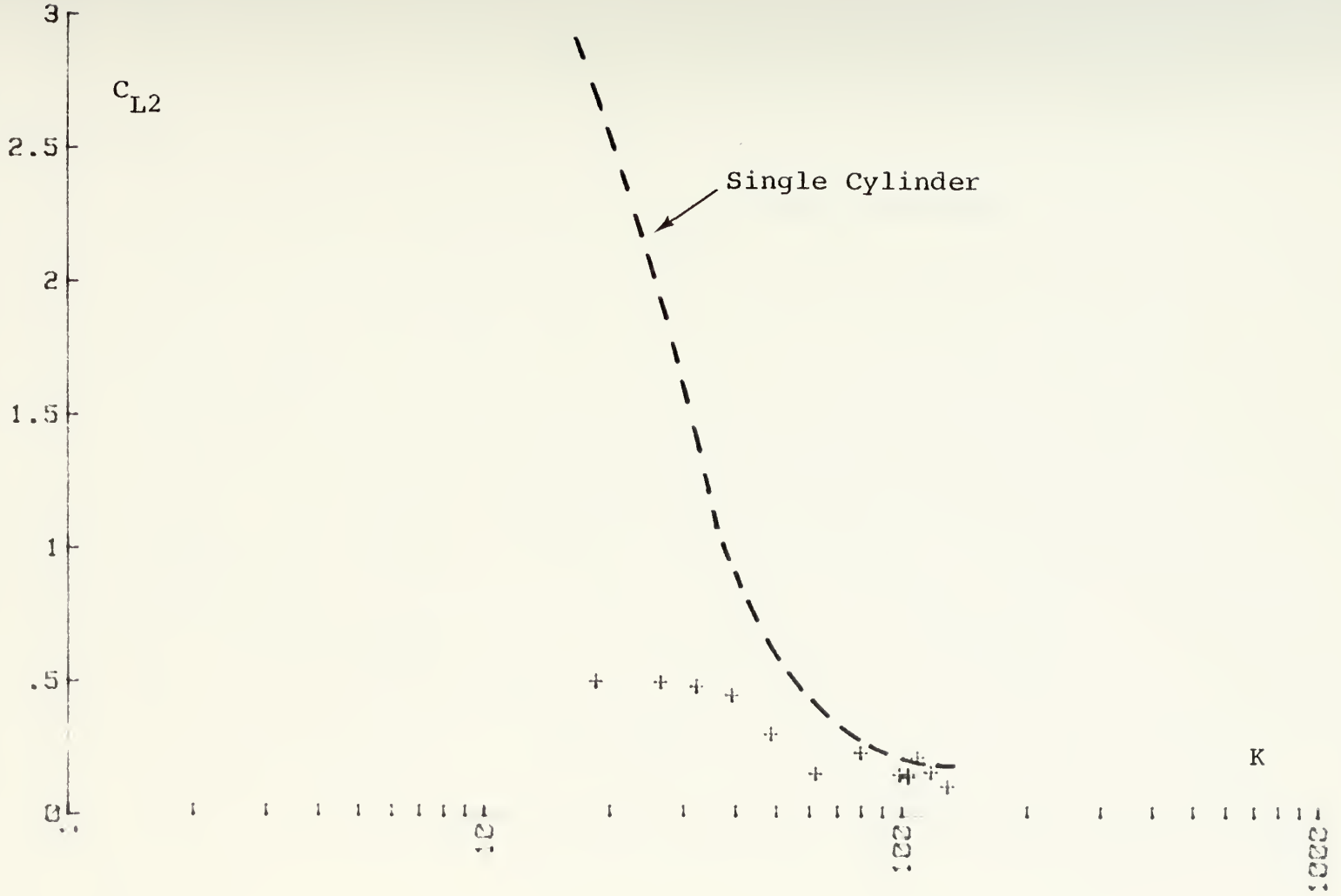

Fig. 37 C_{L2} vs K for N=1.5 and $\alpha=30^{O}$

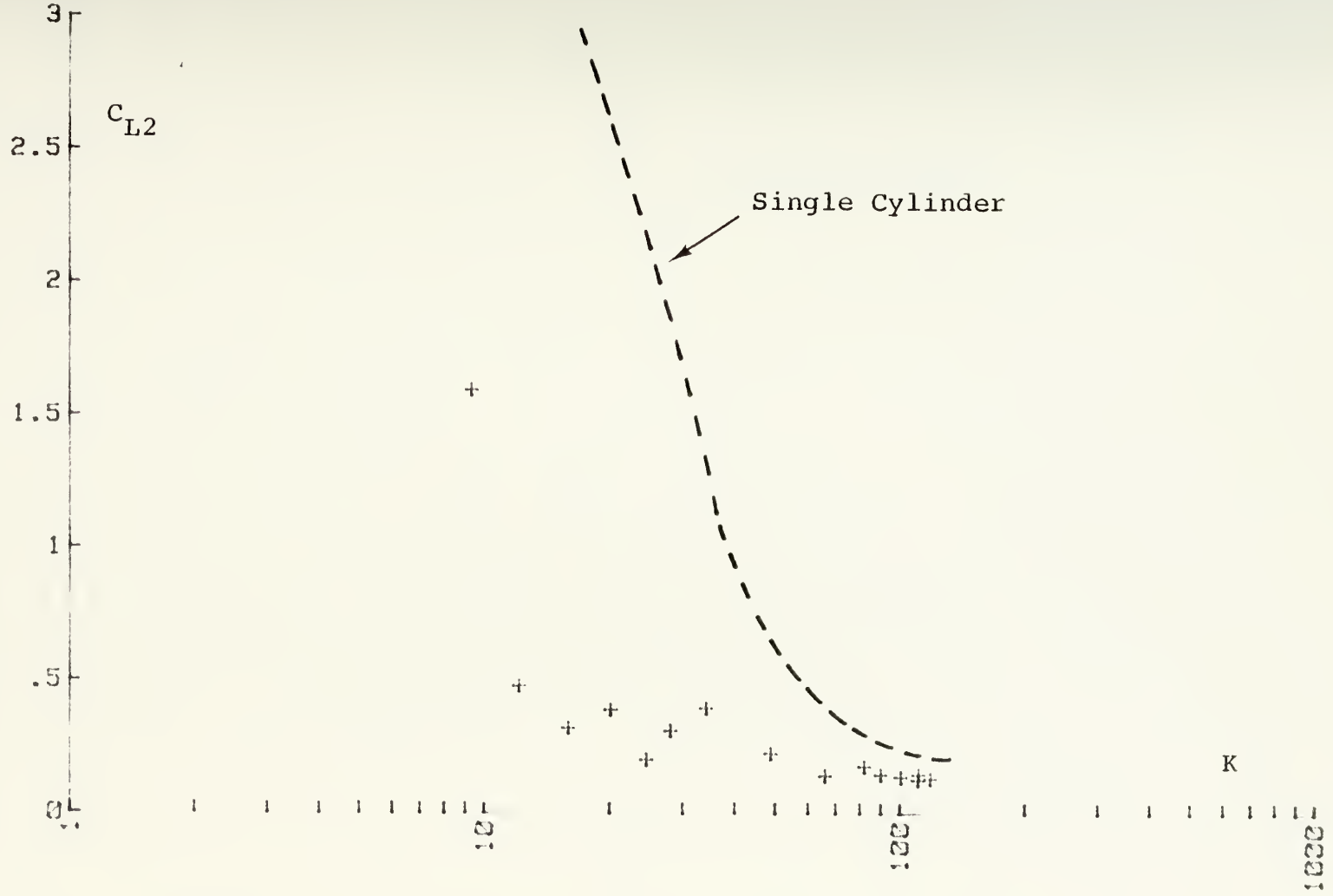

Fig. 39 C_{L2} vs K for N=2 and $\alpha=30^{o}$

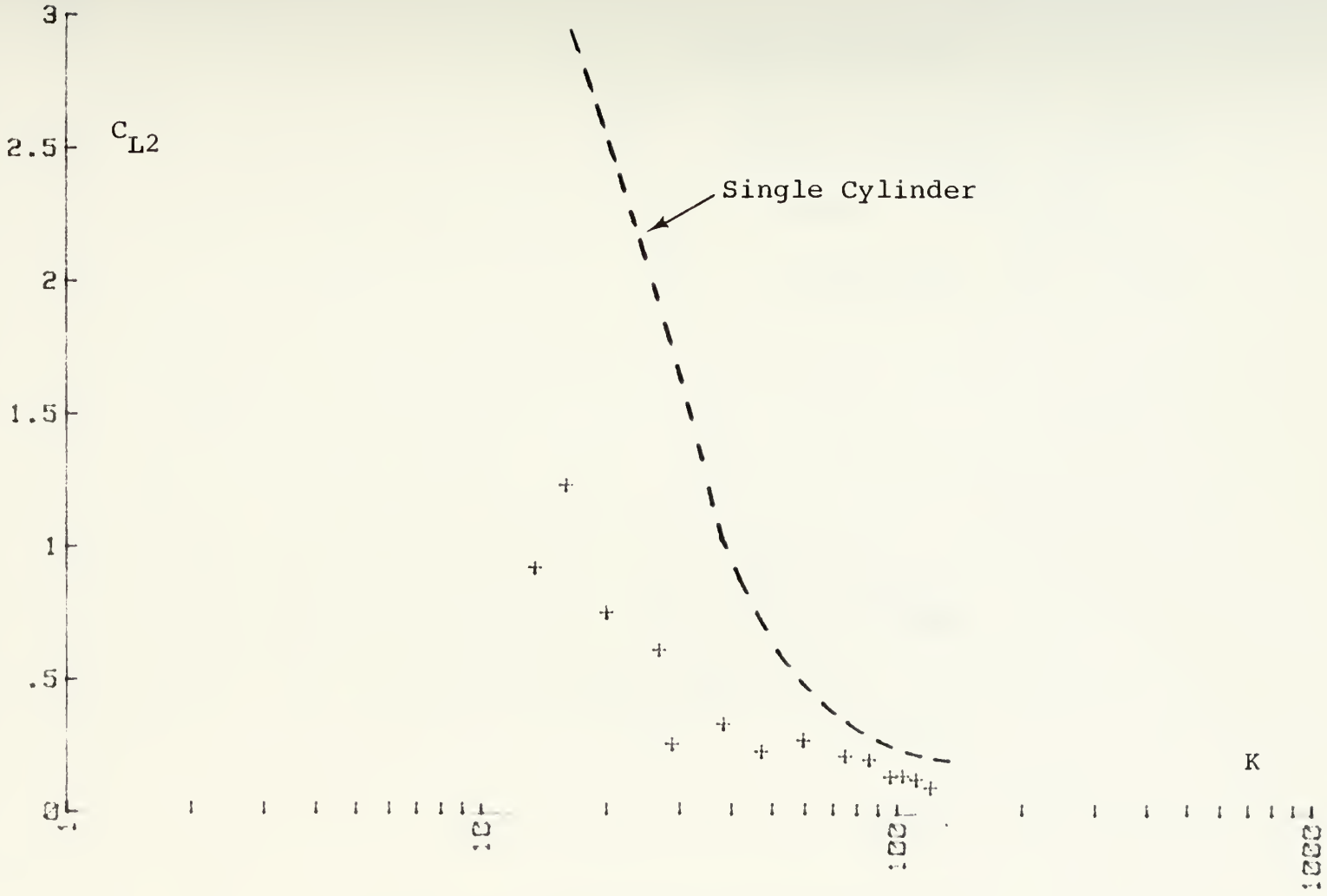

Fig. 40 C_{L2} vs K for N=2.5 and $\alpha=30^{O}$

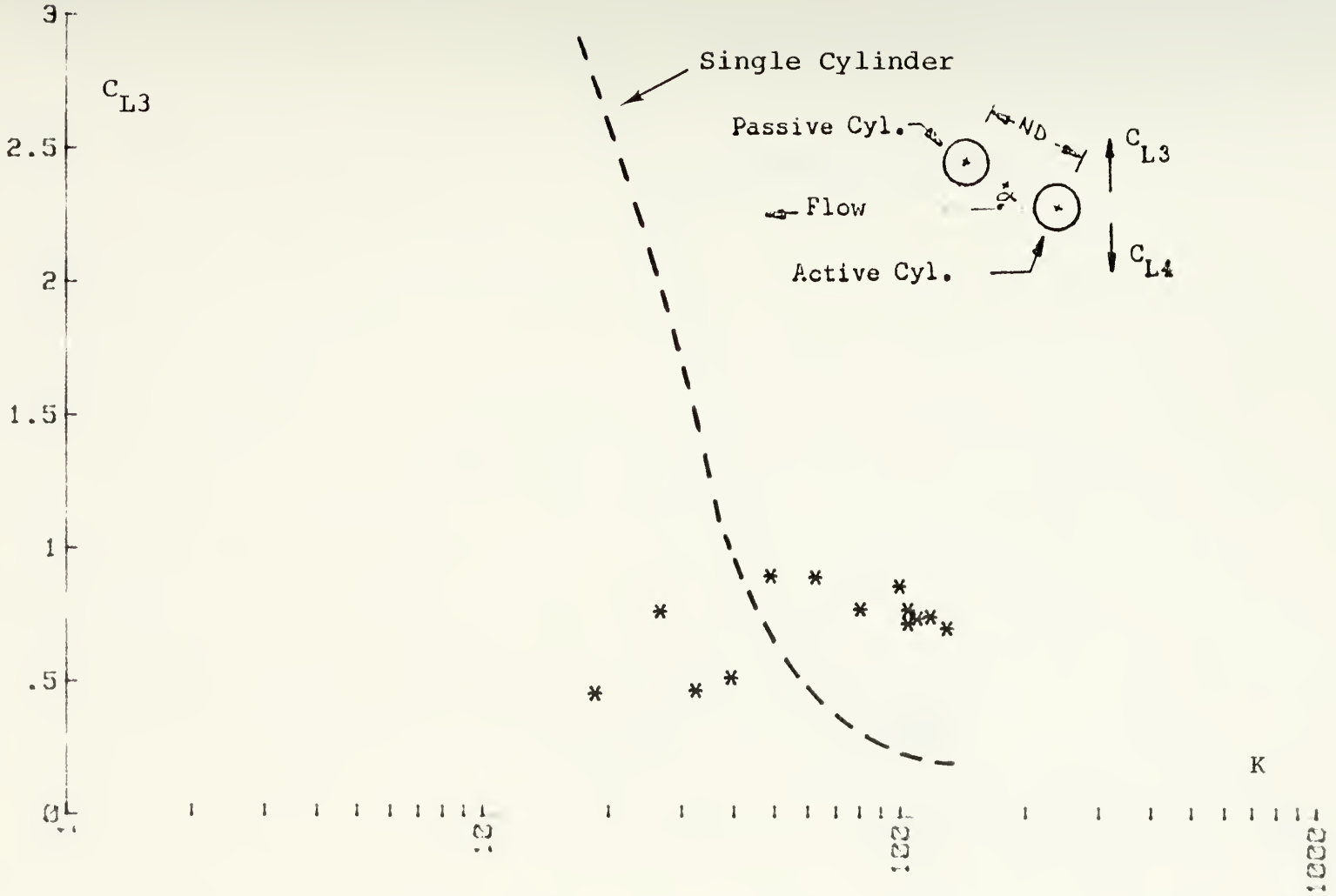

Fig. 41 C_{L3} vs K for N=1.5 and $\alpha=30^{O}$

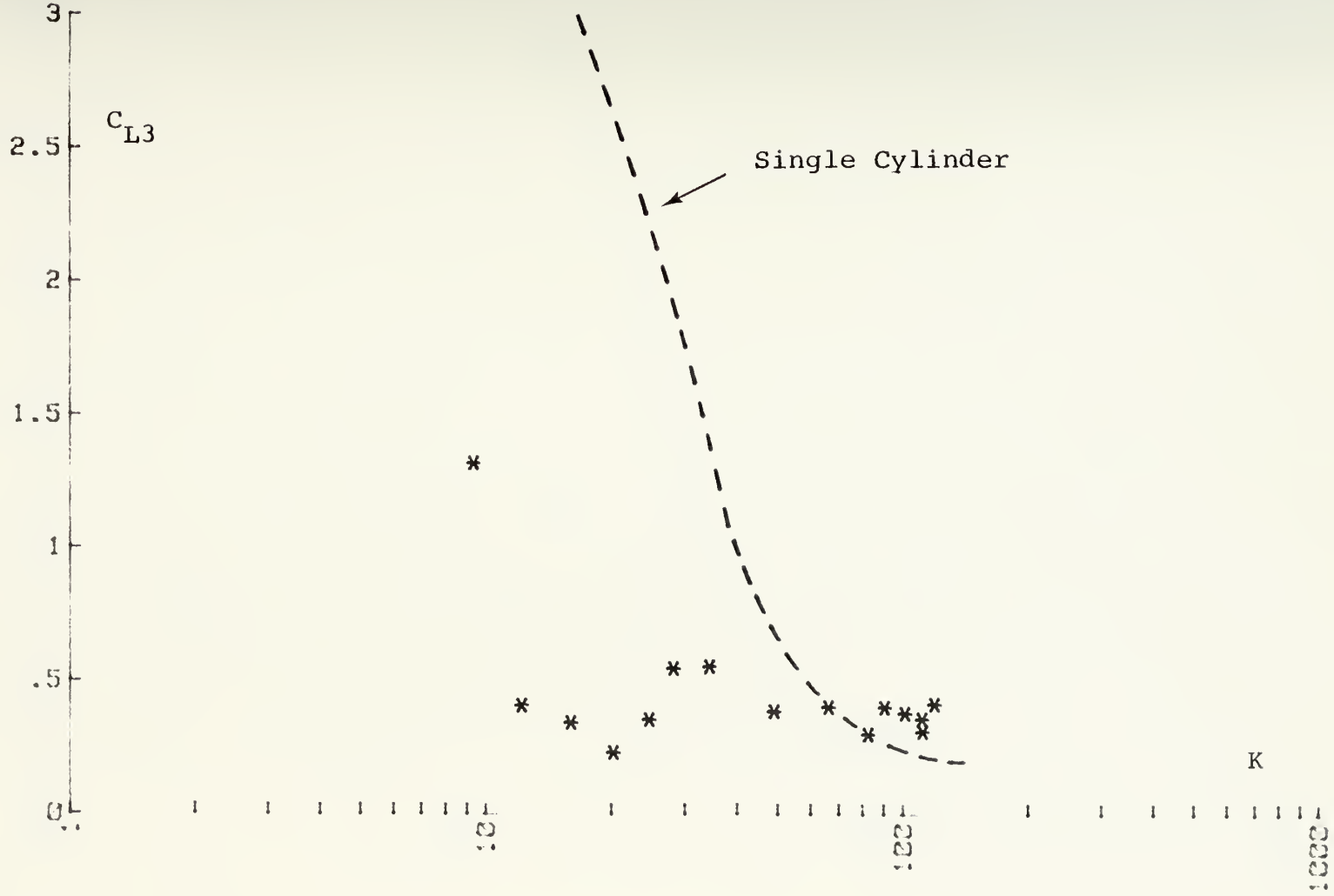

Fig. 42 C_{L3} vs K for N=2 and $\alpha=30^{o}$

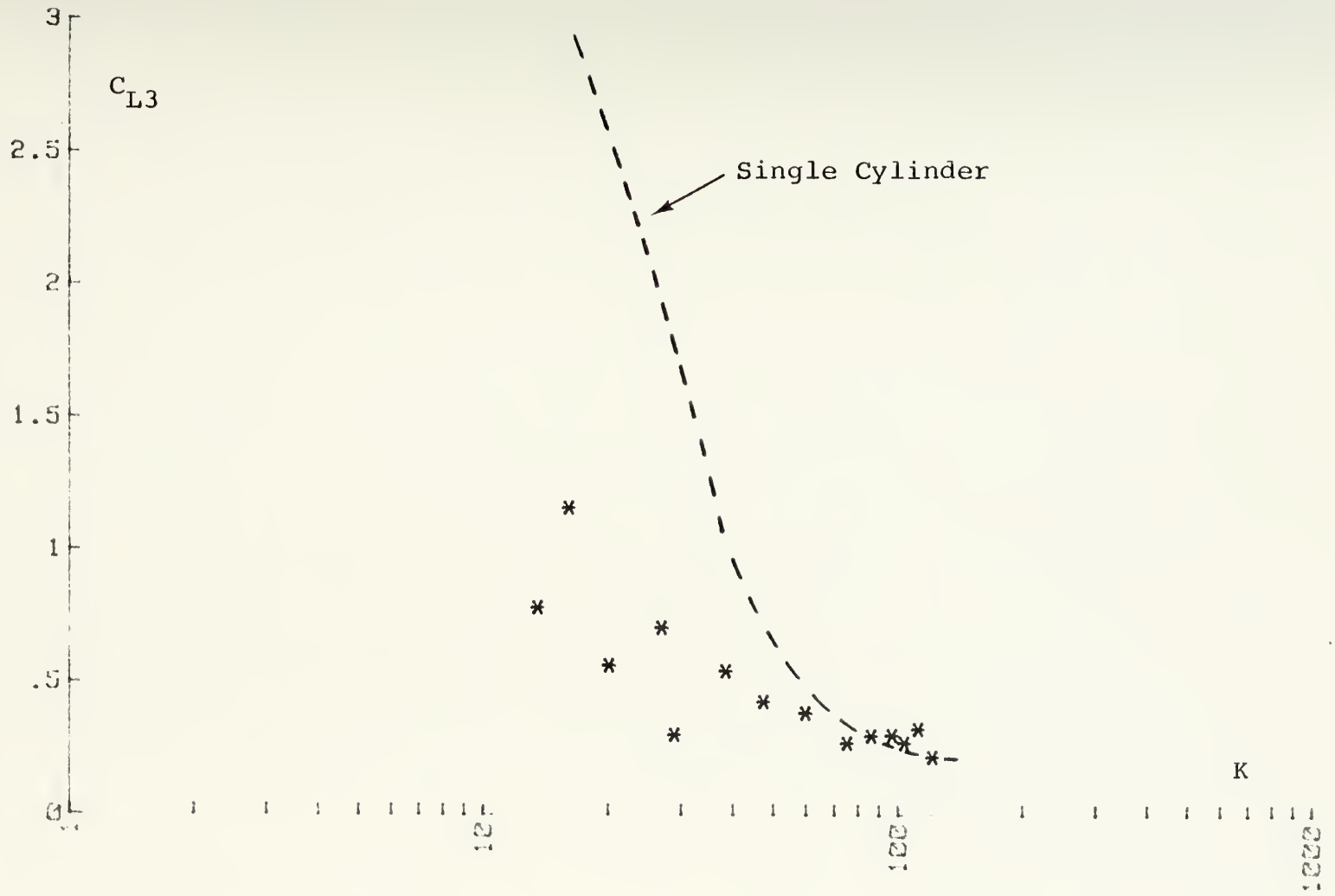

Fig. 43 C_{L3} vs K for N=2.5 and $\alpha=30^{o}$

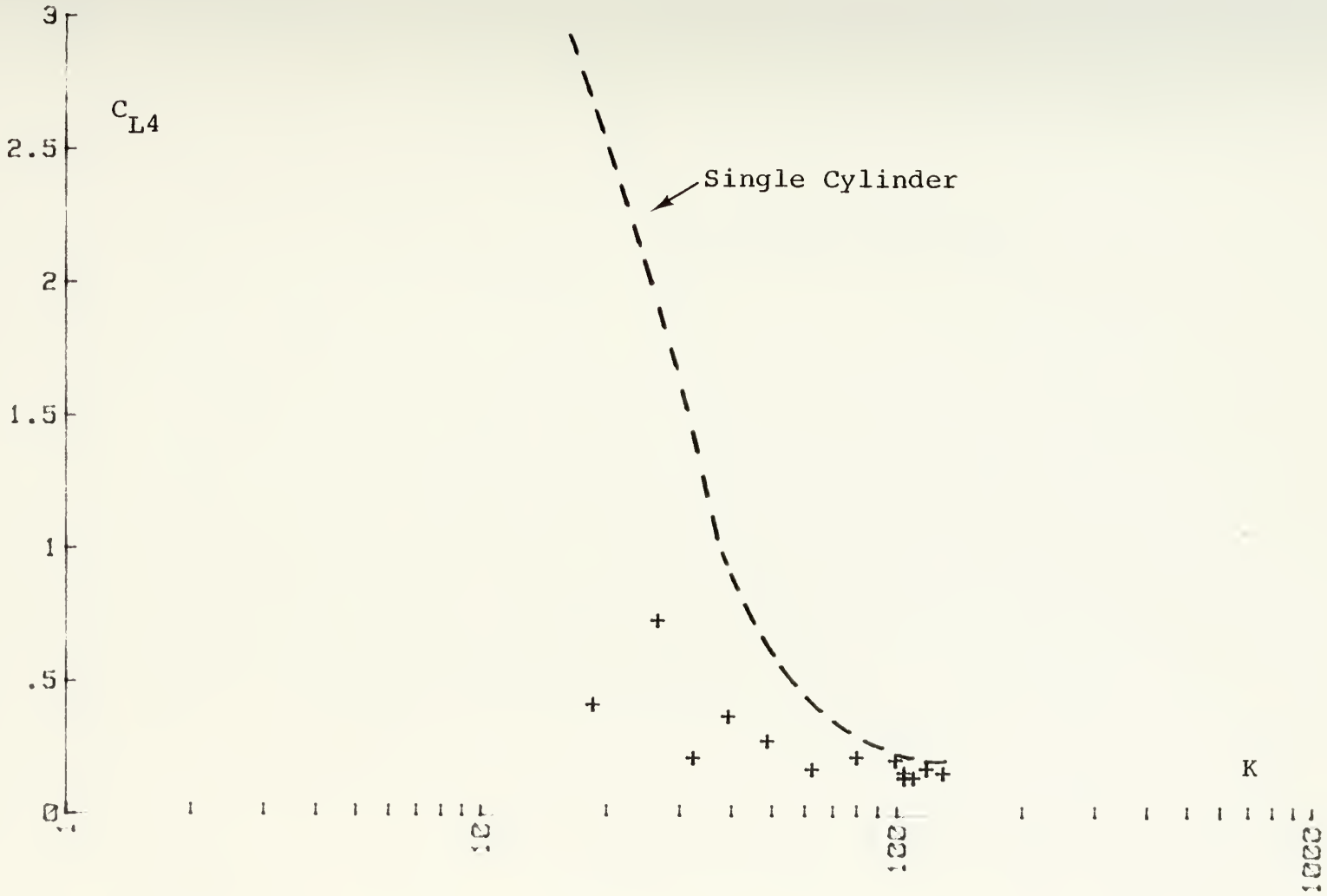

Fig. 44 C_{L4} vs K for N=1.5 and $\alpha=30^{o}$

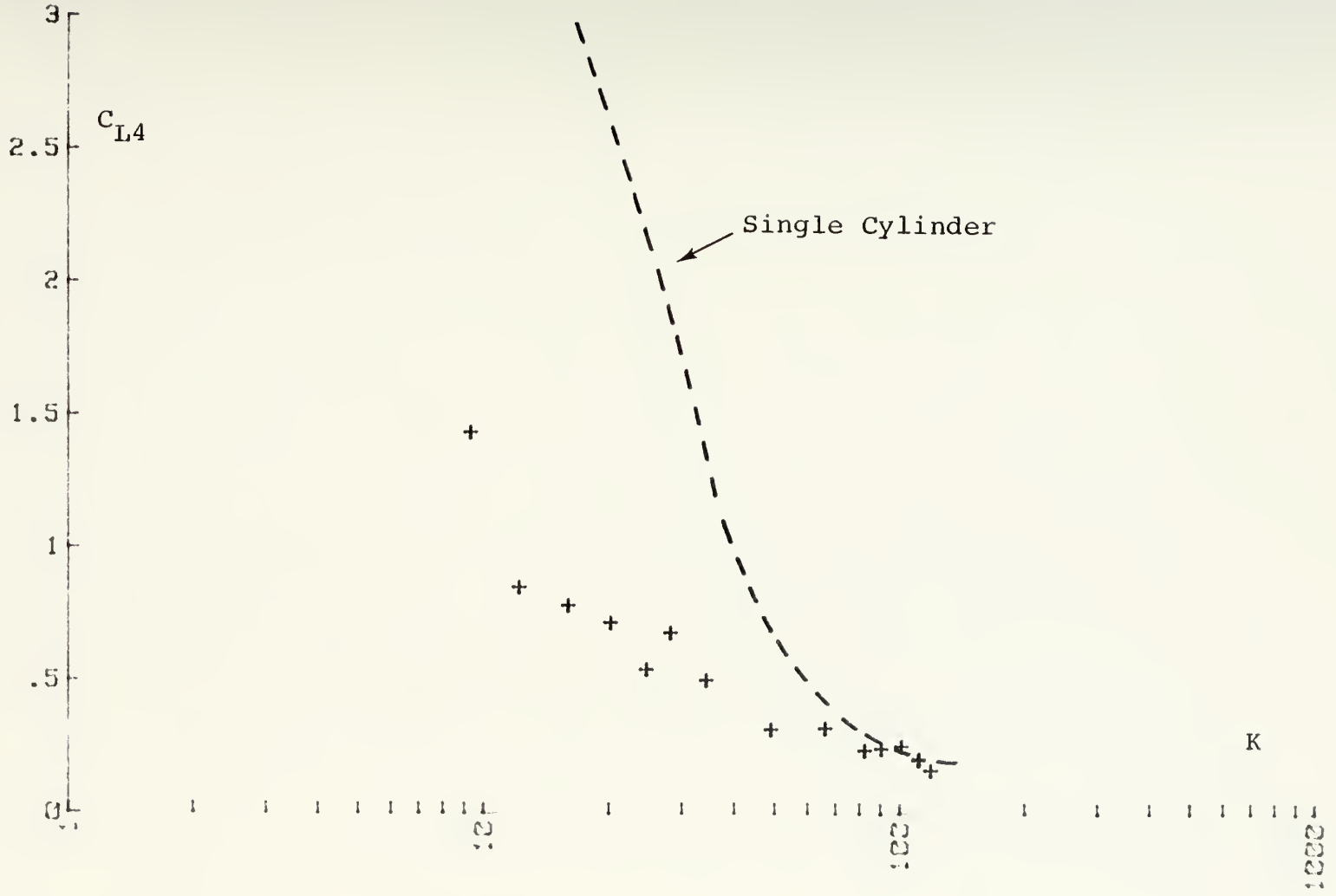

Fig. 45 C_{L4} vs K for N=2 and $\alpha=30^{o}$

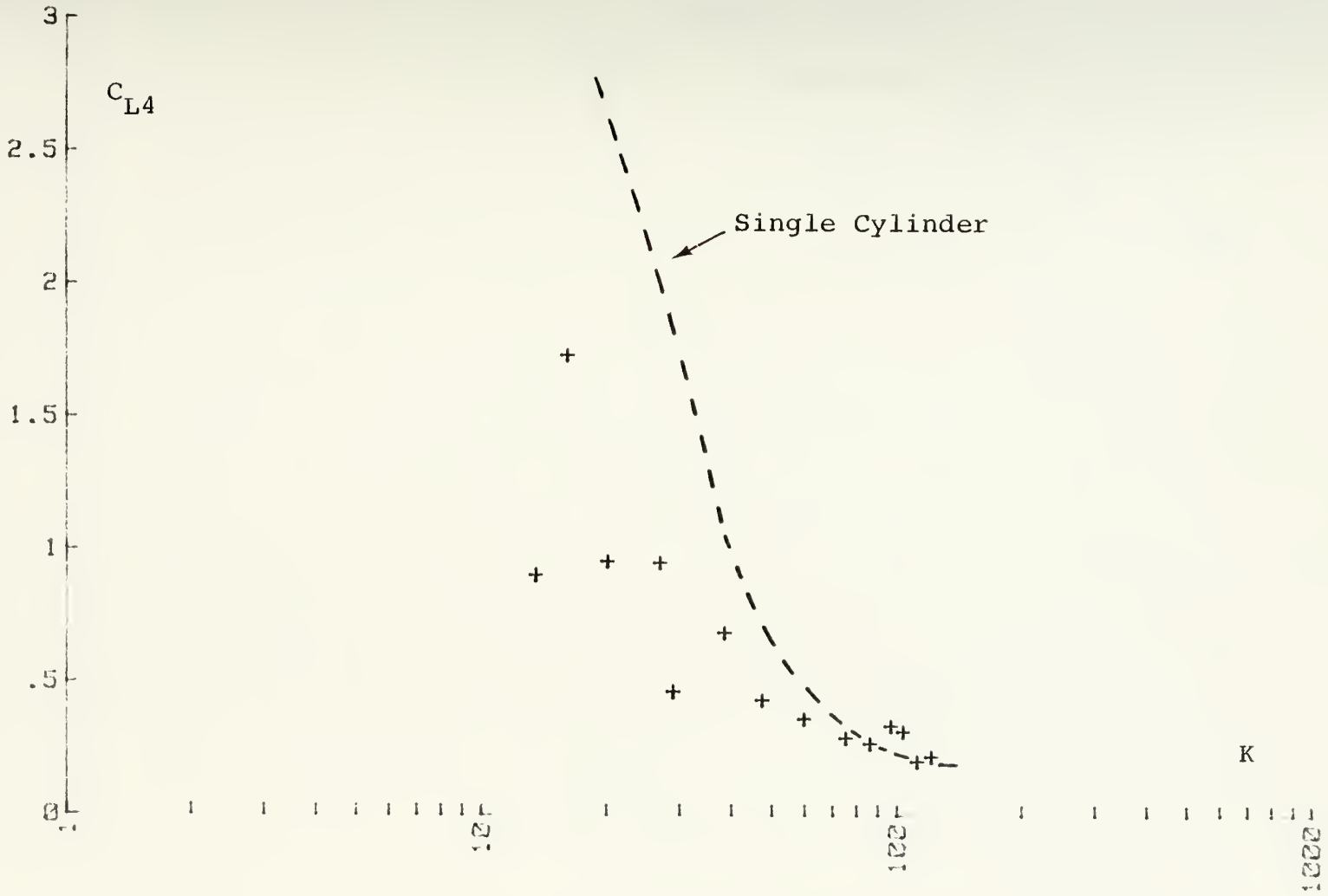

Fig. 46 C_{L4} vs K for N=2.5 and $\alpha=30^{o}$

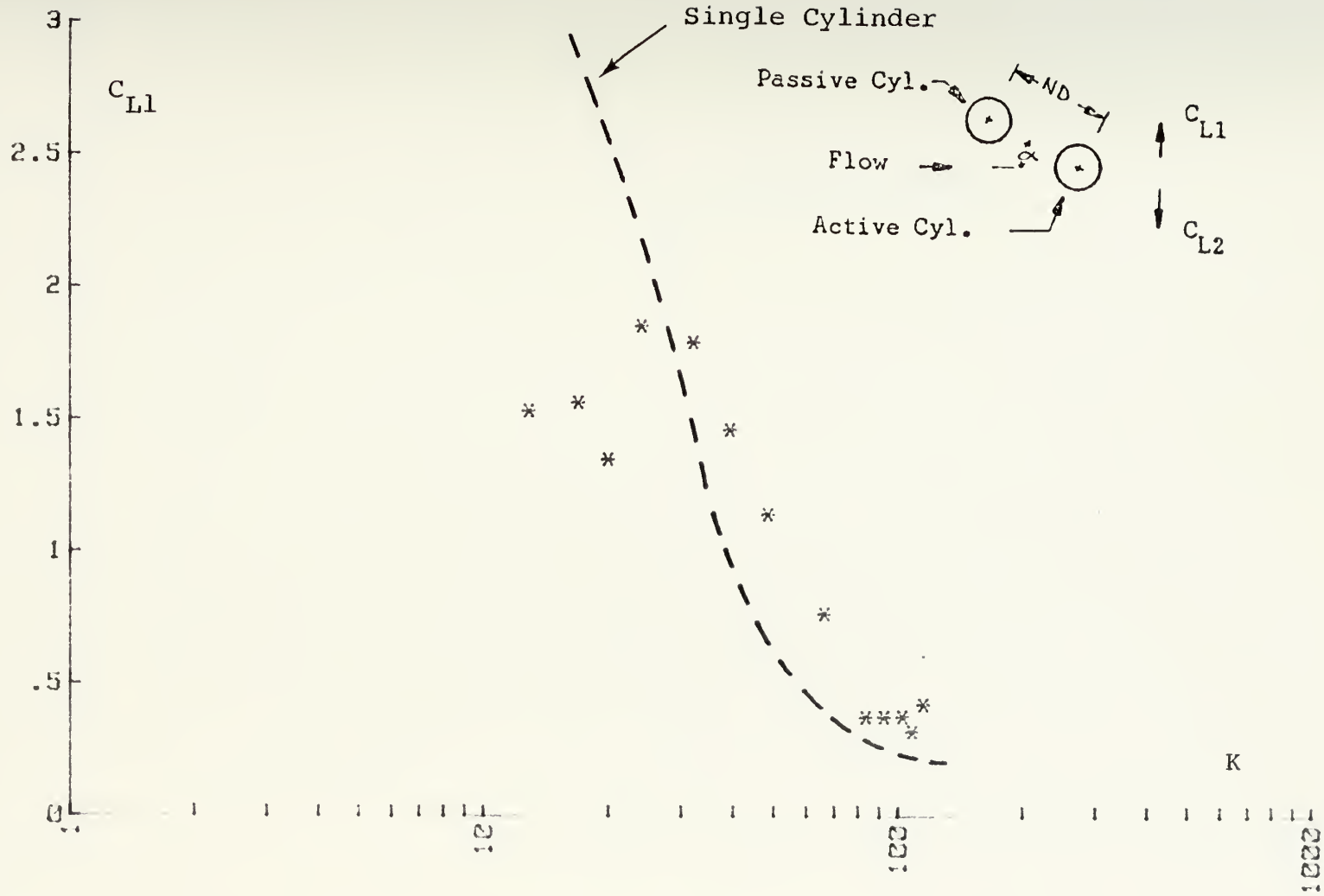

Fig. 47 C_{L1} vs K for N=1.5 and $\alpha=60^{o}$

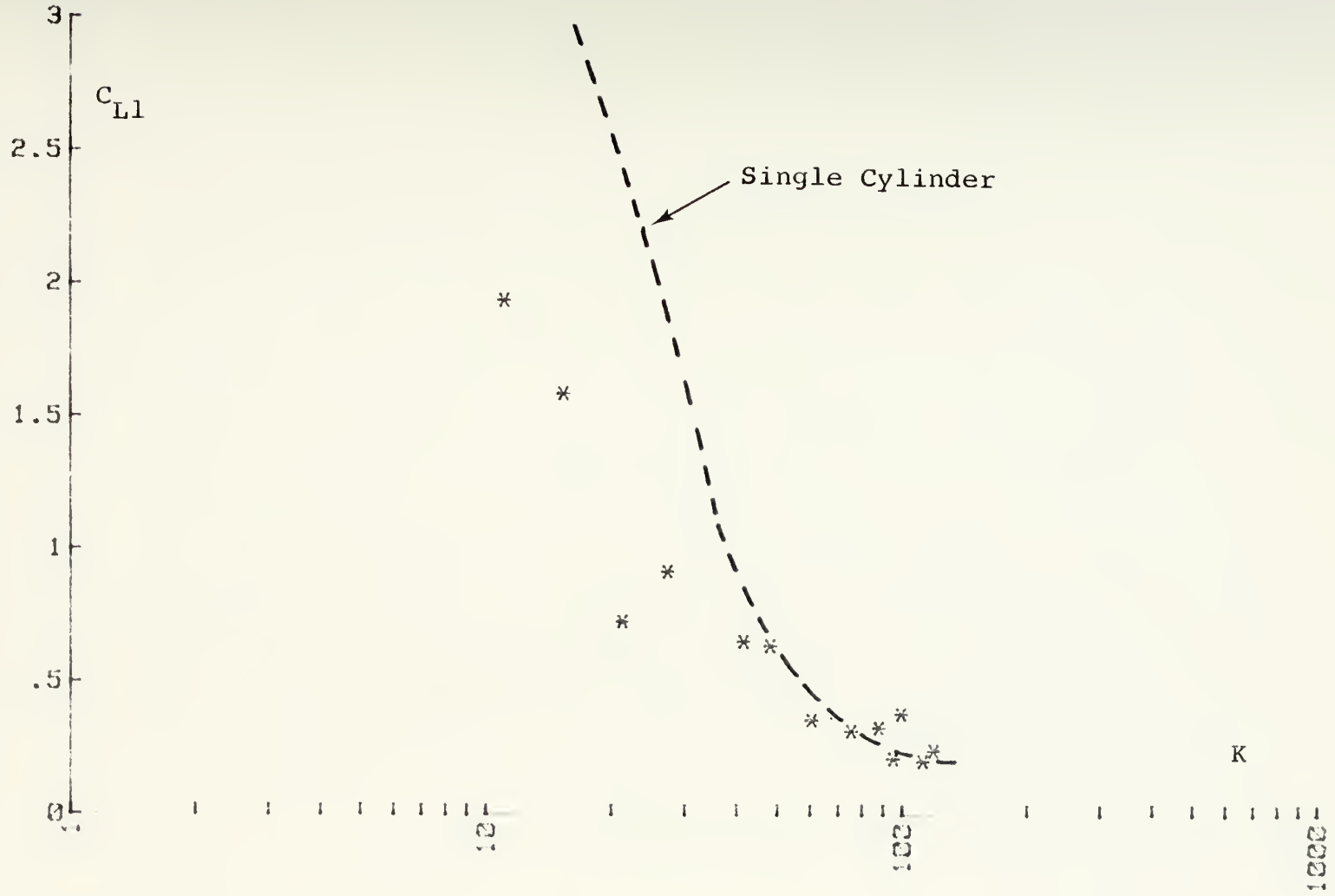

Fig. 48 C_{Ll} vs K for N=2 and $\alpha=60^{o}$

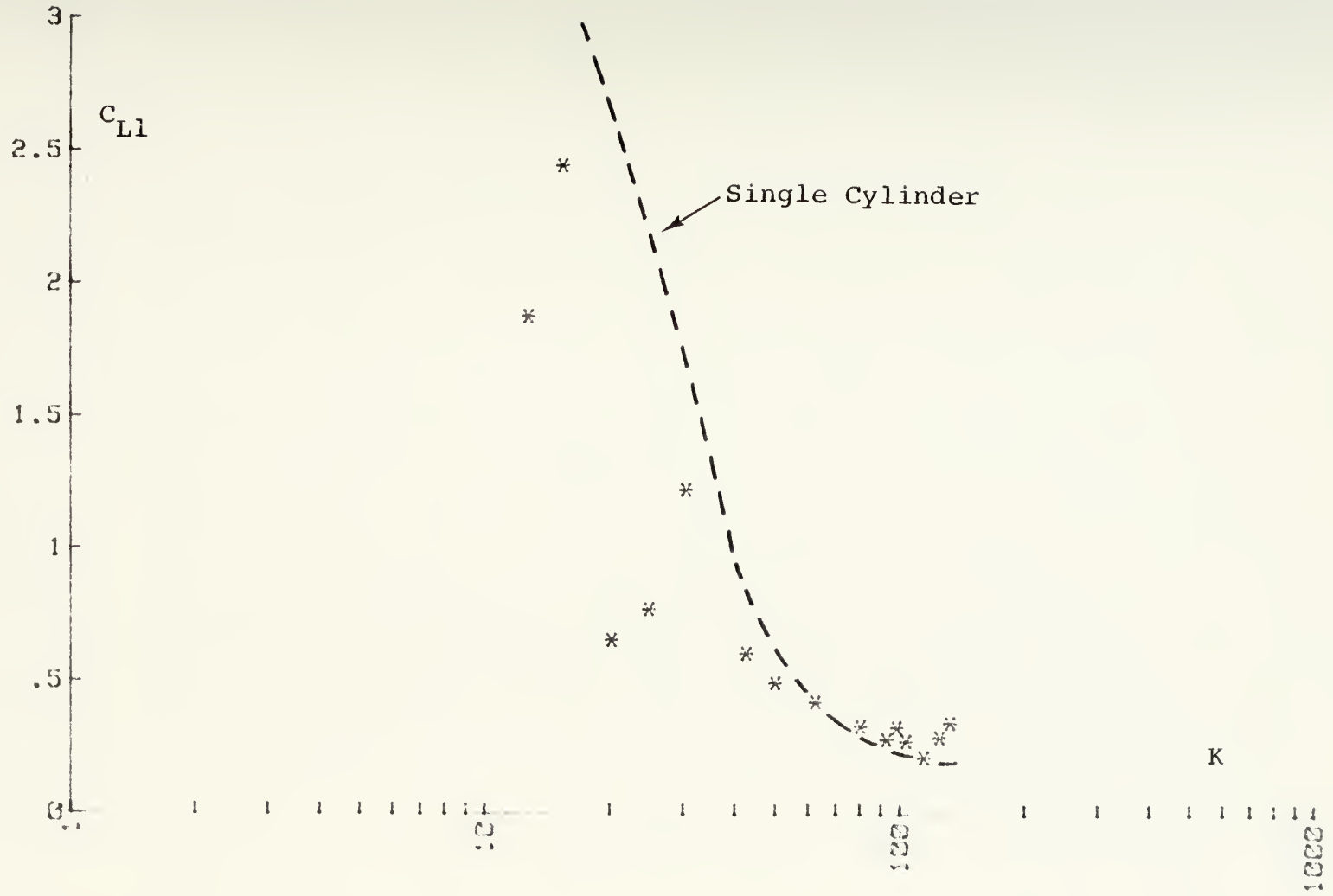

Fig. 49 C_{Ll} vs K for N=2.5 and $\alpha=60^{o}$

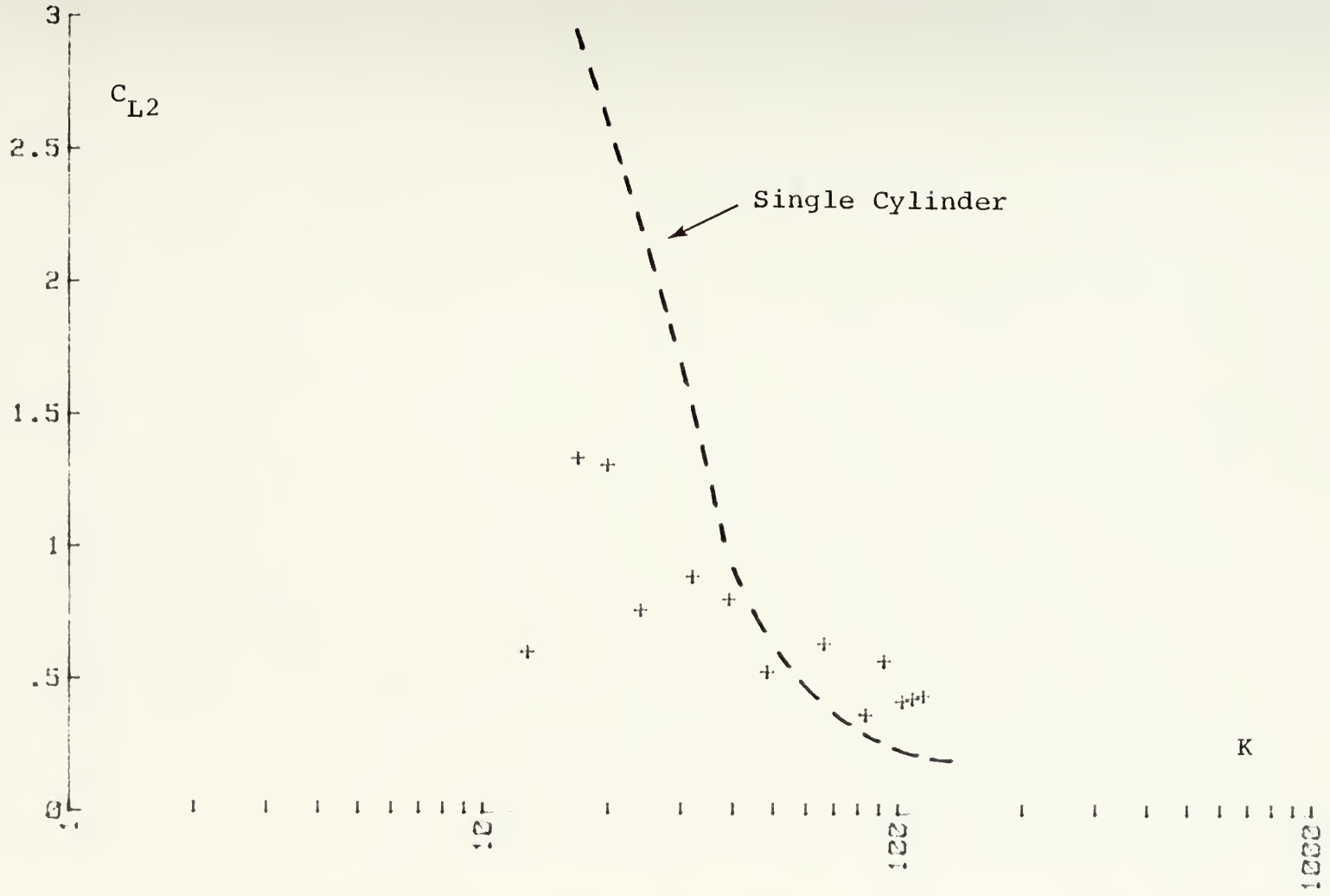

Fig. 50 C_{L2} vs K for N=1.5 and $\alpha=60^{o}$

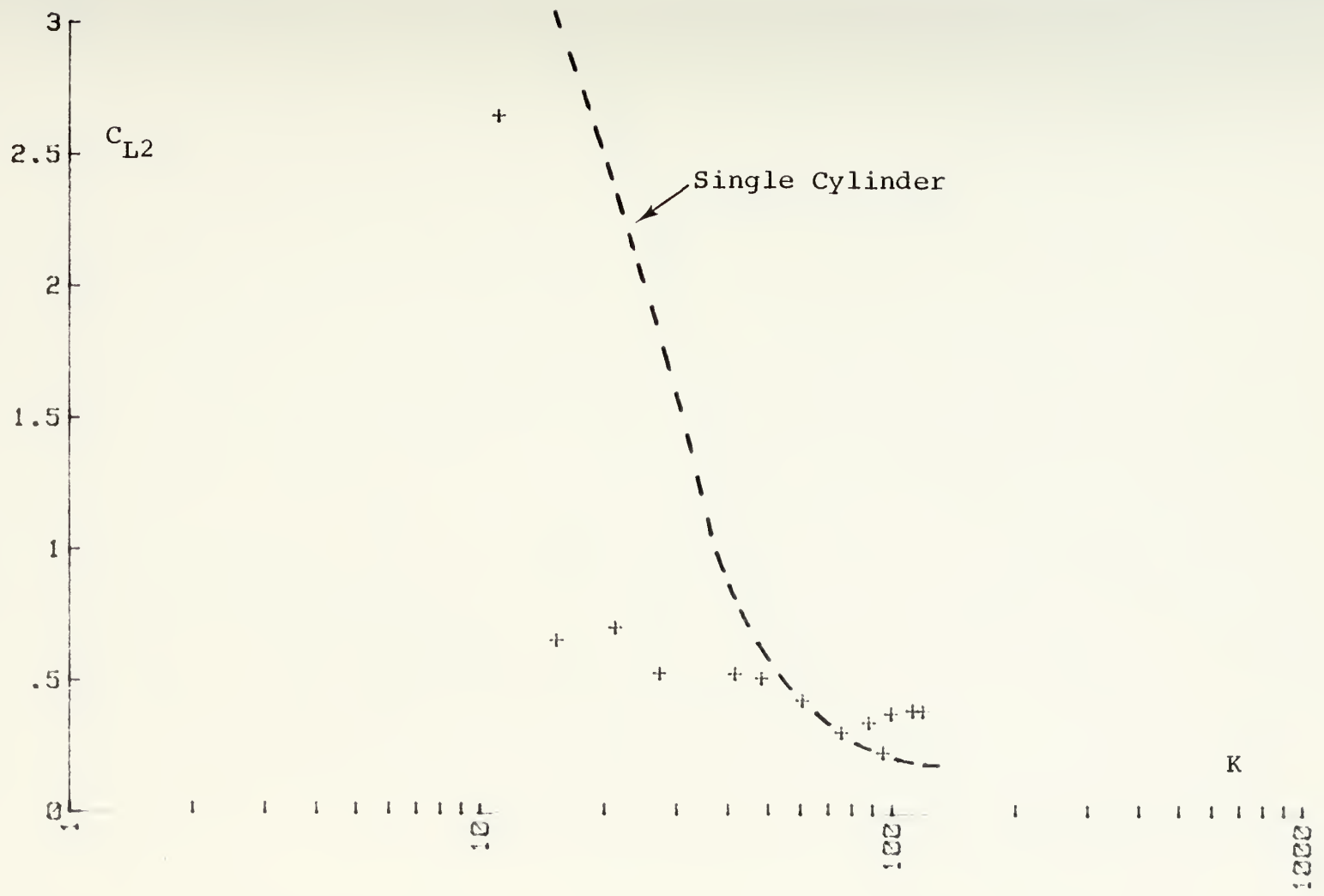

Fig. 51 C_{L2} vs K for N=2 and $\alpha=60^{o}$

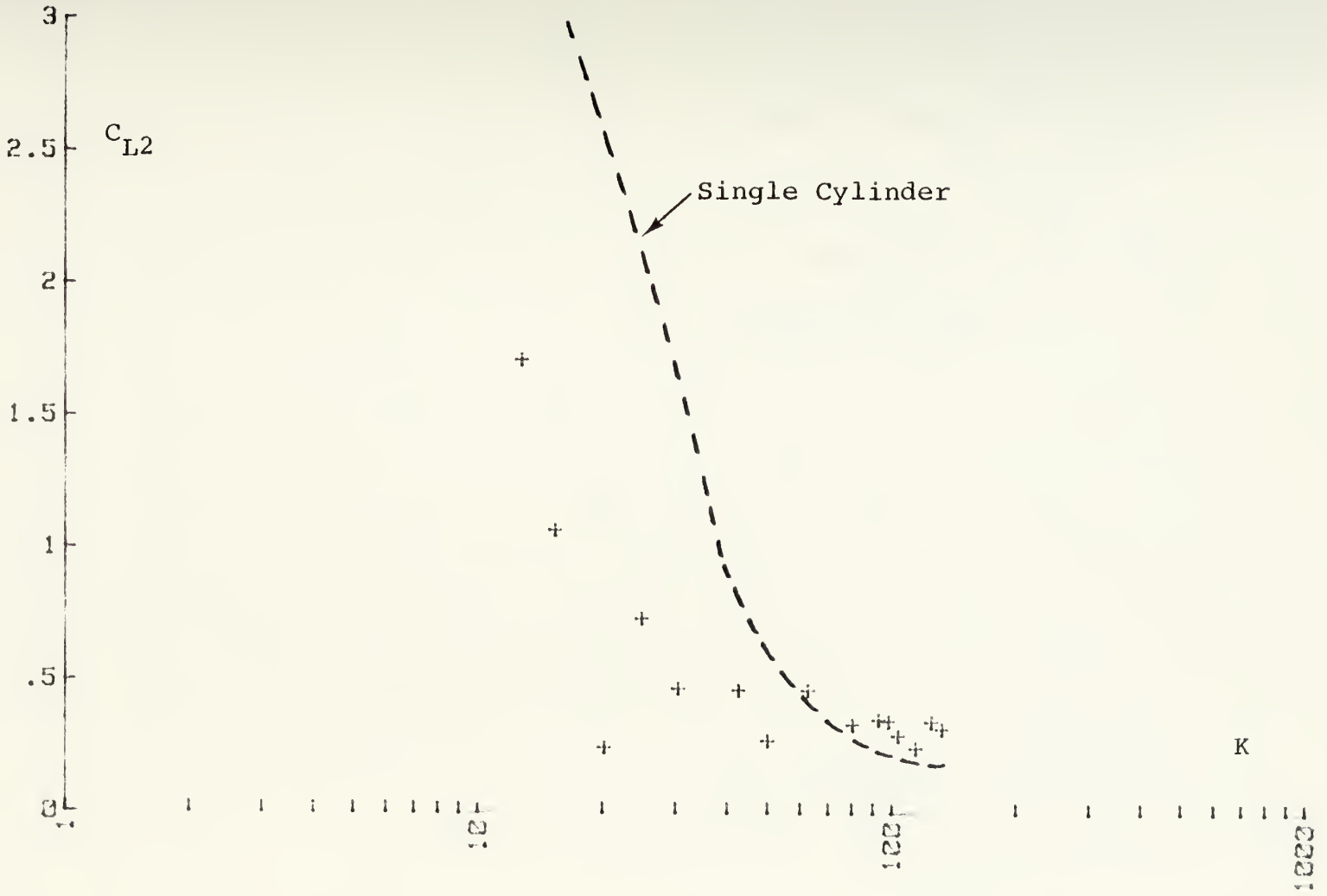

Fig. 52 C_{L2} vs K for N=2 and $\alpha=60^{o}$

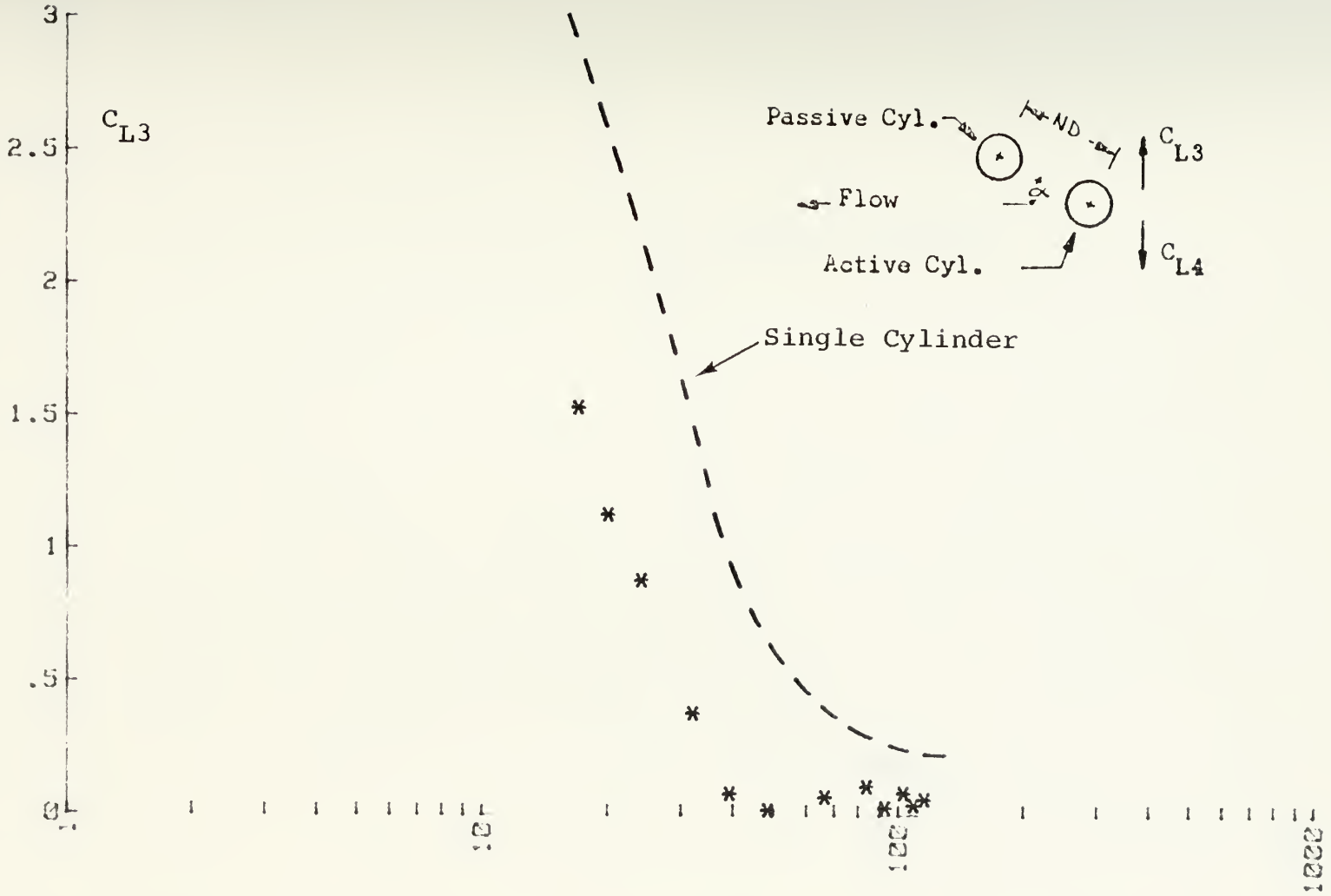

Fig. 53 C_{L3} vs K for N=1.5 and $\alpha=60^{\circ}$

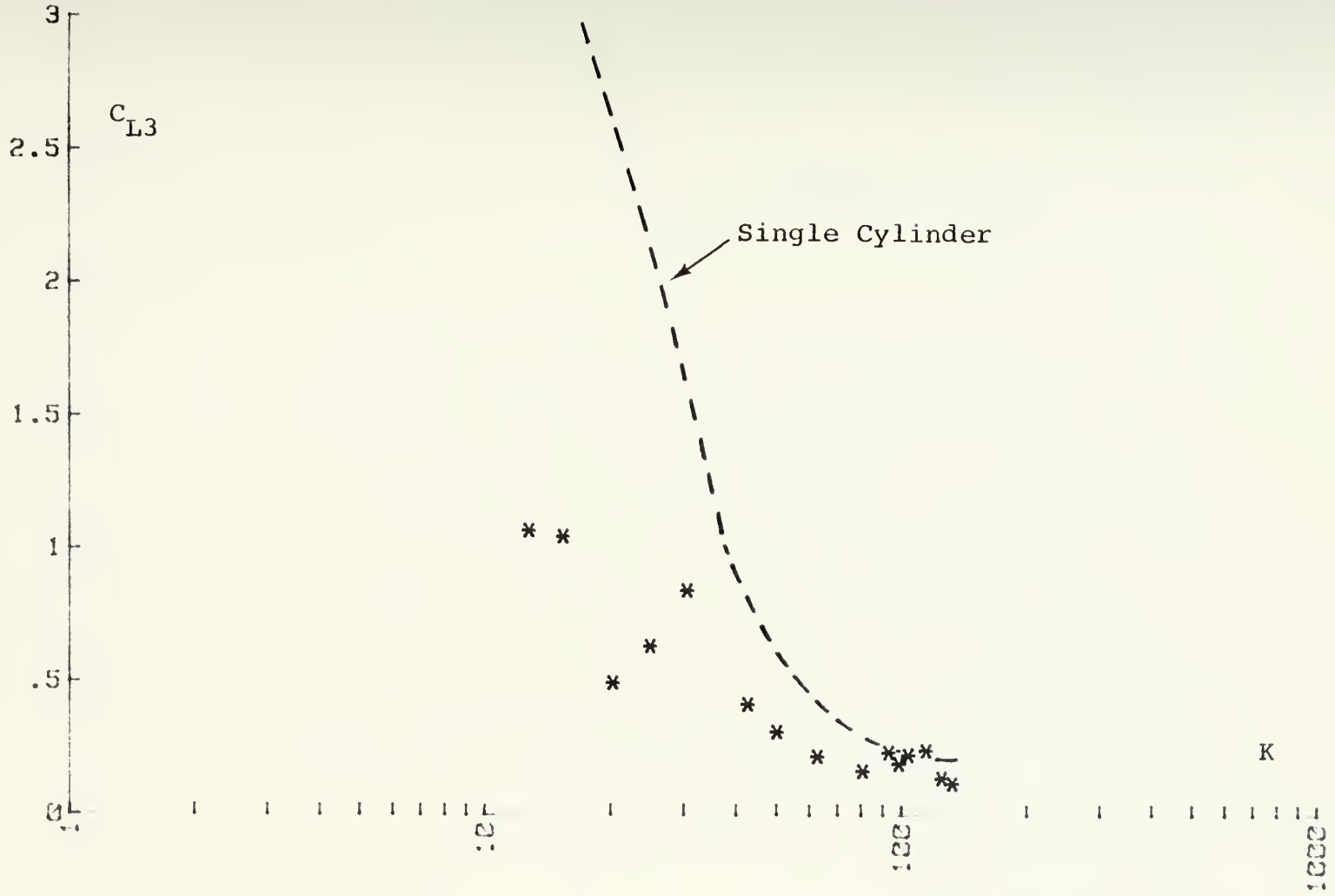

Fig. 55 C_{L3} vs K for N=2.5 and $\alpha=60^{o}$

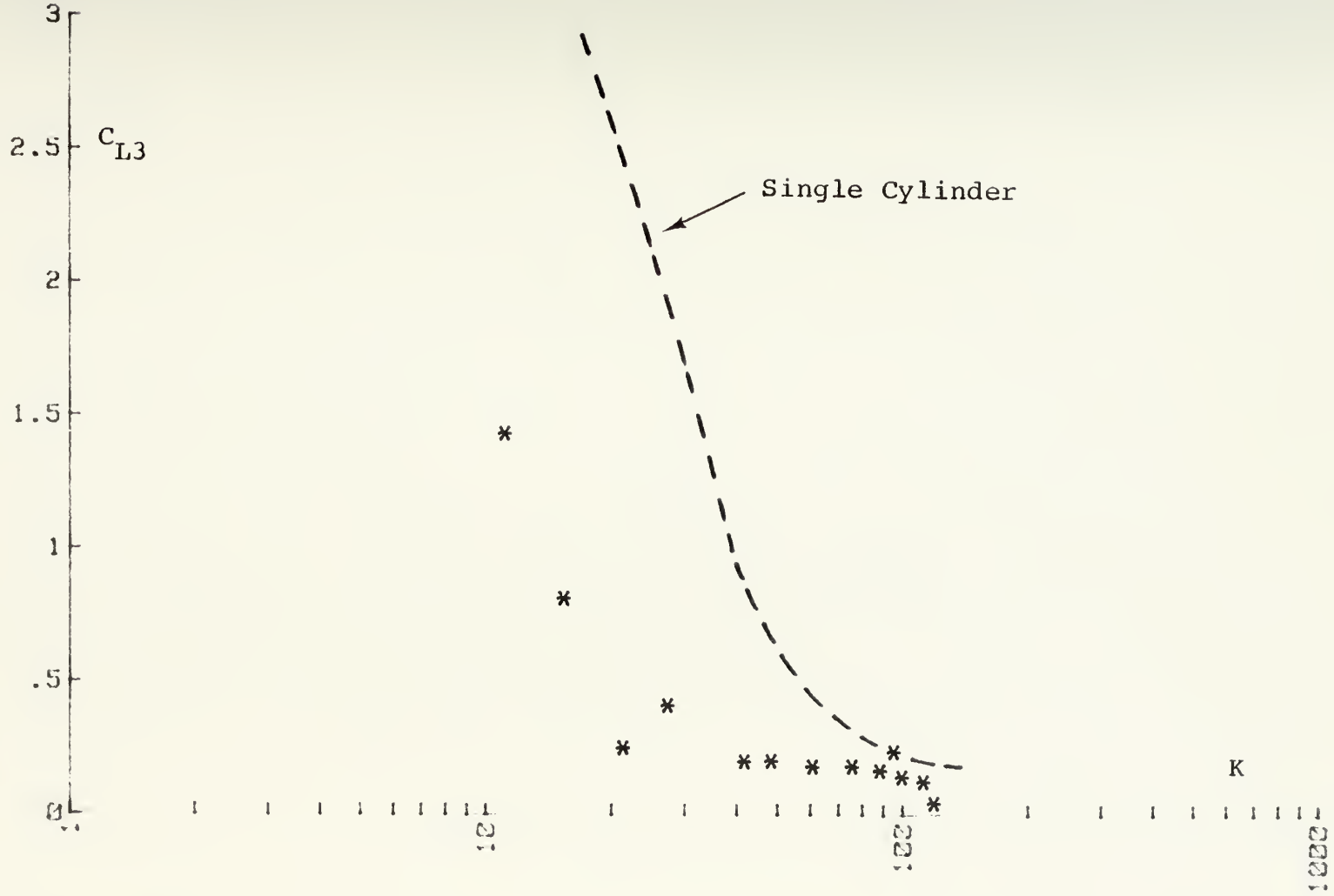

Fig. 54 C_{L3} vs K for N=2 and $\alpha=60^{o}$

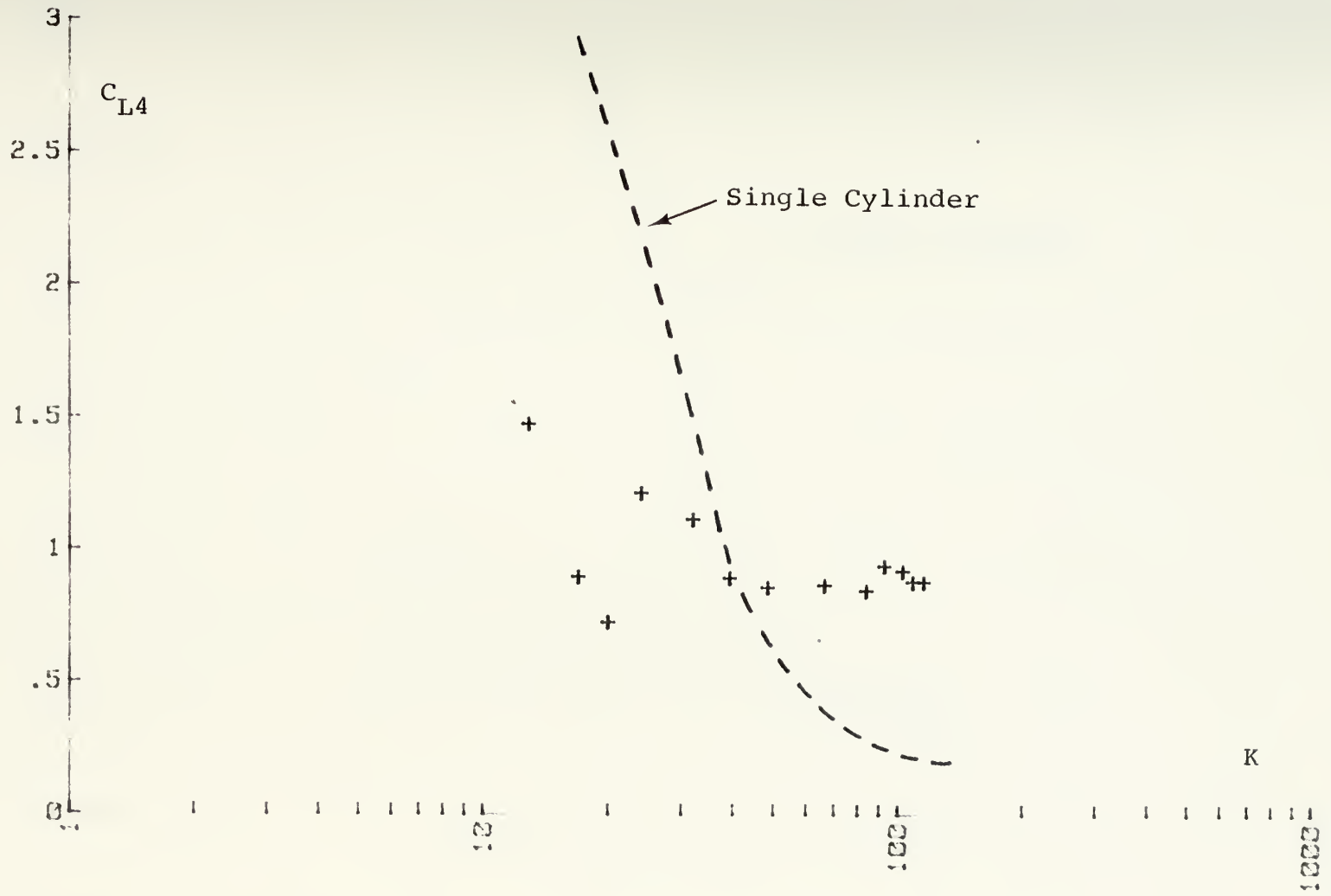

Fig. 56 C_{L4} vs K for N=1.5 and $\alpha=60^{o}$

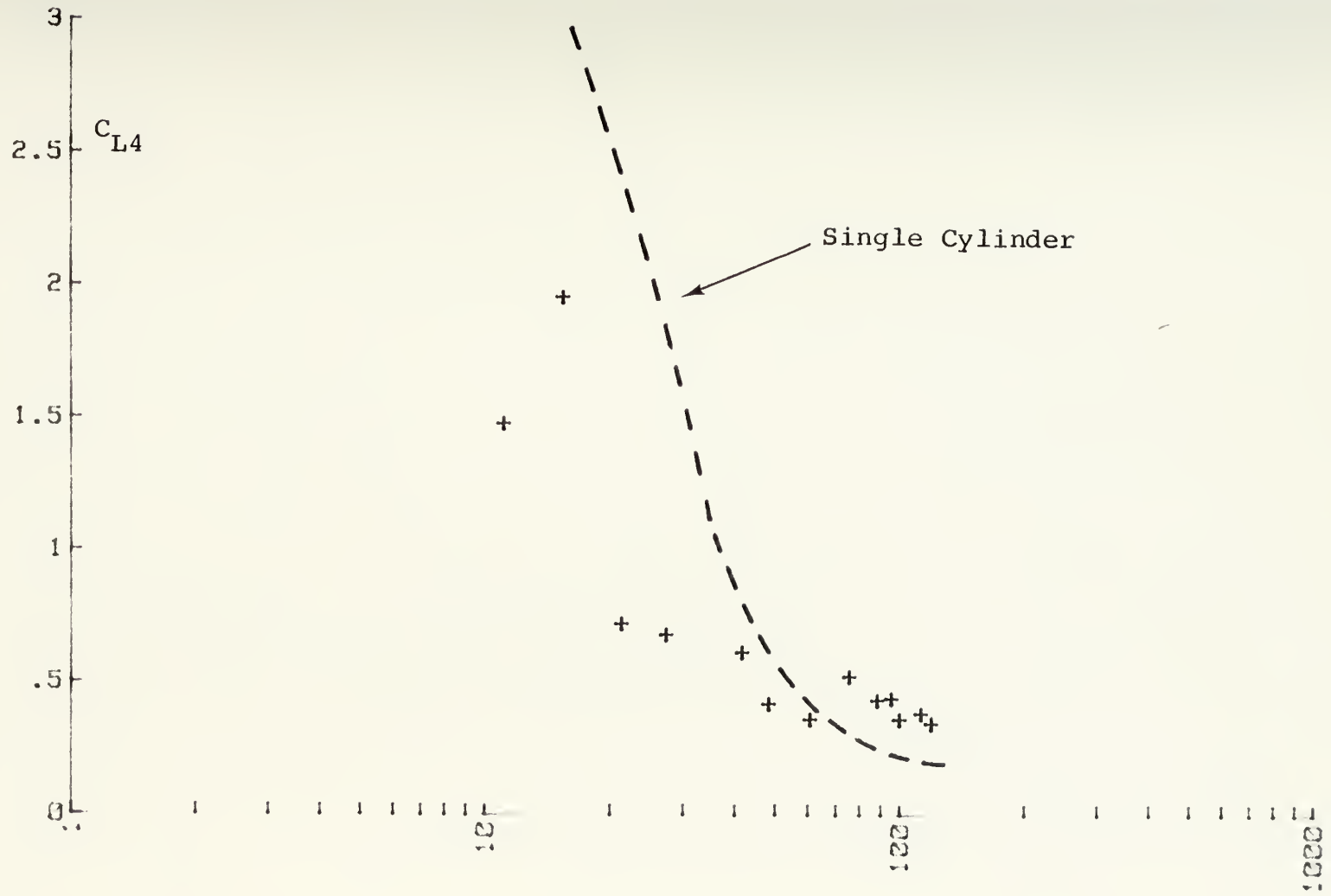

Fig. 57 C_{L4} vs K for N=2 and $\alpha=60^{o}$

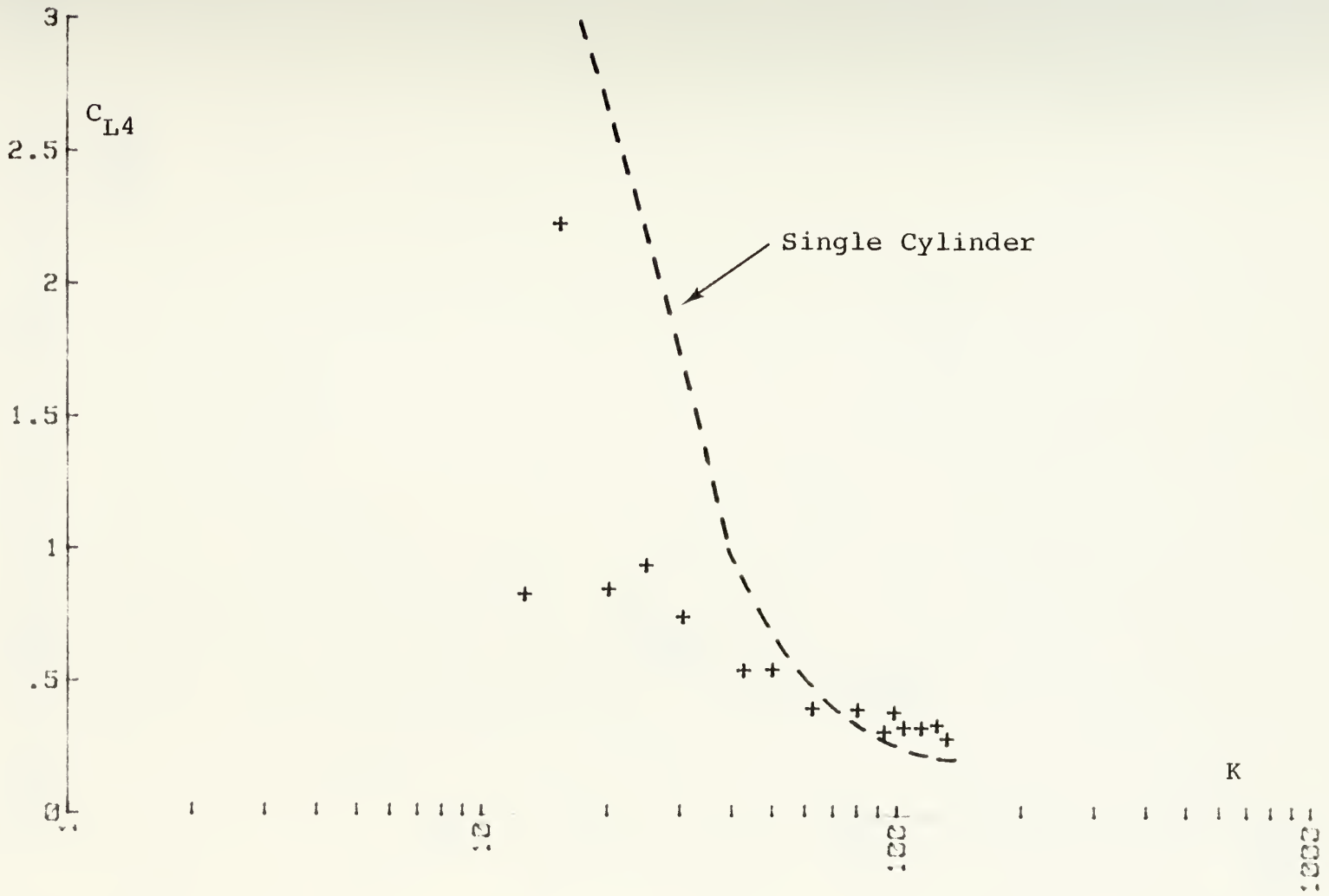

Fig. 58 C_{L4} vs K for N=2.5 and $\alpha=60^{o}$

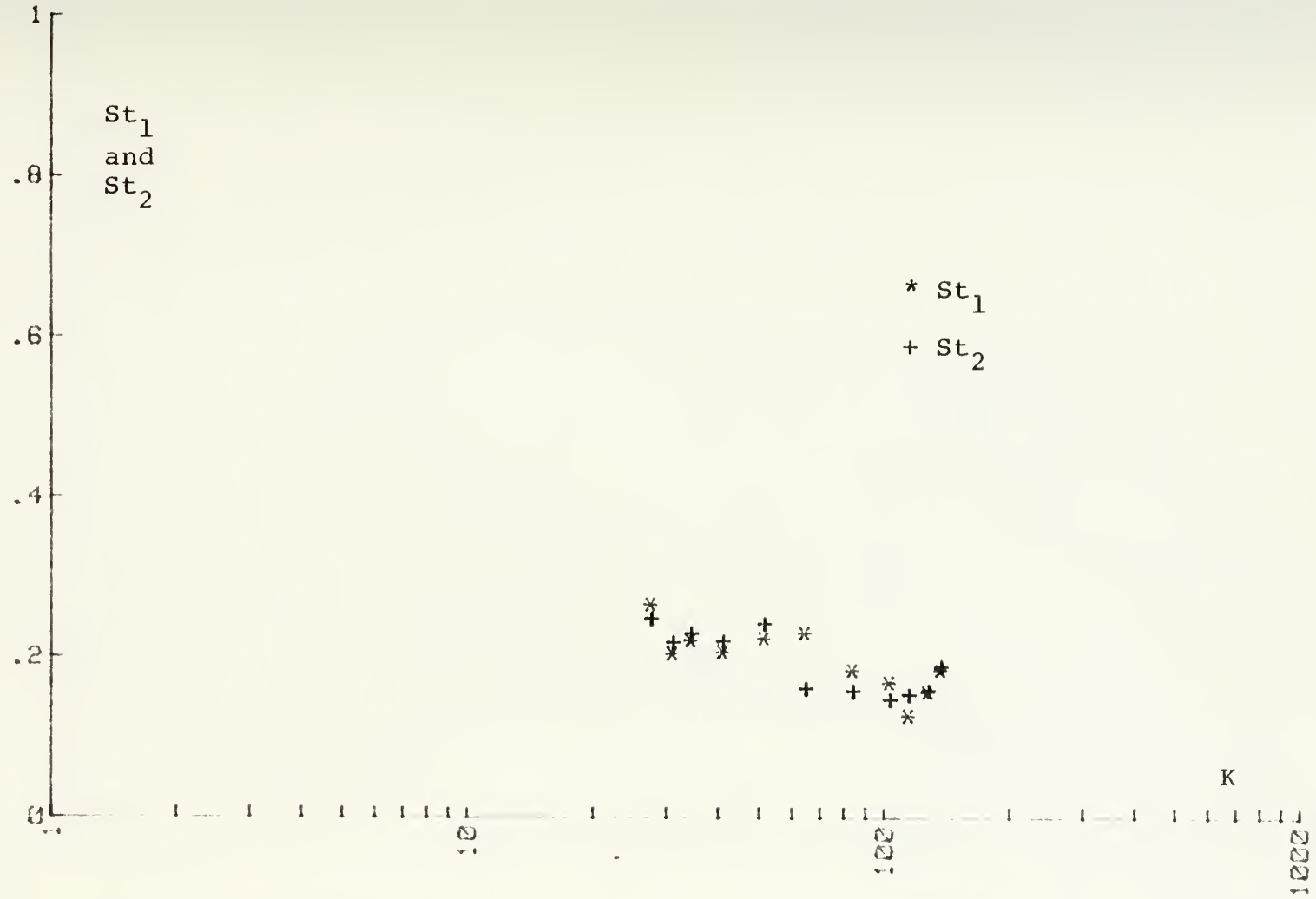

Fig. 59 St_1 and St_2 vs K for N=1.5 and $\alpha=0^o$

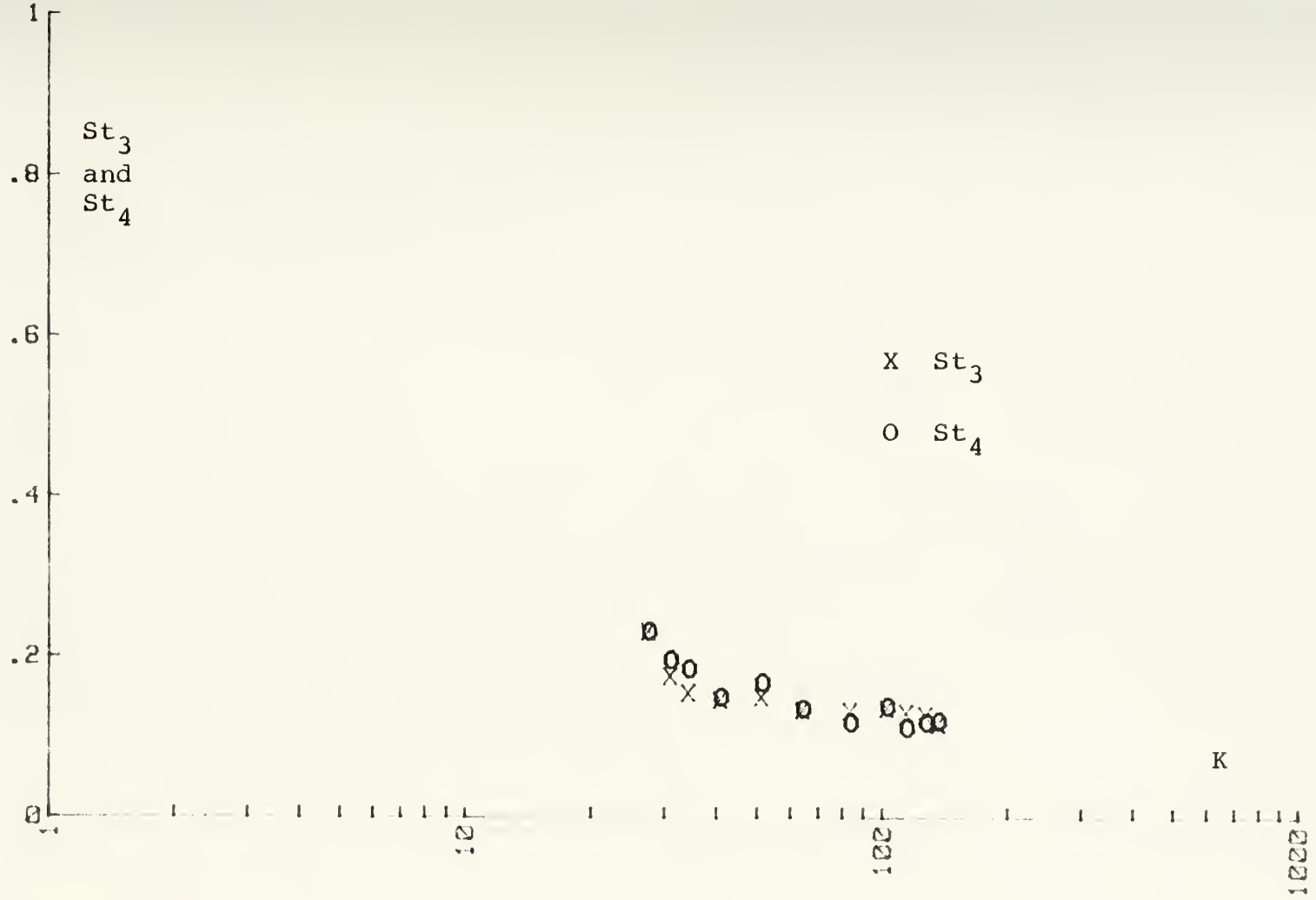

Fig. 60 St_3 and St_4 vs K for N=1.5 and $\alpha=0^{o}$

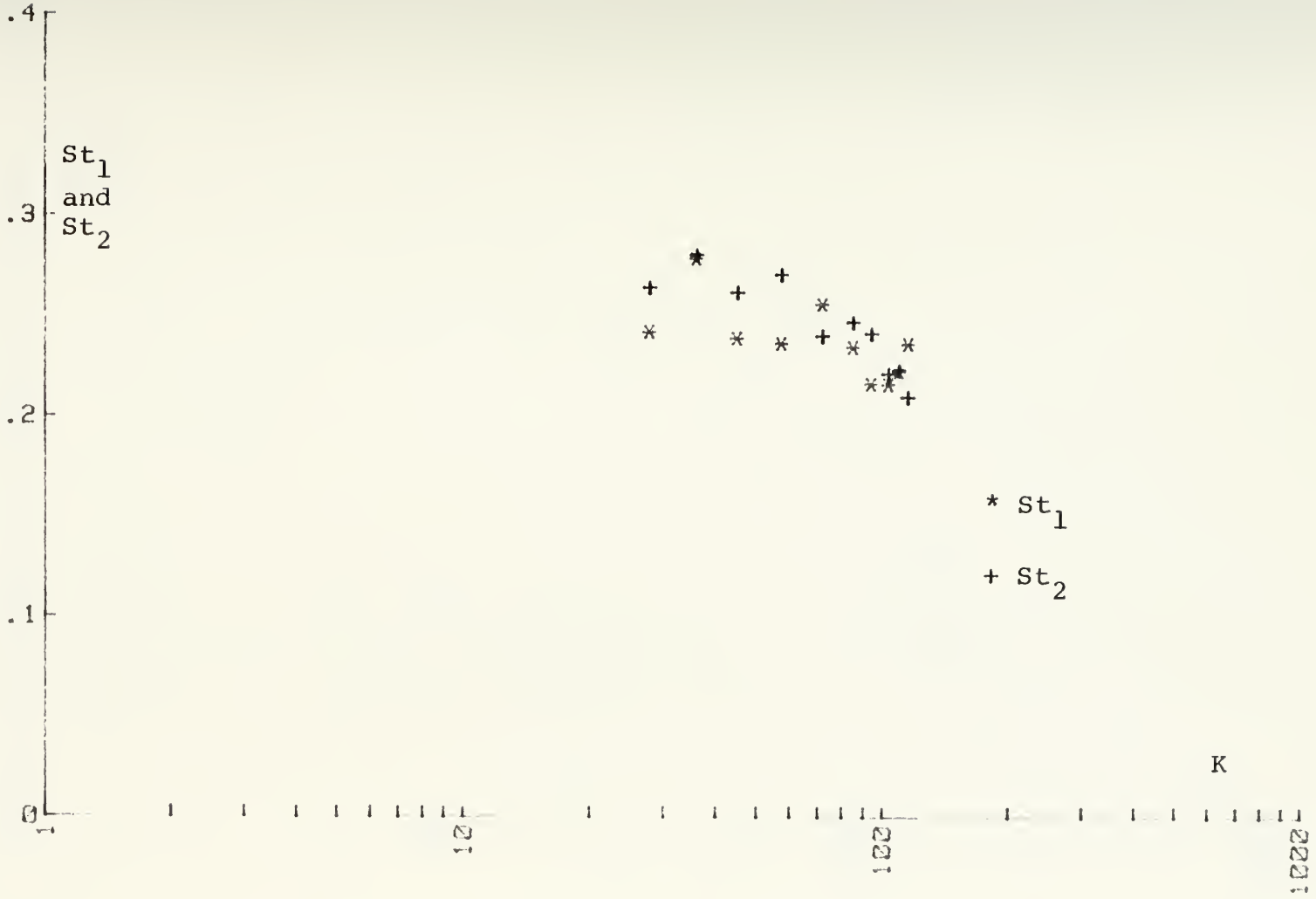

Fig. 61 St_1 and St_2 vs K for N=2 and $\alpha=90^{o}$

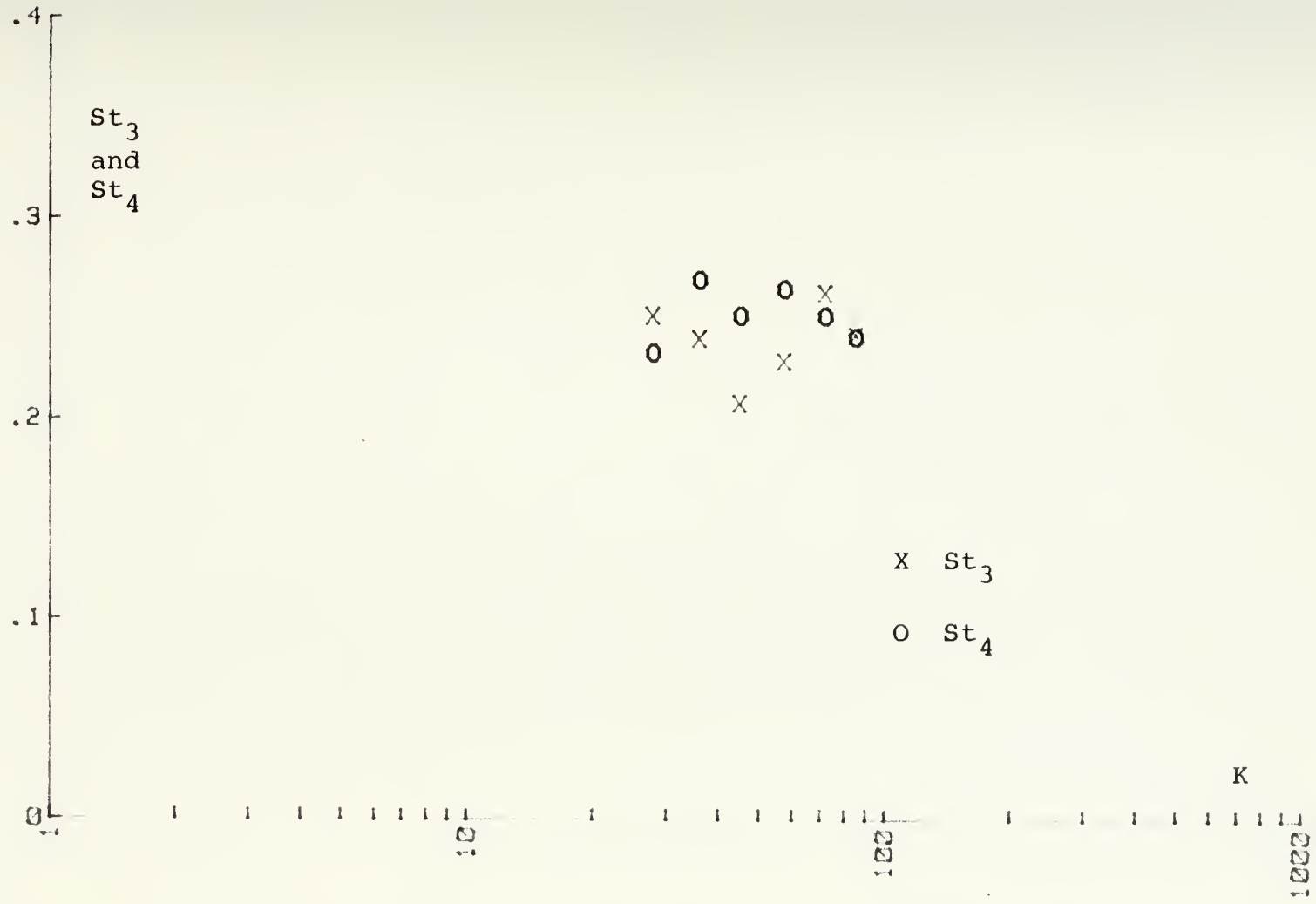

Fig. 62 St_3 and St_4 vs K for N=2 and $\alpha=90^{\circ}$

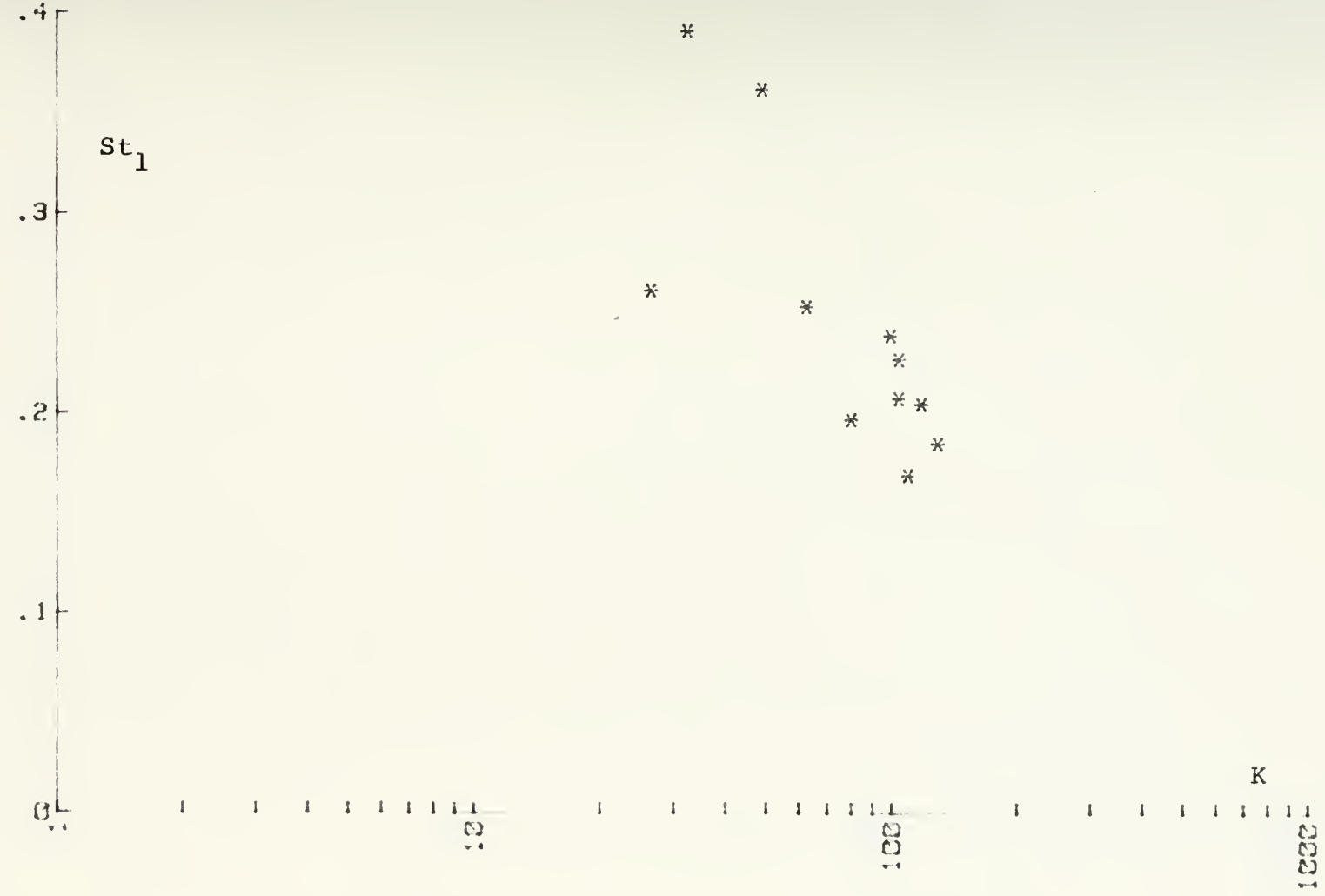

Fig. 63 St_1 vs K for N=1.5 and $\alpha=30^{o}$

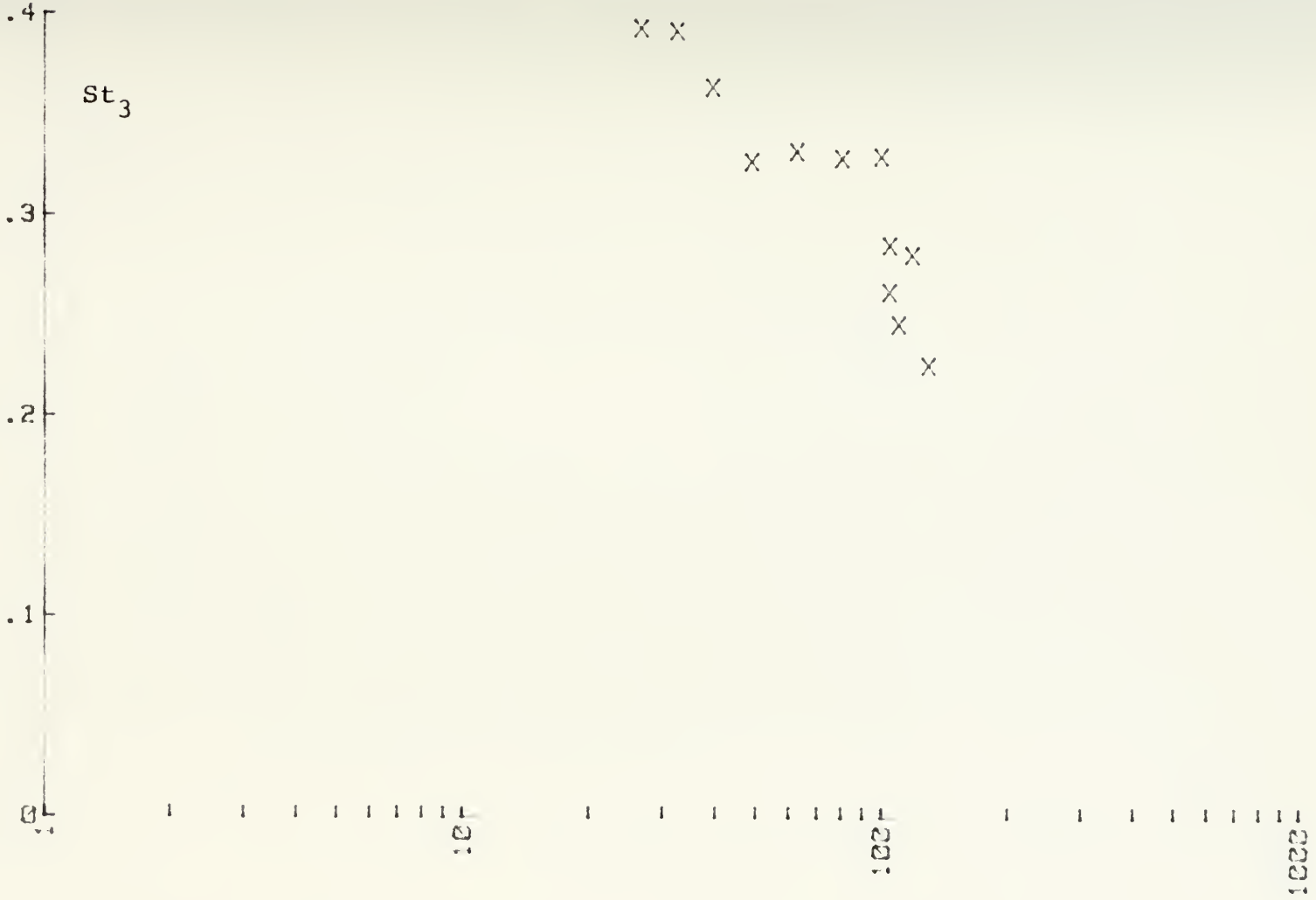

Fig. 64 St_3 vs K for N=1.5 and $\alpha=30^{o}$

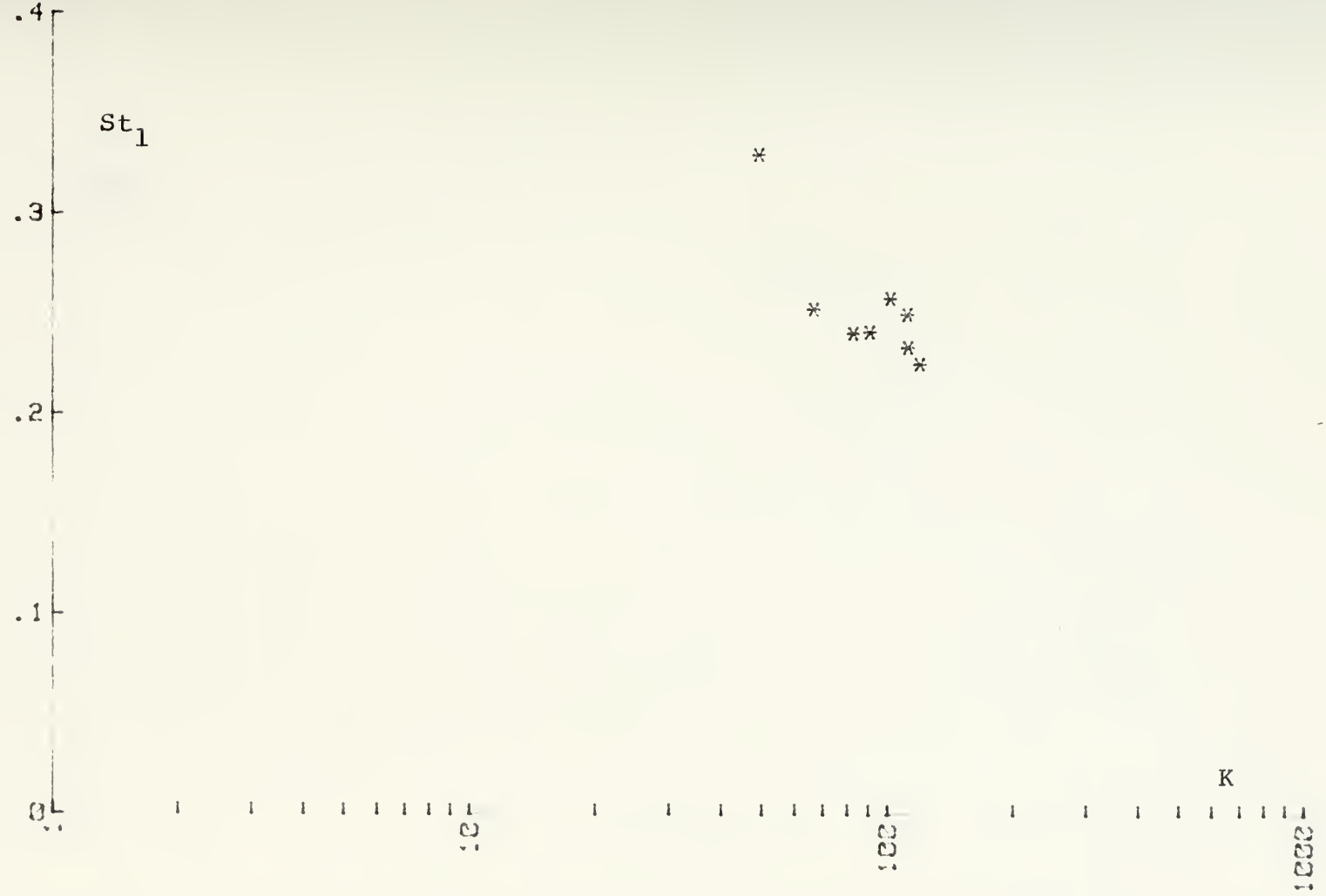

Fig. 65 St_1 vs K for N=2 and $\alpha=30^{o}$

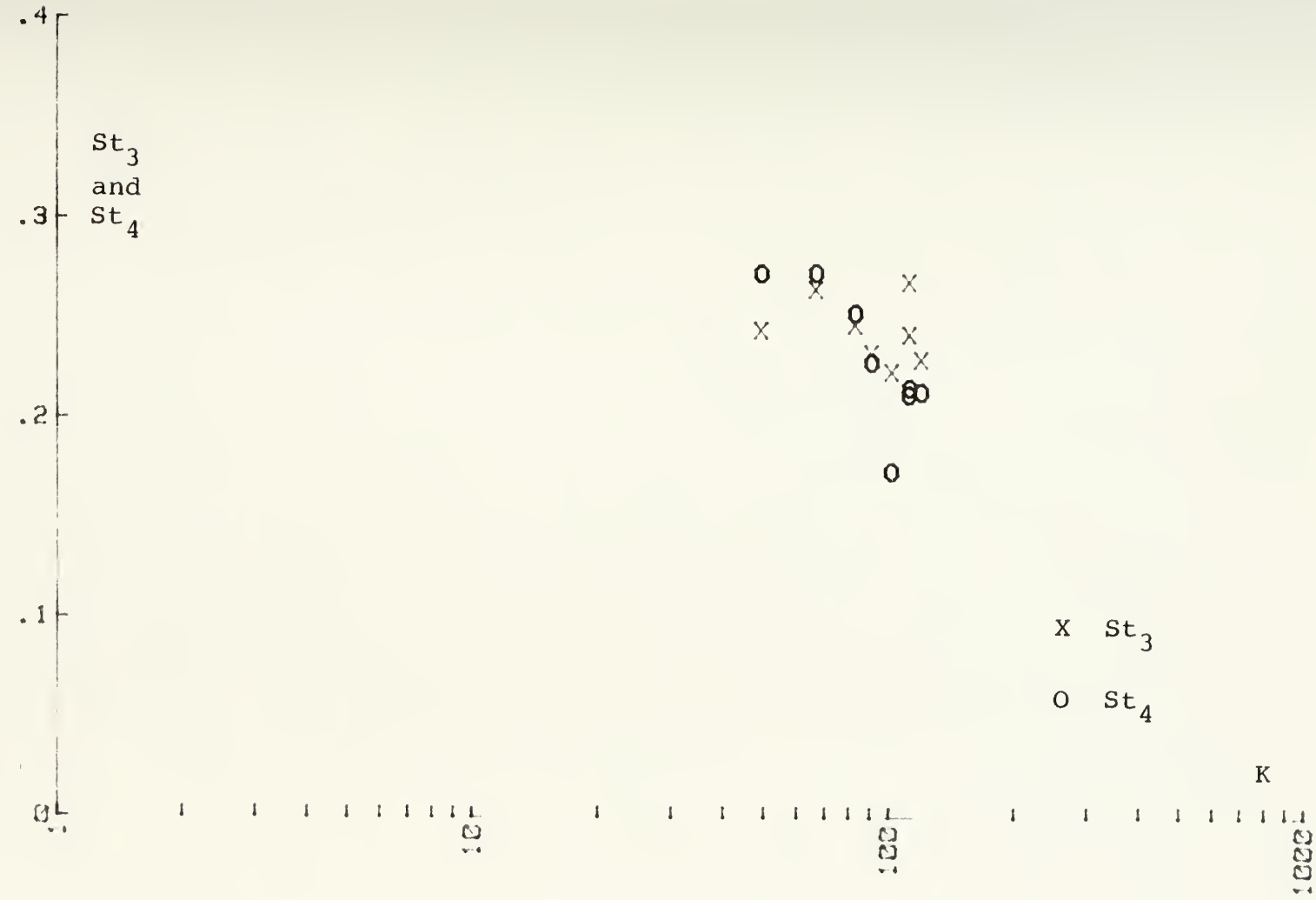

Fig. 66 St_3 and St_4 vs K for N=2 and $\alpha=30^{o}$

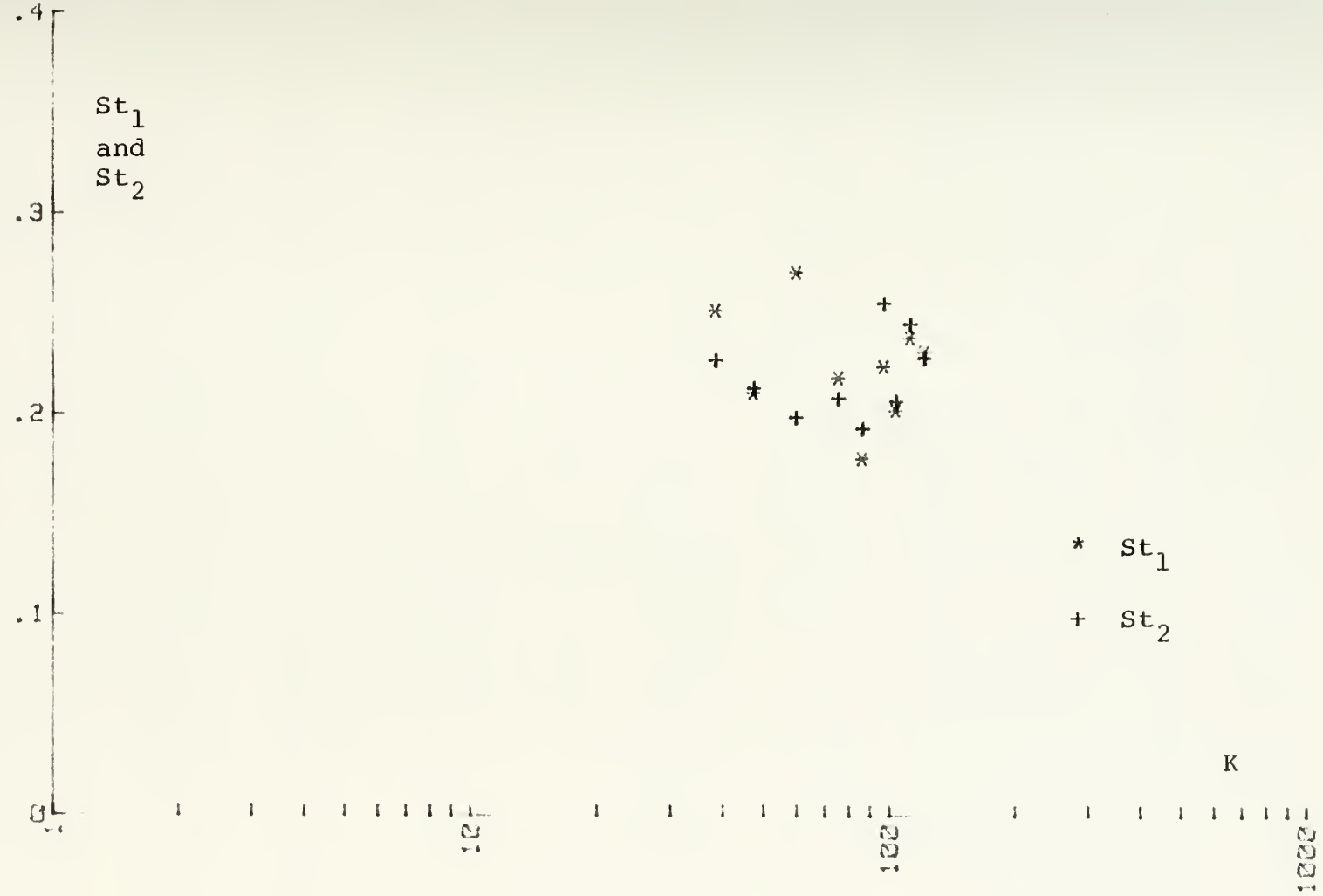

Fig. 67 St_1 and St_2 vs K for N=2.5 and $\alpha=30^{o}$

Fig. 68 St_3 and St_4 vs K for N=2.5 and $\alpha=30^{O}$

LIST OF REFERENCES

1. Dalton, C. and Helfinstine, R. A., "Potential Flow Past a Group of Cylinders," Journal of Basic Engineering, Trans. ASME, Vol. 93, pp. 636-642, 1971.

2. Yamamoto, T., "Hydrodynamic Forces on Multiple Circular Cylinders," Journal of Hydraulics Division, ASCE, Vol. 102, HY9, pp. 1193-1210, 1976.

3. Spring, B. H. and Monkmeyer, P. L., "Interaction of Plane Waves with Vertical Cylinders," Proc. 14th Coastal Engineering Conference, ASCE, Vol. III, pp. 1828-1849, 1974.

4. Chakrabarti, S. K., "Wave Forces on Multiple Vertical Cylinders," Journal of Waterways etc. Div., ASCE, WW2, pp. 145-161, 1978.

5. Zdravkovich, M. M., "Review of Flow Interference Between Two Circular Cylinders in Various Arrangements," Journal of Fluids Engineering, Trans. ASME, Vol. 99, pp. 618-633, 1977.

6. Ball, D. J. and Cox, N. J., "Hydrodynamic Drag Forces on Groups of Flat Plates," Journal of Waterway etc. Div. of ASCE, WW2, pp. 163-173, 1978.

7. Crua, A., "Druckverlustmessunger an Glattrohrbundeln," Sulger Brothers, Report No. 1387, 1967.

8. Hammeke, R., Heinecke, E. and Scholz, F., "Warmeubergangs and Drucklustmessunger ar Queranstromten Glattrohrbundeln, Insbesondere bei Hohen Reynoldsgablem," International Journal of Heat and Mass Transfer, Vol. 10, pp. 427-435, 1967.

9. Laird, A.D.K. and Warren, P. P., "Groups of Vertical Cylinders Oscillating in Water," Journal of Engineering Mechanics Division of ASCE, Vol. 89, EM1, pp. 25-35, 1963.

10. Chen, Y. N., "Fluctuating Lift Forces of the Karman Vortex Streets on Single Circular Cylinders and in Tube Bundles, Part-3, Lift Forcds in Tube Bundles," Journal of Engineering for Industry, Trans. ASME, Vol. 89, pp. 623-628, 1972.

11. Sachs, P., Wind Forces in Engineering, Pegamon Press, Oxford, 1972.

12. Arita, Y., Fujita, H. and Tagaya, K., "A Study of the Force of Current Acting on a Multitubular Column Structure," OTC Paper No. 1815, 1973.

13. ESDU (Engineering Sciences Data Unit), "Fluid Forces on Lattice Structures," Data Sheet 75011, 1975.

14. Dalton, C. and Szabo, J. M., "Drag on a Group of Cylinders," ASME Paper No. 76-Pte-42, 1976.

15. Ross, C. W., "Large Scale Tests of Wave Forces on Piling," U. S. Corps of Engineers Beach Erosion Board, Tech. Memo. No. 111, 1959.

16. Gibson, R. J. and Wang, H., "Added Mass of Pile Group," Journal of Waterway etc. Div. ASCE, WW2, pp. 215-223, 1977.

17. Chakrabarti, S. K., "Discussion of 'Added Mass of Pile Group' (R. J. Gibson and H. Want, Ref. 16)," Journal of Waterway etc. Div. of ASCE, WW2, 1978.

18. Tanida, Y., Okajima, A. and Watanabe, Y., "Stability of a Circular Cylinder Oscillating in Uniform Flow or in a Wake," Journal of Fluid Mechanics, Vol. 61, pp. 769-784, 1973.

19. Bushnell, M. J., "Forces on Cylinder Arrays in Oscillating Flow," OTC Paper No. 2903, 1977.

20. Sarpkaya, T., "Vortex Shedding and Resistance in Harmonic Flow about Smooth and Rough Circular Cylinders at High Reynolds Numbers," Naval Postgraduate School Technical Report No. 59SL76021, Monterey, California, 1976.

21. Sarpkaya, T., "Hydrodynamic Forces on Various Multiple-Tube Riser Configurations," OTC Paper No. 3539, 1979.

INITIAL DISTRIBUTION LIST

		No. Copies
1.	Defense Documentation Center Cameron Station Alexandria, Virginia 22314	2
2.	Library, Code 0142 Naval Postgraduate School Monterey, California 93940	2
3.	Professor T. Sarpkaya, Code 69Sl Mechanical Engineering Naval Postgraduate School Monterey, California 93940	2
4.	Department of Mechanical Engineering, Code 69 Naval Postgraduate School Monterey, California 93940	2
5.	Lieutenant Mehmet Ali Cinar Acibadem Cad. Ismail Hakki Bey Sok. No. 48 Kadikoy, Istanbul, Turkey	2
6.	Bogazici Universitesi P. K. 2 Bebek, Istanbul, Turkey	1
7.	Istanbul Teknik Universitesi Makina Fakultesi Istanbul, Turkey	1
8.	Ortadogu Teknik Universitesi Ankara, Turkey	1
9.	Dz. K. Komutanligi Okullar ve Kurslar Dairesi Bakanliklar, Ankara, Turkey	4

184313
Thesis
C47893 Cinar
C.1
Oscillating flow
about tube bundles.